

Role of Rab5 in Synaptic Vesicle Recycling

Dissertation

Am Fachbereich Biologie, Chemie
der
Universität Kassel

Tanja Wucherpfennig

2002

Als Dissertation genehmigt
von der Fakultät für Biologie/Chemie der Universität Kassel

Tag der mündlichen Prüfung:	21.06.2002
Erstgutachterin:	Prof. Dr. Mireille A. Schäfer
Zweitgutachter:	Prof. Dr. Markus Maniak

Acknowledgements

This study was performed in the laboratory of Dr. Marcos González-Gaitán at the Max-Planck-Institute for Biophysical Chemistry in Göttingen, in the department of Prof. Dr. Herbert Jäckle and at the Max-Planck-Institute for Molecular Cell Biology and Genetics in Dresden.

Foremost, I thank Dr. Marcos González-Gaitán. His critical advise, his respect, his guidance, his encouragement and his support made this study possible.

I thank Prof. Dr. Herbert Jäckle, for his support in Göttingen. I also thank Dr. Ulrich Nauber and countless members of the department of Prof. Jäckle.

I thank Prof. Dr. Mireille A. Schäfer and her colleagues at the University of Kassel for supervising this study and for accepting me as a PhD student in Kassel.

I thank Anja Schwabedissen for her excellent technical support, in particular for the cloning work.

I thank all members of my lab, Eugeni Entchev, Anja Schwabedissen, Veronica Dudu, Periklis Pantazis and Dana Backasch for scientific support, discussions, and a lot of fun.

I wish to thank Dr. Andreas Prokop for teaching me the electron microscopy, Dr. Michaela Wilsch-Bräuninger and Dieter Kötting for support in the electron microscopy.

I acknowledge Heike Taubert and Dana Backasch for the generation of transgenic flies, Rocio Fernández de la Fuente and Dana Backasch for keeping the fly stocks.

I want to thank several people from the electrical and mechanical workshops at the Max-Planck-Institute in Göttingen, in particular D. Herzog, R. Schürkoetter and H. Scheede.

I thank my friend Christian Rosenmund for the introduction to the field of electrophysiology, for many scientific discussions and in particular for being in my life.

I thank my parents for their love and support in whatever I did.

Table of Contents

Introduction	1
SV EXOCYTOSIS	3
COMPENSATORY ENDOCYTOSIS	7
“Kiss-and-run”	8
<i>Clathrin-mediated endocytosis</i>	9
MEMBRANE TRAFFIC THROUGH THE ENDOCYTIC PATHWAY	13
RAB PROTEINS	16
<i>Rab Proteins in the endocytic pathway</i>	21
<i>The early endosome and Rab5</i>	22
<i>The Rab5 domain at the early endosome</i>	23
<i>FYVE domain and FYVE domain containing Rab5 effectors</i>	25
SV RECYCLING IN NEURONS.....	26
MODEL SYSTEMS.....	28
THE DROSOPHILA NEUROMUSCULAR JUNCTION.....	29
Methods	37
TRANSGENE EXPRESSION.....	37
MOLECULAR ANALYSIS AND MUTANT STRAINS	37
LARVAL BODY WALL PREPARATION	39
ANTI-DROSOPHILA RAB5 ANTIBODY	39
IMMUNOHISTOCHEMISTRY.....	40
DEXTRAN UPTAKE IN CELL CULTURE	41
QUANTIFICATION OF THE NMJ SIZE	42
WESTERN BLOTTING.....	43
ELECTRON MICROSCOPY.....	44
SALINES	44
ELECTROPHYSIOLOGY	45
DYE IMAGING.....	46
SHIBIRE ^{TS} DEPLETION/RECOVERY EXPERIMENTS.....	48
FRAP AND WORTMANNIN EXPERIMENTS.....	48
STATISTICAL ANALYSIS	48
Results	50
CHARACTERIZATION OF AN EARLY ENDOSOMAL COMPARTMENT AT THE DROSOPHILA PRESYNAPTIC TERMINAL.....	50
<i>Rab5 defines an endosomal compartment at the synapse</i>	50
<i>2xFYVE localization at the endosome is PI(3)P dependent</i>	55
<i>The endosome is localized within the pool of recycling vesicles</i>	55
<i>The endosome size is stable during synaptic transmission</i>	56
<i>SV recycling involves membrane trafficking through the endosome</i>	59
ANALYSIS OF RAB5 FUNCTION USING RAB5 MUTANTS AND THE DOMINANT NEGATIVE VERSION OF RAB5, RAB5S43N.....	64
<i>Genomic organization of Drosophila Rab5</i>	64
<i>Rab5 mutants show locomotion defects, paralytic phenotypes and defective endosomes</i>	66

<i>Specific interference of Rab5 during presynaptic physiology does not cause a developmental phenotype</i>	69
<i>Endosomes are disrupted in Rab5S43N mutant presynaptic terminals</i>	72
<i>Endocytic intermediates accumulate in Rab5 mutant presynaptic terminals</i>	74
<i>Endocytic trafficking during SV recycling involves Rab5 function</i>	78
<i>Rab5-dependent recycling determines the SV fusion efficacy</i>	83
ANALYSIS OF RAB5 GAIN OF FUNCTION	93
<i>Rab5-mediated endosomal trafficking is rate-limiting during SV recycling and synaptic transmission</i>	93
<i>Overexpression of Rab5 does not cause a developmental phenotype of the NMJ but causes an enlargement of endosomes</i>	94
<i>Rab5 overexpression enhances synaptic performance</i>	94
Discussion.....	97
SYNAPTIC VESICLE RECYCLING	97
<i>SVs recycle through an endosomal compartment at the Drosophila NMJ</i> .	98
<i>Different pathways to recycle synaptic vesicles</i>	99
<i>Is endosomal trafficking activity-dependent?</i>	100
THE ROLE OF RAB5 IN ENDOSOMAL TRAFFICKING	102
<i>Structural phenotypes in Rab5 mutants</i>	102
<i>SV quality control at the endosome and synaptic plasticity</i>	103
Summary.....	107
Zusammenfassung	111
References.....	115

Abbreviations

A	abdominal
AP	action potential
BSA	bovine serum albumin
CCV	clathrin-coated vesicle
CNS	central nervous system
CSP	Cystein string protein
D	dorsal
DRab5	<i>Drosophila</i> Rab5
EEA1	early endosomal antigen 1
EJP	excitatory junction potential
ER	endoplasmic reticulum
FRAP	fluorescence recovery after photobleaching
g	gram
GABA	γ -aminobutyric acid
GAP	GTPase activating protein
GDI	guanine dissociation inhibitor
GEF	guanine nucleotide exchange factor
GFP	green fluorescent protein
h	hours
HRP	horseradish peroxidase
Hrs	hepatocyte growth factor-regulated tyrosine kinase substrate
Hz	hertz
ISN	intersegmental nerve branch
IU	international units
kDa	kilodalton
L	lateral
LPA	lysophosphatidic acid
LTR	long terminal repeat
M	molar
mEJP	miniature excitatory junction potential
mg	milligram
min	minutes
ml	milliliter
mm	millimeter
mM	millimolar
mV	millivolt
M Ω	megaohm
nM	nanomolar
NMJ	neuromuscular junction
NSF	N-ethylmaleimide-sensitive factor
NT	neurotransmitter
OD	outer diameter
ON	over night
ORF	open reading frame
PBS	phosphate buffered saline

PCR	polymerase chain reaction
PEM	PIPES-EGTA-MgCl ₂
PFA	paraformaldehyde
PI(3)P	phosphatidylinositol-3-phosphate
PI(4,5)P ₂	phosphatidylinositol-4,5-bisphosphate
PIs	inositolpolyphosphates
PM	plasma membrane
Rab	ras-like in rat brain
REP	Rab escort protein
rpm	rotations per minute
RT	room temperature
sec	seconds
SDS	sodium-dodecyl-sulphate
SLMV	synaptic-like microvesicle
SN	segmental nerve branch
SNAP	soluble NSF attachment protein
SNAP-25	synaptosome-associated protein of 25 kDa
SNARE	soluble NSF attachment protein receptor
SSR	subs synaptic reticulum
SV	synaptic vesicle
TGN	<i>trans</i> -Golgi network
TN	transverse nerve
UAS	upstream activator sequence
UTR	untranslated region
V	ventral
VAMP	vesicle associated membrane protein

Introduction

A major goal of neuroscience is to understand brain function. What is consciousness? How does the brain perceive and initiate action, how does it learn and remember? To understand how a complex nervous system works requires knowledge at several levels. We need to know how large numbers of neurons interact to produce the complex behavior of an organism. We need to know the properties of individual cells within the nervous system. Finally, we need to understand the molecular mechanisms by which signals are communicated between nerve cells, which is the basis for learning and memory.

Neurons are highly specialized to receive, integrate, conduct and transmit information. Signal transmission over long distances is achieved by an electrical signal, the action potential (AP). Action potentials are invariant electrical signals that are generated in the cell soma. From there, they propagate very fast and without decrement along the axon. Communication between neurons or from neurons to their target cells occurs at a specialized structure called synapse. Two types of synapses are known: electrical and chemical synapses. At electrical synapses, gap junctions connect the cytoplasm of the two cells, allowing ionic currents to directly flow between them.

Chemical synapses consist of a specialized presynaptic part, the synaptic cleft and a specialized postsynaptic part. The presynaptic part appears usually as a swelling, termed bouton, at the nerve terminal. It is characterized by the presence of numerous mitochondria and vesicles of around 40 nm in diameter, the synaptic vesicles (SVs). SVs store a quantum of neurotransmitter (NT) (Katz, 1969), which is released during Ca^{2+} -regulated secretion. NTs are small signaling molecules such as acetylcholine, glutamate, γ -aminobutyric acid (GABA), glycine and the biogenic amines dopamine, noradrenalin and serotonin. Exocytosis of SVs and release of NT is restricted to specialized regions within the presynaptic terminal, called active zones. At the active zones, SV docking sites and Ca^{2+} -channels are clustered together (Burns and

Augustine, 1995; Pumplin *et al.*, 1981; Robitaille *et al.*, 1990). The synaptic cleft between the pre- and the postsynaptic membrane is around 20 nm wide and contains electron-dense extracellular matrix and linker proteins that keep pre- and postsynaptic membranes precisely aligned (Cottrell *et al.*, 2000). The postsynaptic membrane is highly organized and specialized to receive information. It contains clusters of neurotransmitter receptors that are directly opposed to the presynaptic active zones where NT is released (Cottrell *et al.*, 2000; Ehlers *et al.*, 1996; Kneussel and Betz, 2000). During synaptic transmission, chemical synapses first convert the electrical signal into a chemical signal. This conversion is achieved by the action potential induced release of neurotransmitter from the presynaptic terminal into the synaptic cleft. The NT then binds to specific receptors at the postsynaptic cell membrane generating again an electrical signal.

Since neurons are generally elongated cells, their nerve terminal is located distant from the cell soma. This distance can range from a few micrometers to meters as in the case of motoneurons innervating e.g. the feet of giraffes. While the nerve terminal receives electrical signals within milliseconds, transport of components from the cell body is a slow process mediated by two different systems fast and slow axonal anterograde transport (Vale *et al.*, 1992). Fast anterograde transport is mediated by the motor proteins Kinesin and Dynamin moving mainly organelles along microtubuli. The speed of the fast axonal transport system is in the range of 200 mm/day e.g. mitochondria travel around 50 mm/day. In contrast, along the slow axonal transport, most proteins travel with few mm/day. The nerve terminal therefore needs to be independent in many basic functions. It has mitochondria for the local production of energy as well as enzymes and transporters for the synthesis of neurotransmitters. After their synthesis, NTs are transported into SVs by specific transporters located in the vesicle membrane. Each nerve terminal contains a reservoir of NT-filled SVs. This pool of releasable vesicles is essential for synaptic function and needs to be maintained. Since SVs are released by exocytosis during synaptic transmission a mechanism for SV regeneration is required, because otherwise

an active nerve terminal would deplete itself from SVs. New SVs are not delivered from the soma, because axonal transport is a slow process. Instead, they are regenerated within the presynaptic terminal by a local recycling process. After exocytosis, vesicle components are internalized and assembled into new SVs.

SV exocytosis

Within the presynaptic terminal, SVs undergo a cyclic process of docking, priming, exocytosis and endocytosis followed by the maturation and transport of the SVs to the docking sites (Fig. 1). NT exocytosis is a complex and tightly regulated process that involves the sequential interaction of different synaptic proteins. NT-filled SVs are first targeted to specific sites, the active zones, where they become docked. Vesicle docking has been defined by morphological and biochemical criteria. *First*, docked vesicles have been defined at the ultrastructural level as vesicles that are closely opposed to the plasma membrane (PM) (Donrunz and Stevens, 1999; Plattner *et al.*, 1997; Schikorski and Stevens, 1997). *Second*, using imaging techniques and labeled vesicles it has been found that the docked vesicles are less mobile than the cytoplasmic ones (Martin and Kowalchuk, 1997; Oheim *et al.*, 1998; Zenisek *et al.*, 2000). *Third*, a large fraction of the morphologically docked vesicles remains associated with plasma membrane fragments following homogenization (Martin and Kowalchuk, 1997).

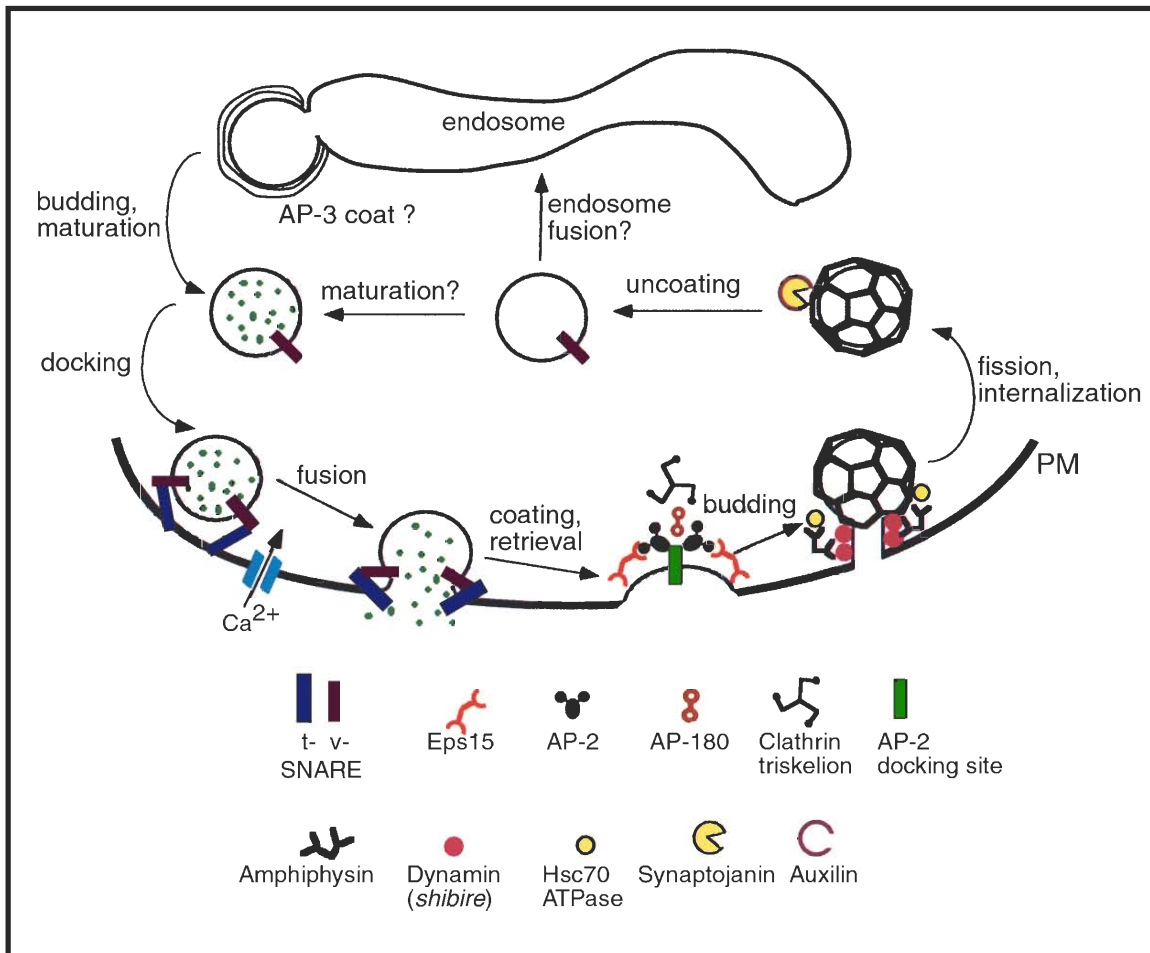


Fig. 1. Scheme of the synaptic vesicle cycle, highlighting proteins with well-established roles in synaptic vesicle recycling. Two models of postinternalization recycling events are shown. After clathrin-mediated endocytosis, uncoated endocytic vesicles may immediately mature into SVs and enter the SV pool. Alternatively, endocytic vesicles may fuse to an intermediate endosomal compartment, where membrane components could be sorted and packed into new SVs, that would bud from the endosome. After filling with neurotransmitter (green spots), SVs are translocated to specific sites at the active zones, where they become morphologically docked. A biochemical priming step renders them fusion competent. Membrane fusion is mediated by vesicle (v) and target membrane (t) SNARE proteins and is triggered by Ca^{2+} . After complete fusion of the SV with the plasma membrane (PM), internalization is initiated by the formation of the clathrin coat. Targeting and assembly of Clathrin on the PM depends on adaptors (AP-2 and AP-180) and may also involve Eps15. Adaptors are targeted to saturable docking sites, probably Synaptotagmin, at the PM. Clathrin-coated vesicles (CCVs) appear to be pinched off by Dynamin. Amphiphysin has been postulated to facilitate fission. CCVs are uncoated by the Hsc70 ATPase in conjunction with Auxilin and Synaptojanin. Modified from Budnik, 1999.

However, only a fraction of the morphologically docked vesicles is fusion-competent, i.e. capable of undergoing rapid exocytosis in response to elevated Ca^{2+} -concentrations (Donrunz and Stevens, 1999; Rosenmund and Stevens, 1996; Schikorski and Stevens, 2001). The pool of fusion-competent SVs is therefore called the readily releasable pool (Donrunz and Stevens, 1999; Kuromi and Kidokoro, 1999; Kuromi and Kidokoro, 2000; Rosenmund and Stevens, 1996). A biochemical priming step is required to render the docked vesicles fusion-competent. Priming involves ATP, the proteins NSF (N-ethylmaleimide-sensitive fusion protein), SNAP (soluble NSF attachment protein) and Munc-13 as well as the synthesis of phosphatidylinositol-4,5-bisphosphate ($\text{PI}(4,5)\text{P}_2$), but the exact events are still largely unknown. Therefore, the term priming is used to include all molecular rearrangements and ATP-dependent protein and lipid modifications that occur after the initial docking and before SV fusion. The final fusion of primed SVs with the PM is triggered by Ca^{2+} -influx through voltage gated Ca^{2+} -channels. Exocytosis is extremely rapid, following Ca^{2+} -influx within milliseconds (Chad and Eckert, 1984; Fogelson and Zucker, 1985; Lim *et al.*, 1990; Lindau *et al.*, 1992; Llinas *et al.*, 1992; Llinas *et al.*, 1982; Mintz *et al.*, 1995; Parsons *et al.*, 1994; Schneggenburger and Neher, 2000; von Ruden and Neher, 1993), reviewed in (Brunger, 2000; Kelly, 1993; Klenchin and Martin, 2000). The speed of exocytosis predicts that only a few molecular rearrangements couple Ca^{2+} -influx to membrane bilayer fusion.

The conserved family of SNARE (soluble NSF attachment protein receptor) proteins has been implicated in all intracellular membrane fusion events (Hay and Scheller, 1997; Jahn and Sudhof, 1999; Sollner *et al.*, 1993b). In particular, SV fusion is mediated by the target membrane SNAREs (t-SNAREs) Syntaxin (Bennett *et al.*, 1992) and SNAP-25 (synaptosomal associated protein of 25 kDa) (Oyler *et al.*, 1989) and the vesicle membrane SNARE (v-SNARE) Synaptobrevin, also called VAMP (vesicle associated membrane protein) (Oyler *et al.*, 1989). The specific cleavage of these SNAREs by clostridial neurotoxins inhibits neurotransmission, supporting their fundamental role in SV fusion

(Hayashi *et al.*, 1994; Jahn and Niemann, 1994; Montecucco and Schiavo, 1995; Schiavo *et al.*, 1992).

As all SNAREs, Syntaxin, SNAP-25 and Synaptobrevin contain an amphipathic α -helix close to their membrane anchor (Fasshauer *et al.*, 1998b). The α -helices of Syntaxin, SNAP-25 and Synaptobrevin twist around each other to form an extremely stable ternary complex (Sollner *et al.*, 1993b), in which the hydrophobic side chains are buried in the center. The crystal structure of this “core complex” revealed a four-helix coiled-coil structure (Sutton *et al.*, 1998). The “zipper model” of SNARE function postulates that the SNARE complex assembles by “zipping up” the SNARE α -helices from the membrane-distant N-termini to the membrane-proximal C-termini. Thus, the formation of the stable SNARE complex is proposed to bring SVs into intimate contact with the plasma membrane (PM). This probably overcomes the energy barrier and drives bilayer fusion (Hanson *et al.*, 1997; Lin and Scheller, 1997).

However, the precise temporal interaction between the SNARE proteins and the mechanism of Ca^{2+} -regulation are unknown. The Ca^{2+} -, phospholipid- and SNARE-binding synaptic vesicle protein Synaptotagmin has been proposed to serve as Ca^{2+} -sensor that regulates exocytosis, (Brose *et al.*, 1992; Desai *et al.*, 2000; Fernandez-Chacon *et al.*, 2001; Geppert and Sudhof, 1998; Littleton and Bellen, 1995; Littleton *et al.*, 1999; Perin *et al.*, 1990). Ca^{2+} -binding to Synaptotagmin causes its rapid insertion into membranes, occurring within milliseconds (Brose *et al.*, 1992; Davis *et al.*, 1999; Li *et al.*, 1995a). It has been thereby speculated that Synaptotagmin causes membrane fusion by a Ca^{2+} -induced morphological change analogous to the mechanism of pH-induced, hemagglutinin-mediated fusion of the influenza virus to its target cell (Kelly, 1993).

After the fusion reaction, v- and t-SNAREs are contained within the same membrane forming cis-SNARE complexes that need to be disassembled prior to the next fusion event. cis-SNARE disassembly is performed by the soluble cofactors NSF and SNAP (Otto *et al.*, 1997; Sollner *et al.*, 1993a; Sollner *et al.*,

1993b; Swanton *et al.*, 1998), but it is not yet known where and when this reaction occurs. Furthermore, following SV exocytosis the vesicle membrane is immediately endocytosed (Fasshauer *et al.*, 1998a; Jahn and Niemann, 1994; Littleton *et al.*, 1998; Poirier *et al.*, 1998). This membrane recapture requires high specificity since SVs and the presynaptic plasma membrane have a distinct membrane composition.

Compensatory endocytosis

Compensatory endocytosis is a process by which a cell retrieves membrane, which has been added to the PM by regulated secretion. As described above, the presynaptic nerve terminal is filled with SVs that are exocytosed during neurotransmission. Synaptic function requires that the pool of SVs, competent for NT release, is maintained even during sustained periods of high frequency stimulation. The regeneration of SVs is achieved by rapid endocytosis of synaptic vesicle components followed by a local recycling mechanism. In addition, compensatory endocytosis is essential to keep the size of the presynaptic terminal constant and to preserve the molecular diversity of SV versus PM.

Recycling of SVs involves at least two distinct pathways, “kiss-and-run” (Ceccarelli *et al.*, 1973; Fesce *et al.*, 1994; Palfrey and Artalejo, 1998) and clathrin-mediated endocytosis (De Camilli and Takei, 1996; Heuser and Reese, 1973). These current endocytic models are based, with some modifications, on observations made in the early 1970s by the groups of Ceccarelli and Heuser (Ceccarelli *et al.*, 1973; Heuser and Reese, 1973). The two groups independently investigated endocytosis at the frog neuromuscular junction (NMJ) using electron-dense endocytic markers and electron microscopy. Heuser and his group observed endocytosis of clathrin-coated vesicles (CCVs) in regions outside the active zones. Ceccarelli and colleagues by contrast observed clathrin-independent endocytosis at or near the active zone. This mechanism was later attributed to the “kiss-and-run” vesicle cycle (Fesce *et al.*, 1994).

“Kiss-and-run”

“Kiss-and-run” (Fesce *et al.*, 1994; Jarousse and Kelly, 2001) is believed to take place at the active zone. According to the model, SVs make only a brief contact with the PM and release their NT through a transient fusion pore (Albillos *et al.*, 1997; Almers and Tse, 1990; Ceccarelli *et al.*, 1973; Klingauf *et al.*, 1998; Pyle *et al.*, 2000). After closure of the fusion pore, the vesicle is simply refilled with NT and can be used again. Thus, no coated intermediate is formed (Ceccarelli *et al.*, 1973; Palfrey and Artalejo, 1998) and the vesicle is recovered without mixing its components with the PM. Therefore, SVs never change their individual identity as defined by their size, protein and lipid-composition. SV recycling through this pathway is thought to be very fast, in the range of 1 to 2 seconds.

There are several lines of evidence supporting the “kiss-and-run” mode. *First*, the detection of uncoated vesicles, labeled with an endocytic tracer at the active zone (Ceccarelli *et al.*, 1973). *Second*, the discrepancy between the amounts of FM-dye released from prelabeled nerve terminals with respect to the released NT. In hippocampal neurons, less dye is released than expected from the amount of NT released. As FM-dyes diffuse slower through a transient fusion pore than the NT, it has been calculated that 20% of the SVs are recycled through the “kiss-and-run” mechanism (Stevens and Williams, 2000). *Third*, two kinetic time constants of endocytosis have been detected in nerve terminals. The faster type of endocytosis is inhibited by prolonged stimulation and could correspond to “kiss-and-run” (Neves and Lagnado, 1999). *Fourth*, Palfrey and colleagues (Palfrey and Artalejo, 1998) observed a fast type of endocytosis that is dynamin-dependent but clathrin-independent. *Fifth*, the opening and closing of fusion pores gives rise to transient increases in the cell surface, which can be detected in endocrine cells electrophysiologically as a quantal change in the membrane capacitance, called “capacitance flicker” (Alvarez de Toledo and Fernandez, 1990; Breckenridge and Almers, 1987; Spruce *et al.*, 1990). Therefore, it seems likely that the “kiss-and-run” mode of SV recycling coexists with the classical pathway, which starts with clathrin-mediated endocytosis.

Clathrin-mediated endocytosis

The process of clathrin-mediated endocytosis (reviewed in (Brodin *et al.*, 2000; Hirst and Robinson, 1998; Jarousse and Kelly, 2001; Kirchhausen, 2000b; Schmid, 1997)) is thought to be slower than the “kiss-and-run” pathway, regenerating SVs within 30 to 60 seconds through coated intermediates. In 1964, coated pits and vesicles were discovered (Roth and Porter, 1964). Clathrin-coated vesicles were first isolated from pig brain in 1969 (Kanaseki and Kadota, 1969) and Clathrin itself was purified in 1975 (Pearse, 1975). Clathrin-mediated endocytosis is involved in a variety of cellular functions such as the uptake of nutrients, growth factors and antigens as well as the regulation of cell surface receptors (Schmid, 1997). Endocytosis via clathrin-coated vesicles has been shown to participate in the recycling of SVs (De Camilli and Takei, 1996; González-Gaitán and Jäckle, 1997; Heuser, 1989; Heuser and Reese, 1973; Shupliakov *et al.*, 1997).

Following the complete collapse of the SV into the PM clathrin-mediated endocytosis (Ceccarelli *et al.*, 1979; Heuser and Reese, 1973; Matteoli *et al.*, 1992; Torri-Tarelli *et al.*, 1987; Valtorta *et al.*, 1988) ensures the specific retrieval of SV components and their reassembly into new SVs (Maycox *et al.*, 1992; Takei *et al.*, 1996) (Fig. 1). Within the presynaptic terminal, this process takes place at specialized sites, the centers of endocytosis, which surround the active zones where exocytosis occurs (González-Gaitán and Jäckle, 1997; Jarousse and Kelly, 2001; Ringstad *et al.*, 1999; Roos and Kelly, 1998; Roos and Kelly, 1999; Teng and Wilkinson, 2000).

Clathrin-mediated endocytosis involves a number of highly coordinated sequential steps controlled by different proteins. These steps include 1) targeting of coat components to the PM, 2) the formation of clathrin-coated membrane invaginations, termed pits, into which cargo-molecules are concentrated, 3) the formation of clathrin-coated vesicles (CCVs) by pinching off clathrin-coated pits from the PM and, finally, 4) the removal of the Clathrin coat, called uncoating.

1) Coat assembly

The main coat constituents are Clathrin, the Clathrin adaptor protein complex AP-2 and a synaptic protein called AP-180. Clathrin-mediated endocytosis is initiated by the binding of AP-2 to the PM. AP-2 then recruits Clathrin to the membrane and triggers its polymerization. The heterotetrameric AP-2 complex is composed of four closely associated subunits called α , β 2, μ 2 and σ 2. It has two essential functions during clathrin-mediated endocytosis: *First*, recruitment of the Clathrin coat to the PM and *second*, selection of specific cargo molecules destined for internalization.

The α subunit also called α -Adaptin is responsible for targeting AP-2 to specific, saturable docking sites at the PM (Gaidarov *et al.*, 1996; Gaidarov and Keen, 1999; Mahaffey *et al.*, 1989; Mahaffey *et al.*, 1990; Moore *et al.*, 1987), defined probably by Synaptotagmin (Chapman *et al.*, 1998; Haucke *et al.*, 2000; Zhang *et al.*, 1994). In addition, specific inositolpolyphosphates (PIs) in particular PI(4,5)P₂ is required to recruit AP-2 to the PM (Gaidarov *et al.*, 1996; Gaidarov and Keen, 1999). The σ 2 subunit is involved in the selection of cargo molecules to be internalized. It interacts with tyrosine- and dileucine-based endocytic sorting signals present in the cytoplasmic domains of certain transmembrane receptors (Boll *et al.*, 1996; Ohno *et al.*, 1996; Ohno *et al.*, 1995; Sorkin *et al.*, 1995). Binding of the σ 2 subunit to these sorting motifs causes a concentration of cargo molecules at the sites of endocytosis. Finally, the β subunit of AP-2 recruits Clathrin (Ahle and Ungewickell, 1989; Gallusser and Kirchhausen, 1993; Shih *et al.*, 1995) and triggers its polymerization.

Clathrin was named in reference to the cage like structure it forms (Pearse, 1976). It is the major structural component of the Clathrin coat (Pearse, 1975) and forms triskelions consisting of three heavy chains of around 180 kDa and three light chains of around 30 kDa (reviewed in (Kirchhausen, 2000a)). Triskelions can be viewed after negative staining in the electron microscope and appear as three-legged structures (Ungewickell and Branton, 1981). They self-assemble *in vitro* into lattices containing pentagons and hexagons. The Clathrin

coat consists of 12 pentagons and a variable number of hexagons (Crowther and Pearse, 1981; Kanaseki and Kadota, 1969). 12 pentagons are required in order to form a closed structure, whereas the number of hexagons determines the size of the coat (Shraiman, 1997).

Two models for the assembly process have been proposed. According to Liu (Liu *et al.*, 1995), Clathrin triskelions first assemble into a flat network of hexagons some of which are later converted into pentagons generating membrane curvature. Alternatively, because of a certain membrane curvature, determined by other factors, hexagons and pentagons are incorporated during the assembly process (Cupers *et al.*, 1994). Another factor involved in the assembly of Clathrin coats is the monomeric protein AP-180. AP-180 binds to both Clathrin and AP-2 (Ahle and Ungewickell, 1986; Morris *et al.*, 1993) and has been implicated in controlling the size of endocytic vesicles (Nonet *et al.*, 1999; Zhang *et al.*, 1998).

2) Invagination

Much less is known about the process of invagination. Invagination is accompanied by an increase in the negative membrane curvature. The lysophosphatidic acid (LPA) acyl transferase Endophilin might be involved in the process of invagination. This enzyme converts LPA, by addition of the fatty acid arachidonate into phosphatidic acid, thereby increasing the negative membrane curvature (Ringstad *et al.*, 1999; Schmidt *et al.*, 1999).

3) Fission

The most extensively studied protein involved in the fission of clathrin-coated vesicles is Dynamin. Dynamin has been originally linked to endocytosis through its temperature-sensitive *Drosophila* mutant *shibire^{ts}*. In *shibire^{ts}*, endocytosis is inhibited at the restrictive temperature because clathrin-coated pits cannot be pinched off from the PM (Kosaka and Ikeda, 1983b). Later, the mutation in *shibire* was mapped to Dynamin (Chen *et al.*, 1991; van der Bliek and

Meyerowitz, 1991). Because Dynamin forms rings and tubules *in vitro* (Carr and Hinshaw, 1997; Hinshaw and Schmid, 1995) and is located at the neck of the coated pits (Sever *et al.*, 1999), it has been proposed to act as a “pinchase” that mechanically pinches off the clathrin-coated vesicle from the PM (Sweitzer and Hinshaw, 1998). However, since Dynamin contains several protein-protein interaction domains, it has been alternatively proposed to recruit the actual severing activities around the neck of the budding vesicle (Kirchhausen, 1999; Sever *et al.*, 1999; Yang and Cerione, 1999).

Recently, two dynamin-binding proteins Amphiphysin (David *et al.*, 1996) and Endophilin (Ringstad *et al.*, 1999) have been postulated to facilitate the fission step (Barr and Shorter, 2000; Zimmerberg, 2000).

4) Uncoating

Uncoating of clathrin-coated vesicles is thought to occur rapidly, since free, coated vesicles are rarely seen in stimulated synapses. The clathrin-binding protein Auxilin (Holstein *et al.*, 1996) recruits the uncoating ATPase Hsc70 to clathrin-coated vesicles and stimulates its ATPase activity (Barouch *et al.*, 1997; Holstein *et al.*, 1996; Schroder *et al.*, 1995; Ungewickell *et al.*, 1995). Hsc70 subsequently releases Clathrin triskelions (Kirchhausen and Harrison, 1981; Ungewickell and Branton, 1981) and other coat proteins from the vesicles by undergoing multiple cycles of Clathrin binding and ATP hydrolysis (Barouch *et al.*, 1994; Braell *et al.*, 1984; Chappell *et al.*, 1986; Schlossman *et al.*, 1984). Furthermore, the polyphosphoinositide phosphatase Synaptojanin (Guo *et al.*, 1999; McPherson *et al.*, 1996) has also been implicated in the uncoating reaction, since disruption of its function causes the accumulation of CCVs (Cremona *et al.*, 1999; Harris *et al.*, 2000).

In the case of the synapse, little is known about the fate of uncoated endocytic vesicles. In particular, the process of endocytic vesicle recycling and maturation into NT-filled, releasable SVs is a matter of debate. In contrast, it is well established that in cultured mammalian cells uncoated endocytic vesicles fuse

to an intermediate endosomal compartment, the early sorting endosome and that recycling takes place through the endocytic pathway.

Membrane traffic through the endocytic pathway

Eukaryotic cells contain an elaborate system of intracellular organelles and membrane trafficking routes (Fig. 2). The biosynthetic pathway of eukaryotic cells serves to deliver newly synthesized molecules to different intracellular organelles. Along this route components usually travel through endoplasmic reticulum (ER) and Golgi complex to their target destinations including mitochondria, lysosomes and PM. The other major route, the endocytic pathway, is responsible for the recycling of endocytosed components. The endocytic pathway involves several distinct endocytic compartments and each trafficking step between the different intracellular organelles is mediated by small membrane carriers.

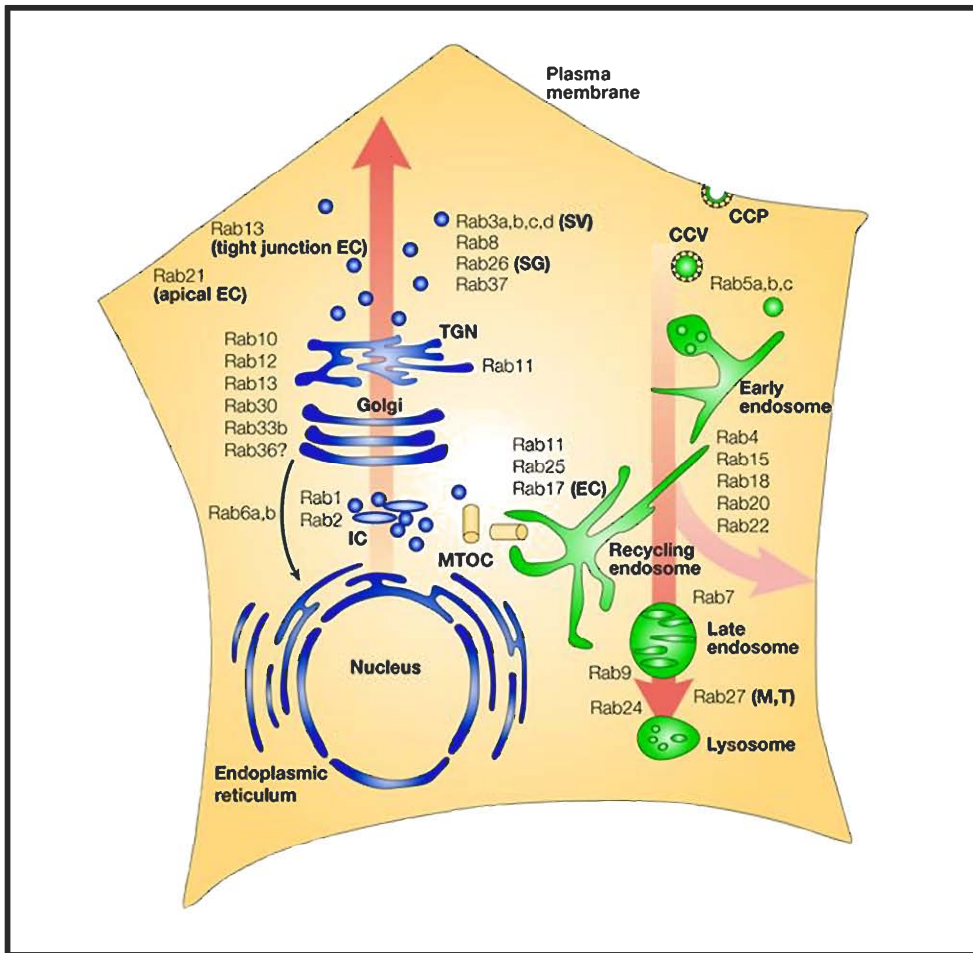


Fig. 2. Schematic illustration of the trafficking routes in mammalian cells and the specific Rab proteins involved (from Zerial, 2001). Along the biosynthetic pathway (left) molecules travel through endoplasmic reticulum and Golgi complex to the plasma membrane. The endocytic route (right) is composed of different endocytic compartments, including early endosome, recycling endosome, late endosome and lysosome. Each trafficking step between the different compartments is mediated by a specific protein of the Rab family. The localization of different Rab proteins to the different intracellular compartments is summarized. Abbreviations: CCV, clathrin-coated vesicle; CCP, clathrin-coated pit; EC, epithelial cells; IC, ER-Golgi intermediate compartment; M, melanosomes; MTOC, microtubule-organizing centre; SG, secretory granules; SV, synaptic vesicle; T, T-cell granules; TGN, *trans*-Golgi network. Note that some Rab proteins are cell specific (for example Rab3a in neurons) or show cell-type-specific localization (for example, Rab13 in tight junctions).

The first step in the formation of these transport vesicles is the assembly of a coat at specific sites of the donor organelle (reviewed in (Hirst and Robinson, 1998; Robinson and Bonifacino, 2001; Schmid, 1997; Takei and Haucke, 2001; Zhang *et al.*, 1999)). The coat generally assembles from multiple hetero-oligomeric, cytosolic protein complexes. Coats are believed to be involved in the physical formation of transport vesicles as well as in the selective packaging of their cargo. Several different coat complexes are known: 1) Clathrin with AP-2 driving endocytic vesicle formation at the PM. 2) Clathrin with AP-1 generating transport vesicles at the *trans*-Golgi network (TGN). 3) The AP-3 complex generates vesicles at the TGN and probably also at the endosome. 4) The AP-4 complex associated to the TGN. 5) The coatamer protein complex assembles together with ARF-1 to form COPI-coated vesicles that mediate retrograde transport within the Golgi and between Golgi and ER. 6) A protein complex including sec23p/sec24p, sec13/31p and sar1p that assembles to form COPII vesicles at the ER. Each type of transport vesicle mediates the flow of certain cargo molecules to certain destination.

Membrane traffic requires high specificity and tight regulation because cargo molecules need to be delivered to the correct acceptor compartments, while organelle integrity and biochemical composition have to be maintained. Furthermore, the compartment size needs to be stable, which requires that fusion of vesicles with a given compartment is in balance with budding of vesicles from the same compartment.

A typical transport reaction can be viewed as a four-step process. It consists of *first*, the formation of a vesicular (Rothman and Orci, 1992) or tubular (Klausner *et al.*, 1992) transport intermediate from the donor compartment. This reaction is controlled by different coat proteins (Kreis, 1992). *Second*, the movement of the vesicle along microtubules (Brady, 1991; Kuznetsov *et al.*, 1992; Mitchison, 1992) towards the target compartment. *Third*, tethering/docking of the vesicle with the target compartment (Pfeffer, 1999) and *fourth*, finally the fusion of the lipid bilayers. The specificity of these events is critical to preserve organelle integrity and to control cargo flow within the cell. To achieve this, each

trafficking step is tightly regulated by a different protein of the Rab family of small GTPases (Pfeffer, 1994).

Rab proteins have been proposed to determine vesicular transport specificity by mediating in conjunction with their effector proteins the specific tethering of vesicles to their target organelle. In addition, Rab proteins are thought to be upstream modulators of the SNARE proteins, regulating the formation of a complex between the v- and its cognate t-SNARE (Lian *et al.*, 1994; Lupashin and Waters, 1997; McBride *et al.*, 1999; Sogaard *et al.*, 1994). The family of SNARE proteins is involved in the final event of membrane fusion (see below) (McNew *et al.*, 2000; Parlati *et al.*, 2000; Rothman, 1994; Weber *et al.*, 1998). This view is supported by several recent studies reporting direct molecular interactions between Rab effector proteins and components of the SNARE machinery (McBride *et al.*, 1999; Peterson *et al.*, 1999; Price *et al.*, 2000; Sato *et al.*, 2000; Tall *et al.*, 1999). The interactions between Rab effectors and components of the SNARE machinery may coordinate the Rab-dependent membrane tethering and docking with the SNARE-dependent membrane fusion.

Rab Proteins

Rab proteins are small (21 – 25 kDa), monomeric GTPases (Fig. 3A) forming the largest branch of the Ras superfamily of small GTPases. There are probably 63 different Rab proteins in humans (Bock *et al.*, 2001; Zerial and McBride, 2001), 11 in yeast (Lazar *et al.*, 1997) and around 30 in *Drosophila* (Littleton, 2000). The first Rab gene was identified in *Saccharomyces cerevisiae* in 1983 (Gallwitz *et al.*, 1983). The first mammalian homologs were cloned in 1987 and termed Rab (ras-like in rat brain) (Touchot *et al.*, 1987).

Rab proteins regulate vesicle-mediated transport of proteins and lipids between different organelles (Bucci *et al.*, 1992; Huber *et al.*, 1993; Lombardi *et al.*, 1993; Martinez *et al.*, 1994; Pfeffer, 1996; Rothman, 1994; Salminen and Novik, 1987; Segev, 1991; Tisdale *et al.*, 1992; van der Sluijs *et al.*, 1992) (Fig. 2). They directly or indirectly affect vesicle budding (Benli *et al.*, 1996; McLauchlan

et al., 1998; Nuoffer and Balch, 1994; Riederer *et al.*, 1994) and play important roles in vesicle docking (Christoforidis *et al.*, 1999a; Novick and Zerial, 1997; Nuoffer and Balch, 1994; Pfeffer, 1994). In addition, some members have been implicated in motility by interactions with the cell cytoskeleton (Nielsen *et al.*, 1999).

Each Rab protein is localized to the cytoplasmic surface of a distinct membrane bound organelle (Ferro-Novick and Novick, 1993; Novick and Zerial, 1997; Pfeffer, 1994; Takai *et al.*, 1992; Zerial and McBride, 2001; Zerial and Stenmark, 1993) (Fig. 2). Membrane attachment and function of Rab proteins requires their isoprenylation. After their synthesis, Rab proteins are bound to a Rab escort protein (REP) (Seabra *et al.*, 1992a; Seabra *et al.*, 1992b) that presents the unprenylated Rab protein to the geranylgeranyl-transferase type II (Andres *et al.*, 1993). This heterodimeric protein geranylates Rab proteins, by the addition of the C-20 isoprenyl lipid geranylgeranyl, to usually two cysteine residues at the C-terminus of Rab proteins (Marshall, 1993; Seabra *et al.*, 1992a). Geranyl groups render Rab proteins hydrophobic and are required for their reversible membrane association (Alexandrov *et al.*, 1994).

The double geranylated Rab protein is thought to remain associated with REP, which delivers the GTPase to a specific organelle or transport vesicle. The specificity of Rab localization is mediated by interactions between the hypervariable, C-terminus of a Rab protein with distinct proteins on the organelle surface (Chavrier *et al.*, 1991; Soldati *et al.*, 1994; Ullrich *et al.*, 1994). Rab proteins are predominantly localized to membranes of transport vesicles and to their specific target compartments. In the steady state, Rab proteins accumulate at their target compartment and have thereby been used as markers for different organelles (Bucci *et al.*, 1992; Chavrier *et al.*, 1991; Chavrier *et al.*, 1990; Ullrich *et al.*, 1996). Only a minor fraction of each Rab protein is localized to the cytosol where it is complexed with a protein called guanine dissociation inhibitor (GDI) (Garrett *et al.*, 1993; Regazzi *et al.*, 1992; Sasaki *et al.*, 1991; Sasaki *et al.*, 1990; Soldati *et al.*, 1993; Ullrich *et al.*, 1993).

Rab proteins act as molecular switches that cycle between an active GTP-bound, membrane associated and an inactive GDP-bound cytosolic conformation. The GTP–GDP cycle is required for Rab function and is mediated by the accessory proteins GDI, GDI displacement factor, guanine nucleotide exchange factor (GEF) and GTPase activating protein (GAP). Within the cytosol, the GDP-bound form of Rab proteins, Rab–GDP, is bound to Rab–GDI, which masks the hydrophobic prenyl groups of Rab proteins (Pfeffer *et al.*, 1995). Upon membrane attachment, GDI is released by a GDI displacement factor (Dirac-Svejstrup *et al.*, 1997). Subsequently, a GEF catalyzes the exchange of GDP against GTP (Burton *et al.*, 1993; Burton *et al.*, 1994; Moya *et al.*, 1993), thereby converting Rab proteins into their active, GTP-bound form (Bourne, 1988; Goud and McCaffrey, 1991; Soldati *et al.*, 1994; Ullrich *et al.*, 1994; Zerial and Stenmark, 1993). Activated Rab proteins recruit soluble factors that act as specific effector molecules regulating downstream docking and fusion events. Finally, GAPs stimulate GTP hydrolysis (Ferro-Novick and Novick, 1993; Strom *et al.*, 1993) converting Rab proteins into their inactive, GDP-bound form. Rab-GDI then recognizes and extracts Rab-GDP from the membrane and recycles them back to the appropriate membrane (Araki *et al.*, 1990; Garrett *et al.*, 1993; Regazzi *et al.*, 1992; Soldati *et al.*, 1993; Takai *et al.*, 1992; Ullrich *et al.*, 1993).

One of the key approaches to manipulate and investigate Rab protein function was the mutagenesis of specific amino acids essential for the GTP/GDP cycle of Rab proteins (Fig. 3A). The choice of the amino acids to be mutagenized was based on the well-characterized mutations described in the Ras oncoprotein. Mutations corresponding to the glutamine 61 to lysine (Q61L) mutation in Ras cause a decreased intrinsic and GAP-stimulated GTPase activity, while the ability to bind nucleotides is not changed (Adari *et al.*, 1988; Der *et al.*, 1986; Stenmark *et al.*, 1994; Tanigawa *et al.*, 1993; Tisdale *et al.*, 1992; Walworth *et al.*, 1992). Therefore, dominant active Rab proteins are stabilized in their active, GTP-bound conformation (Adari *et al.*, 1988; Der *et al.*, 1986; Hoffenberg *et al.*, 1995; Stenmark *et al.*, 1994). In contrast, mutants equivalent to the serine 17 to

asparagine (S17N) mutation of the Ras protein (Farnsworth and Feig, 1991; Feig and Cooper, 1988), have a lower affinity for GTP than for GDP, causing a dominant inhibitory effect by blocking the protein in its inactive, GDP-bound conformation. Comparable mutations in Rab proteins have been discovered, including for Rab3A (T36N) (Burstein *et al.*, 1992), Rab1A (S25N) (Nuoffer *et al.*, 1994), Rab9 (Riederer *et al.*, 1994) and Rab5 (Li and Stahl, 1993; Stenmark *et al.*, 1994). They all show dominant negative phenotypes, probably by binding to, and titrating out the respective effector molecules, that are thereby not available for the endogenous Rab protein (Burstein *et al.*, 1992).

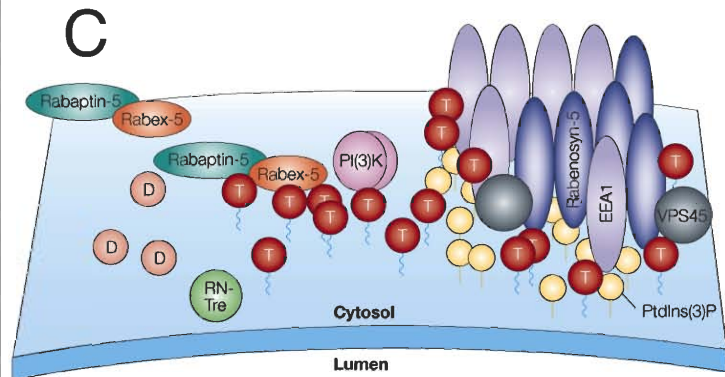
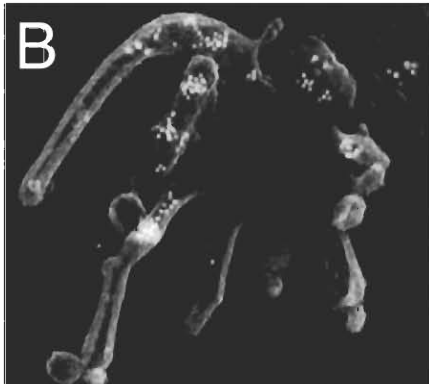
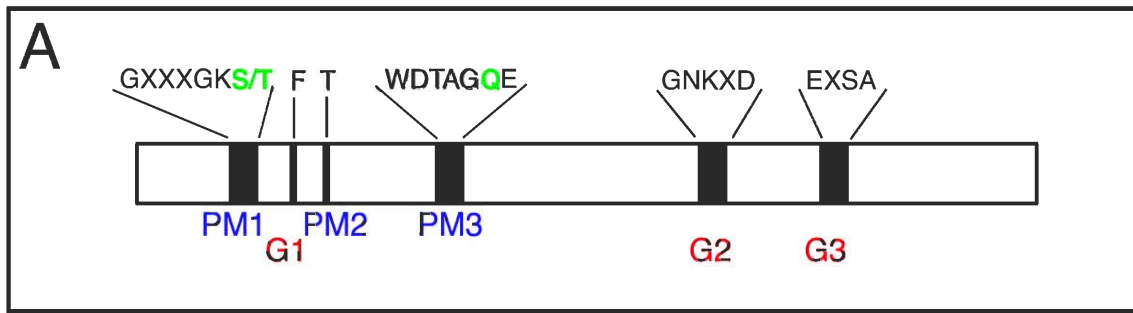


Fig. 3. Rab GTPases. (A) Linear representation of the Rab GTPase structure (modified from Olkkonen, 1997). The conserved residues involved in nucleotide binding and hydrolysis are indicated in black. The residues mutated in the dominant active and dominant negative versions are indicated in green. PM1-3 (blue) represents the phosphate/Mg²⁺-binding motifs and G1-3 (red) the guanine base-binding motifs. The highly conserved amino acid residues (in one-letter code) in these motifs are shown above the diagram. (B) Early endosome visualized by freeze-etch electron microscopy (from Gruenberg, 2001). The endosome contains a gold-labeled fluid-phase marker (white spots) internalized for 5 min. (C) Schematic illustration of the Rab5 domain at the early endosome (from Zerial, 2001). The Rab5 domain at the early endosome is, according to a model, designed to generate a local enrichment of active, GTP-bound Rab5 through positive feedback-loops. Rab5-GTP (T) undergoes continuous cycles of GTP hydrolysis (Rab5-GDP is shown as D), catalyzed by RN-Tre, a newly identified Rab-GAP (GTPase activating protein), and nucleotide exchange. The Rabaptin-5/Rabex-5 complex activates Rab5 through the nucleotide exchange activity of Rabex-5 and gets recruited to the endosomal membrane through Rabaptin-5. Active Rab5 interacts with PI(3)-kinases (PI(3)K) coupling phosphatidyl-inositol-3-phosphate (PtdIns(3)P) production to Rab5-GTP localization. The presence of Rab5-GTP and PtdIns(3)P allows the recruitment of FYVE-domain containing Rab5 effectors such as the early endosomal antigen 1 (EEA1) and Rabenosyn-5. In addition, molecular links between distinct Rab5 effectors and the SNARE machinery have been described, e.g. VPS45 that has been implicated in SNARE pairing.

Rab Proteins in the endocytic pathway

The endocytic pathway mediates recycling and degradation of endocytosed molecules. The endocytic pathway is composed of several biochemically and morphologically distinct stations, (Hubbard, 1989; Rodman *et al.*, 1990) including early sorting endosomes, recycling endosomes, late endosomes and lysosomes (Fig. 2). Membrane traffic between these compartments is mediated by different proteins of the Rab family, in particular by Rab5, Rab4, Rab11 and Rab7.

The first step along the endocytic pathway is the formation of endocytic vesicles by clathrin-mediated endocytosis (see above). Endocytic vesicles subsequently fuse to the first station within the endocytic pathway, the early sorting endosome. The early sorting endosome is a complex and dynamic membrane system (Fig. 3B) in which endocytosed components are sorted to their different destinations (Dunn *et al.*, 1989; Ghosh *et al.*, 1994; Gruenberg and Kreis, 1995; Gruenberg and Maxfield, 1995; Mellman, 1996).

Endocytosed components are directed from the early sorting endosome either into the degradative or into the recycling pathway. The degradative pathway leads to the late endosomes and lysosomes where degradation by acid hydrolases occurs (Gruenberg and Maxfield, 1995; Mellman, 1996). Other proteins such as the recycling receptors transferrin- or the LDL-receptor are recycled back to the PM (Dunn *et al.*, 1989; Ghosh and Maxfield, 1995). Two recycling routes are known. The fast recycling pathway, which leads from the early endosome directly back to the PM (Daro *et al.*, 1996; Mayor *et al.*, 1993; Schmid *et al.*, 1988; Sheff *et al.*, 1999; van der Sluijs *et al.*, 1992), whereas the second route involves another compartment the perinuclear recycling endosome (Hopkins, 1983; Prekeris *et al.*, 2000; Schlierf *et al.*, 2000; Ullrich *et al.*, 1996; Yamashiro *et al.*, 1984). More recently, a transport route that connects early endosomes and the TGN was discovered (Rohn *et al.*, 2000; Wilcke *et al.*, 2000).

Each trafficking step along the endocytic pathway is regulated by a different Rab protein (Chavrier *et al.*, 1990; Lombardi *et al.*, 1993; Olkkonen *et al.*, 1993; Ullrich *et al.*, 1996; van der Sluijs *et al.*, 1991). Rab5 mediates traffic from the PM to the early endosome (Bucci *et al.*, 1992), Rab7 the step from the early sorting endosome to the degradative compartment (Bucci *et al.*, 2000; Feng *et al.*, 1995; Méresse *et al.*, 1995; Vitelli *et al.*, 1997; Wichmann *et al.*, 1992) and Rab4 and Rab11 trafficking within the recycling pathway. In particular, Rab4 controls the fast recycling from the early endosome directly back to the PM (Daro *et al.*, 1996; Sheff *et al.*, 1999; van der Sluijs *et al.*, 1992), whereas Rab11 recycling through the recycling endosome (Prekeris *et al.*, 2000; Schlierf *et al.*, 2000; Ullrich *et al.*, 1996). In the steady state, these Rab proteins are localized to their target compartments and have thereby been used as markers for the different endocytic compartments. Both Rab5 (Bucci *et al.*, 1992; Chavrier *et al.*, 1991) and Rab4 (van der Sluijs *et al.*, 1991) are associated to early sorting endosomes. Rab7 serves as a marker for the degradative compartment (Chavrier *et al.*, 1990) and Rab 11 is localized to the recycling endosome (Ullrich *et al.*, 1996).

The early endosome and Rab5

The early endosome is the primary sorting station in the endocytic pathway (Ghosh and Maxfield, 1995; Gruenberg and Kreis, 1995; Gruenberg and Maxfield, 1995; Mellman, 1996) and the small GTPase Rab5 has been used as an early endosomal marker (Bucci *et al.*, 1992; Chavrier *et al.*, 1991). Rab5 regulates the first step of the endocytic pathway between the PM and the early sorting endosome. Thus, Rab5 has been implicated in the formation of clathrin-coated endocytic vesicles at the PM (McLauchlan *et al.*, 1998) as well as in the fusion of endocytic vesicles with the early endosome (“heterotypic fusion”) (Bucci *et al.*, 1992). In addition, Rab5 regulates in a rate-limiting manner the “homotypic fusion” between early endosomes (Barbieri *et al.*, 1994; Gorvel *et al.*, 1991; Li *et al.*, 1994; Roberts *et al.*, 1999; Rybin *et al.*, 1996). Furthermore, it mediates attachment to, and motility of early endosomes towards the minus

end of microtubules and thereby the distribution of early endosome within the cell (Nielsen *et al.*, 1999).

Three Rab5 isoforms have been identified in mammals, Rab5a, Rab5b, Rab5c (Bucci *et al.*, 1995) and in yeast (Novick and Zerial, 1997), whereas only one isoform is present in *C. elegans* (Grant and Hirsh, 1999). Rab5 function requires the interaction with specific effector molecules. Using affinity-chromatography more than 20 proteins have been purified from bovine brain, which directly or indirectly interact specifically with the GTP-bound, active form of Rab5 (Christoforidis *et al.*, 1999b). They include Rabaptin-5 (Stenmark *et al.*, 1995), Rabex-5 (Horiuchi *et al.*, 1997), Rabaptin-5b (Gournier *et al.*, 1998), EEA1 (Christoforidis *et al.*, 1999a) and Rabenosyn-5 (Nielsen *et al.*, 2000).

The Rab5 domain at the early endosome

The early endosome is composed of at least two functionally different subdomains, visualized by the distinct localization of the two Rab proteins Rab4 and Rab5 (De Renzis *et al.*, 2002; Sonnichsen *et al.*, 2000). Endocytic vesicles fuse to the endosome at the Rab5 domain, while components destined for the fast recycling back to the PM are sorted in the Rab4 domain. Two effector proteins, Rabaptin-5 (Vitale *et al.*, 1998) and Rabenosyn-5 (De Renzis *et al.*, 2002) have been shown to bind both Rab5 and Rab4. It has therefore been proposed that these divalent Rab effectors control the sub-compartmental organization of early endosomes. They might connect the Rab5 and Rab4 domains and thereby regulate protein sorting and recycling.

The Rab5 domain is known to be required for the specificity of vesicle tethering/docking. The Rab5 domain is enriched in activated, GTP-bound Rab5, several different Rab5 effector proteins as well as the lipid phosphatidylinositol-3-phosphate (PI(3)P) (Fig. 3C). The Rab5 effector proteins are recruited in a cooperative fashion to the Rab5 domain. First, Rab5 is delivered to the endosomal membrane complexed to GDI as described above. At the

membrane, a GDI displacement factor dissociates the Rab5-GDI complex releasing GDI into the cytosol (Ayad *et al.*, 1997; Dirac-Svejstrup *et al.*, 1997).

Subsequently, Rab5 is activated by a complex composed of Rabaptin-5 and Rabex-5 (Horiuchi *et al.*, 1997; Lippe *et al.*, 2001). Rabex-5 acts as a specialized Rab5-GEF, catalyzing the exchange of GDP against GTP (Horiuchi *et al.*, 1997). Rabaptin-5, which was identified as the first Rab5 effector in a two-hybrid screen (Stenmark *et al.*, 1995), increases the activity of Rabex-5 on Rab5 (Lippe *et al.*, 2001). In addition, Rabaptin-5 stabilizes Rab5 in its active, GTP-bound form by down-regulating GTP-hydrolysis, (Rybin *et al.*, 1996). Furthermore, as the C-terminal domain of Rabaptin-5 binds active Rab5 (Vitale *et al.*, 1998), activation of Rab5 at the endosomal membrane starts a positive feedback mechanism: Rabaptin-5 binds and stabilizes active Rab5 at the endosome and recruits Rabex-5, which in turn generates more active Rab5.

Active Rab5 directly recruits two PI(3)-kinases (Christoforidis *et al.*, 1999b) and PI(3)-kinase activity in turn is required for efficient endosome fusion (Jones and Clague, 1995; Li *et al.*, 1995b; Spiro *et al.*, 1996). The PI(3)-kinase p85 α /p110 β is a type I kinase that mainly phosphorylates phosphatidylinositol-4-phosphate (PI(4)P) and PI(4,5)P₂ generating phosphatidylinositol-3,4,5-trisphosphate (PI(3,4,5)P₃). This enzyme has been also implicated in signal transduction pathways (Vanhaesebroeck *et al.*, 1997). The other PI(3)-kinase is hVPS34/p150 the mammalian homolog of the yeast Vps34p/Vps15 (Volinia *et al.*, 1995). It preferentially phosphorylates PI to PI(3)P. In summary, active Rab5 recruits PI(3)-kinases to the early endosome generating a domain enriched in PI(3)P (Christoforidis *et al.*, 1999b). Several Rab5 effector proteins specifically bind PI(3)P through their FYVE protein domain (Gaullier *et al.*, 2000; Lawe *et al.*, 2000; Nielsen *et al.*, 2000; Raiborg *et al.*, 2001b; Stenmark *et al.*, 1996).

FYVE domain and FYVE domain containing Rab5 effectors

The FYVE domain is a zinc finger domain that coordinates two Zn^{2+} ions and specifically binds PI(3)P (Burd and Emr, 1998; Gaullier *et al.*, 1998; Lawe *et al.*, 2000; Patki *et al.*, 1998; Stenmark and Aasland, 1999). It was named after the first proteins shown to contain it, namely Fab1, YOTB/ZK632.12, Vac1 and EEA1 (Stenmark *et al.*, 1996). Later, a tandem repeat of the FYVE domain of Hrs (hepatocyte growth factor-regulated tyrosine kinase substrate) called 2xFYVE^{Hrs} was shown to specifically localize to the early endosome (Gillooly *et al.*, 2000). The 2xFYVE domain can therefore be used as an independent marker for the early endosome.

The best-studied FYVE-containing effector protein of Rab5 is EEA1. It has been originally identified as an early endosomal antigen, hence the name, in a patient with a subacute form of lupus erythematosus (Mu *et al.*, 1995). The specific targeting of EEA1 to the endosomal membrane (Rubino *et al.*, 2000) is mediated via the cooperative binding of its C-terminal FYVE- and Rab5-binding domains (Gaullier *et al.*, 2000; Gaullier *et al.*, 1998; Simonsen *et al.*, 1998; Stenmark *et al.*, 1996). EEA1 is absent from CCVs and the PM (Mu *et al.*, 1995; Nielsen *et al.*, 2000; Wilson *et al.*, 2000), because they do not contain PI(3)P. EEA1 may therefore provide directionality for the transport from the PM to the early endosome. At the endosomal membrane, EEA1 is found in large oligomeric structures, complexed with Rabaptin-5, Rabex-5 and NSF (McBride *et al.*, 1999). EEA1 has been implicated in the tethering/docking of endocytic vesicles at the endosome (Christoforidis *et al.*, 1999a). In addition, it interacts with Syntaxin 13 (McBride *et al.*, 1999), the t-SNARE involved in endosome fusion. EEA1 could therefore connect tethering/docking with the final event of membrane fusion mediated by the SNARE proteins.

Rabenosyn-5, another FYVE-containing Rab5 effector protein that is specifically localized to the early endosome, interacts indirectly with the SNARE complex (Nielsen *et al.*, 2000; Wilson *et al.*, 2000). Hrs has been shown to be targeted to the endosome via its FYVE and coiled-coil domains (Raiborg *et al.*, 2001b). In

addition, Hrs binds directly to Clathrin. It has thereby been suggested to play a role in Clathrin recruitment to early endosomes and to be involved in trafficking from early to late endosomes (Raiborg *et al.*, 2001a).

In summary, the early endosome contains a highly specialized Rab5-domain, enriched in activated Rab5, PI(3)P and Rab5 effector molecules. This domain regulates the fusion of endocytic vesicles with the early endosome.

SV recycling in neurons

In contrast to the well-established endocytic pathway in cultured mammalian cells, little is known about how neurons regenerate their SVs. Two main recycling pathways, “kiss-and-run” and clathrin-mediated endocytosis have been proposed and might act in parallel. However, the precise intracellular steps in SV recycling are unknown. It has been suggested that fully equipped SVs are directly regenerated at the PM after clathrin-mediated endocytosis (De Camilli and Takei, 1996; Takei *et al.*, 1996). Alternatively, internalized endocytic vesicles could fuse to an endosomal compartment from which SVs are subsequently regenerated. Tubules and cisternae, i.e. organelles with morphological features of endosomes have been suggested to be involved as intermediates of SV recycling, at least after strong stimulation (Heuser and Reese, 1973; Holtzman *et al.*, 1971). In addition, endosomal structures have been described in the presynaptic terminal of different cultured neurons (Parton *et al.*, 1992; Sulzer and Holtzman, 1989; Teichberg and Holtzman, 1975).

In neuroendocrine PC12 cells, different endosomal subcompartments have been observed using endocytic tracers and immunoelectron microscopy (de Wit *et al.*, 1999). In addition, synaptic-like microvesicles (SLMVs) have been shown to bud from sorting endosomes in PC12 cells (de Wit *et al.*, 1999). Furthermore, a population of vesicles, in size and protein composition distinct from SVs, has been characterized biochemically in PC12 cells (Provoda *et al.*, 2000). The authors suggested that these vesicles correspond to primary endocytic vesicles, delivering SV proteins to the endosome. However, since PC12 cells are not

comparable to differentiated neurons, these structures might rather correspond to the conventional endosomal pathway of cultured mammalian cells than to the SV recycling route of differentiated neurons.

Endosomal trafficking during SV recycling in neurons has been suggested in a study in which Rab5 was found on a subpopulation of SVs isolated from rat brain (Fischer von Mollard *et al.*, 1994). Therefore, the same mechanisms and endosomal compartments as in cultured cells could possibly be involved during SV recycling in neurons, with Rab5 regulating membrane influx into an endosomal compartment. Recently, the AP-3 adaptor protein complex has been implicated in vesicle budding from the endosome because AP-3 specifically binds to SVs purified from rat brain and to SLMVs from PC12 cells (Faundez *et al.*, 1998). Furthermore, the neuron-specific isoform of the AP-3 complex specifically binds to purified SLMVs and is required for SLMV-formation from PC12 cell endosomes (Blumstein *et al.*, 2001), suggesting that SV recycling involves an intermediate endosomal compartment.

In contrast, SV recycling experiments in cultured hippocampal neurons suggested that the SV membrane does not mix with an intracellular compartment, arguing against SV recycling through endosomes (Murthy and Stevens, 1998). However, it is not known whether SV membrane would mix with the membrane of an intracellular compartment after fusing to it. Alternatively, the SV membrane could travel through intracellular compartments as an intact structure similar to membrane rafts (Ikonen, 2001). Furthermore, synapses of hippocampal neurons are less than 1 μm in diameter and intracellular compartments may therefore be rather small. In addition, the association between SV membrane and compartment membrane may be transient and thereby limiting the degree of membrane mixing. Finally, SV fusion to an intermediate compartment may not be an obligatory step during the recycling process or may occur only under certain conditions. Together, the pathway of SV recycling in neurons is therefore still controversial.

Model systems

Synaptic function is studied in several different model systems. They include large synapses such as the lamprey reticulospinal synapse, the Calyx of Held in the mammalian auditory system or NMJs of frog and fly as well as rather small central synapses in brain slices or in primary cell cultures. This work was performed using the NMJ of *Drosophila melanogaster* third instar larvae. The fruit fly *Drosophila melanogaster* has been used as a model organism for research for almost a century because it is small, cheap, and easy to be kept in large numbers and has a short life cycle of around 10 days. *D. melanogaster* was originally used as a model organism in genetics by Thomas Hunt Morgan, who discovered in 1910 the first spontaneous mutants, with white eye color. Using *Drosophila* genetics, he also developed the chromosome theory of heredity for which he got the Nobel Prize in 1933.

Later, the fruit fly served to study the development from an egg cell into a multicellular organism. In the 80s, Christiane Nüsslein-Volhard and Eric Wieschaus performed a systematic genome-wide mutational screen in *Drosophila* and discovered genes controlling early embryonic development (Nüsslein-Volhard and Wieschaus, 1980). Still today, *Drosophila* is one of the most attractive model organisms. A large collection of mutants in any of several thousand genes is available and large-scale genetic screens can be performed to identify genes of unknown function. In addition, the genome can be easily manipulated by standard genetic techniques including P-element-mediated germ-line transformation (Rubin and Spradling, 1982; Spradling and Rubin, 1982). Enhancer traps can be used to screen for genes based on their pattern of expression (O'Kane and Gehring, 1987) and site-specific recombination can be induced to generate chromosomal rearrangements (Golic and Lindquist, 1989). Furthermore, the UAS/GAL4 technique allows to efficiently inactivate known genes and to ectopically express target genes (Brand and Perrimon, 1993). Proteins can thereby be overexpressed, dominant negative, gain of function or GFP-tagged versions of certain proteins can be expressed under the control of tissue-specific promoters. Balancer chromosomes, which are

chromosomes bearing inversions allow the stable maintenance of lethal mutations as heterozygotes without the need of selection. Double stranded RNA interference has also emerged as a powerful tool for silencing gene function (Brown *et al.*, 1999; Carthew, 2001; Hunter, 1999; Kalidas and Smith, 2002; Schmid *et al.*, 2002).

In March 2000, the entire *Drosophila* genome was sequenced and estimated to contain only around 14.000 genes (Adams *et al.*, 2000). A new annotation of the *Drosophila* genome raises this number to around 20.000 genes (The Heidelberg consortium, unpublished). Therefore, the fly has a relatively small genome size. For comparison, the genome of the unicellular yeast *Saccharomyces cerevisiae* has already half the size of the *Drosophila* genome. Nevertheless, many basic cellular functions and processes are highly conserved from flies to mammals. Consistently, most mammalian proteins have well conserved homologues in *Drosophila*, e.g. 60% of the known human disease-causing genes were found in *D. melanogaster*.

The Drosophila neuromuscular junction

The larval NMJ of *Drosophila melanogaster* has emerged as a powerful model system to investigate the physiological significance of molecules involved in synaptic development and synaptic function (Keshishian *et al.*, 1996). Since many of the molecules involved in synaptic transmission are conserved between *Drosophila* and vertebrates, it is assumed that the basic function of vertebrate and *Drosophila* synapses is identical. The larval dissection is straightforward, the synapses are large (around 5 µm in diameter) and therefore well accessible for various techniques such as laser-scanning confocal microscopy and imaging including the use of fluorescent dyes. In addition, the preparation is an established model system for conventional transmission electron microscopy as well as for standard electrophysiological studies.

A major advantage of the *Drosophila* NMJ is that it is composed of a relatively small number of muscles and motoneurons each of which is uniquely

identifiable (Fig. 4, 5). The body wall musculature is well characterized and organized in a stereotyped and segmentally repeated pattern of multinucleated muscle cells (Fig. 4). Each abdominal (A) hemisegment from A2 to A7 contains a fixed set of 30 uniquely identifiable muscle fibers (Fig. 4) (Anderson *et al.*, 1988; Campos-Ortega and Hartenstein, 1997; Crossley, 1978). The pattern in A1 is slightly different, and there are other specialized muscles in the more anterior and posterior segments. Each muscle fiber has a characteristic position, orientation, morphology, size, body wall insertion site, expression pattern of molecular markers and innervation pattern (Bate, 1990; Budnik *et al.*, 1990; Campos-Ortega and Hartenstein, 1997; Chiba *et al.*, 1993; Johansen *et al.*, 1989a; Johansen *et al.*, 1989b; Keshishian *et al.*, 1996; Schmid *et al.*, 1999). According to the nomenclature of Bate (Bate, 1993), the muscles in the segments A2 to A7 are divided into dorsal (D), lateral (L) and ventral (V) muscles and based on their orientation into longitudinal muscles (muscles oriented in an anterior-posterior direction), “acute” muscles (from ventral-anterior to dorsal-posterior) or “oblique” muscles (from dorsal-anterior to ventral-posterior). Furthermore, the somatic muscles are organized into three layers, the internal, intermediate and external layer (Fig. 4). A different nomenclature simply numbers the muscles (Anderson *et al.*, 1988).

All larval and adult muscle cells derive from a group of ventral blastoderm cells that invaginate during embryonic gastrulation to form an internal layer of the mesoderm (Bate, 1993). In *Drosophila*, the muscle development precedes the differentiation of the central nervous system (CNS) (Broadie and Bate, 1993c; Halpern *et al.*, 1991; Johansen *et al.*, 1989a; Johansen *et al.*, 1989b; Sink and Whitington, 1991a; Sink and Whitington, 1991b; Sink and Whitington, 1991c). Consequently, innervation plays no role in the muscle patterning of the embryo (Bate, 1990; Broadie and Bate, 1993b; Johansen *et al.*, 1989b) and muscle differentiation proceeds normally in the absence of innervation (Broadie and Bate, 1993a). However, later stages of NMJ development require interactions between motoneurons and muscles (Broadie and Bate, 1993a; Broadie and

Bate, 1993c; Guan *et al.*, 1996; Keshishian *et al.*, 1996; Keshishian *et al.*, 1993; Petersen *et al.*, 1997; Prokop *et al.*, 1996; Saitoe *et al.*, 1997).

The somatic musculature is innervated by motoneuron axons that are grouped into six major nerve branches: ISN (intersegmental nerve branch), SNa (segmental nerve branch a), SNb (segmental nerve branch b), SNc (segmental nerve branch c), SNd (segmental nerve branch d) and TN (transverse nerve) (Fig. 5). Motoneurons derive from neuroblasts in the neuroectoderm. Their cell bodies are located within the CNS and they project in a stereotypic manner to the muscle fibers, generating a precise and invariant innervation pattern (Broadie and Bate, 1993c; Halpern *et al.*, 1991; Sink and Whittington, 1991b; Sink and Whittington, 1991c). Approximately 40 motoneurons innervate the 30 muscle fibers in each abdominal hemisegment. Each hemisegment is innervated by motoneurons from both its own and from the next anterior CNS segment, with cell bodies of the motoneurons located on both, the ipsi- and the contralateral sides. However there is no organized motoneuron topography in the CNS with respect to the locations of the innervated muscles (Sink and Whittington, 1991b).

Each motoneuron can be identified based on its specific contacts on particular target muscles, the degree of terminal branching, the bouton morphology and the cotransmitters (Johansen *et al.*, 1989b). The entire motoneuron population uses glutamate as the excitatory neurotransmitter, which is as well the main excitatory neurotransmitter in the vertebrate brain (Jan and Jan, 1976b; Johansen *et al.*, 1989a; Johansen *et al.*, 1989b). Different motoneuron subsets express cotransmitters including octopamine (Monastirioti *et al.*, 1995) and the peptide neurotransmitters proctolin (Anderson *et al.*, 1988), insulin-like peptide (Gorczyca *et al.*, 1993) and leukokinin I-like peptide (Cantera and Nassel, 1992).

The *Drosophila* body wall muscle fibers are polyinnervated (Atwood *et al.*, 1993; Budnik and Gorczyca, 1992; Jan and Jan, 1976a; Jan and Jan, 1976b; Jia *et al.*, 1993; Johansen *et al.*, 1989a; Kurdyak *et al.*, 1994). Some motoneurons

innervate only a single muscle fiber, whereas others project to muscle fiber pairs or even to larger subsets of the body wall muscles (Halpern *et al.*, 1991; Keshishian *et al.*, 1993; Sink and Whitington, 1991b). The axon endings can be divided into 3 morphologically defined classes (reviewed in (Budnik, 1996)). Type I boutons typically project onto one or two muscle fibers and innervate all body wall muscles (Johansen *et al.*, 1989a). The boutons are round in shape and enclosed by a prominent subsynaptic reticulum (SSR), a postsynaptic specialization made by the highly folded sarcolemma (Atwood *et al.*, 1993; Jia *et al.*, 1993). Type I boutons are filled with SVs that contain glutamate (Atwood *et al.*, 1993; Jia *et al.*, 1993) and may in addition contain vesicles with peptide cotransmitters (Atwood *et al.*, 1993; Jia *et al.*, 1993). The active zones of type I boutons are characterized by the presence of electron dense T-bars, where SVs are morphologically docked (Atwood *et al.*, 1993; Jia *et al.*, 1993). Type I boutons are further subdivided according to their size into I big (Ib) and I small (Is) (Atwood *et al.*, 1993; Budnik, 1996). Type Ib boutons are 3 to 6 μm in diameter, whereas type Is boutons are 2 to 4 μm in diameter. In addition, type Is boutons contain less SVs and are surrounded by a less developed SSR than type Ib boutons.

Only two motoneurons per hemisegment form type II boutons. However, these two motoneurons innervate as many as 24 muscles per hemisegment (Budnik and Gorczyca, 1992; Monastirioti *et al.*, 1995). Type II boutons are the smallest, with a diameter of 1 to 2 μm , but the most numerous bouton type. Type II boutons are formed from a thin axonal process, and extend over nearly the entire length of the muscle (Johansen *et al.*, 1989a). They are localized in grooves on the muscle surface, with little or no surrounding SSR (Jia *et al.*, 1993). Type II boutons are filled with glutamate containing SVs and with peptide containing dense-core vesicles (Gorczyca *et al.*, 1993; Jia *et al.*, 1993).

Type III boutons innervate only one muscle, VL1 (Gorczyca *et al.*, 1993; Hoang and Chiba, 2001). The boutons are elongated and have an intermediate size. Similar to type II endings, they have a superficial localization and almost completely lack SSR (Jia *et al.*, 1993). Type III boutons are mostly filled with

insulin-like peptide containing large dense-core vesicles and only few small translucent vesicles (Gorczyca *et al.*, 1993; Jia *et al.*, 1993).

Most studies focus on the NMJ of the ventral longitudinal abdominal muscles VL3 (muscle 6) and VL4 (muscle 7) (see Fig. 4). They are innervated by two glutamatergic motoneurons called MNSNb/d-Is (RP3) and MN6/7b-Ib, or axon 1 and axon 2 respectively (Hoang and Chiba, 2001; Lnenicka and Keshishian, 2000). The single motoneuron axon of MN6/7b-Ib innervates the cleft between muscle 6 and 7 and forms all of the type Ib boutons at this NMJ. In contrast, MNSNb/d-Is is a multi-innervating motoneuron, innervating muscle 6 and 7 and in addition 6 other ventral muscles. MNSNb/d-Is forms type Is boutons (Atwood *et al.*, 1993).

Electrophysiological studies are usually performed on muscle 6, because of its prominent size and positioning in the internal muscle layer, which makes it well accessible to recording electrodes. As described above muscle 6 is innervated by two glutamatergic motoneurons, MNSNb/d-Is (RP3) and MN6/7b-Ib causing a compound excitatory junction potential (EJP).

In this study the *Drosophila* NMJ of third instar larvae was used as a model system to investigate the recycling pathway of SVs. Particularly, the questions of whether the presynaptic terminal contains endosomal compartments and if they are involved in the process of SV recycling were addressed. *First*, endosomal markers were used to visualize endosomes at the presynaptic terminal of the larval NMJ. *Second*, it was addressed whether SVs traffic through the endosome. SV recycling through the endosome was studied using the thermosensitive Dynamin mutant *shibire^{ts}* to specifically block clathrin-mediated endocytosis, uncoupling endo- from exocytosis. *Third*, the role of the small GTPase Rab5 during endocytic trafficking and SV recycling was analyzed using loss of function, dominant negative and gain of function mutants of Rab5. The effects of interfering with Rab5 function were analyzed using laser-

scanning confocal microscopy as well as at the ultrastructural level. *Fourth*, the function of endosomal trafficking during synaptic transmission was studied by performing FM1-43 dye recycling experiments and standard electrophysiological recordings on the mutant NMJs.

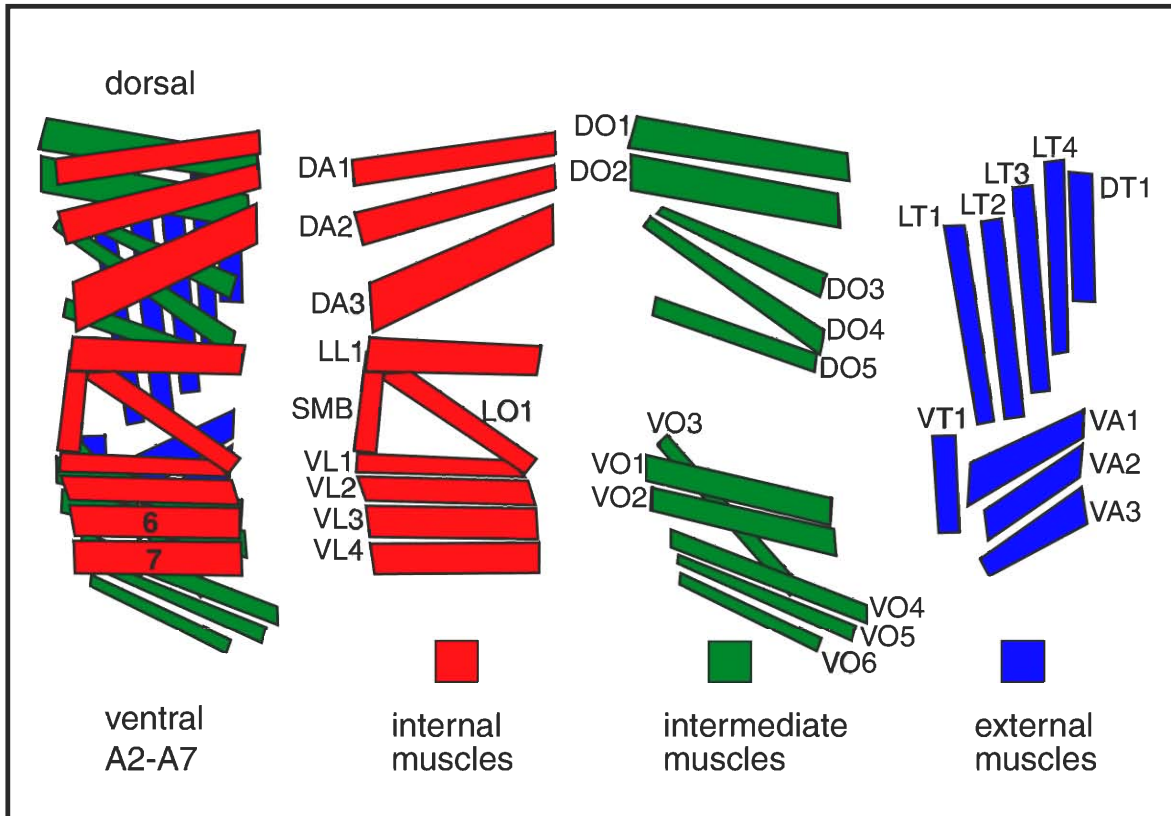


Fig. 4. Schematic representation of the larval somatic musculature. Shown is the stereotypic muscle pattern of a single abdominal hemisegment A2 - A7. The muscles are organized into an internal (red), an intermediate (green) and an external layer (blue). Left panel, overlay of the three layers. Anterior is left, posterior is right, dorsal is up and ventral is down. Each muscle is characterized by its position, orientation, size and body wall insertion site. Nomenclature according to Bate (Bate, 1993). Abbreviations: DA, dorsal-"acute"; DO, dorsal-"oblique"; DT, dorsal-transversal; LL, lateral-longitudinal; LO, longitudinal-"oblique"; LT, lateral-transversal; VA, ventral-"acute"; VO, ventral-"oblique"; VL, ventral-longitudinal; VT; ventral-transversal; SMB, segment border muscle. Numbers in the left panel indicate the two ventral-longitudinal muscles most studies focus on. According to the nomenclature of Anderson (Anderson, 1988) they are referred to as muscle 6 and muscle 7.

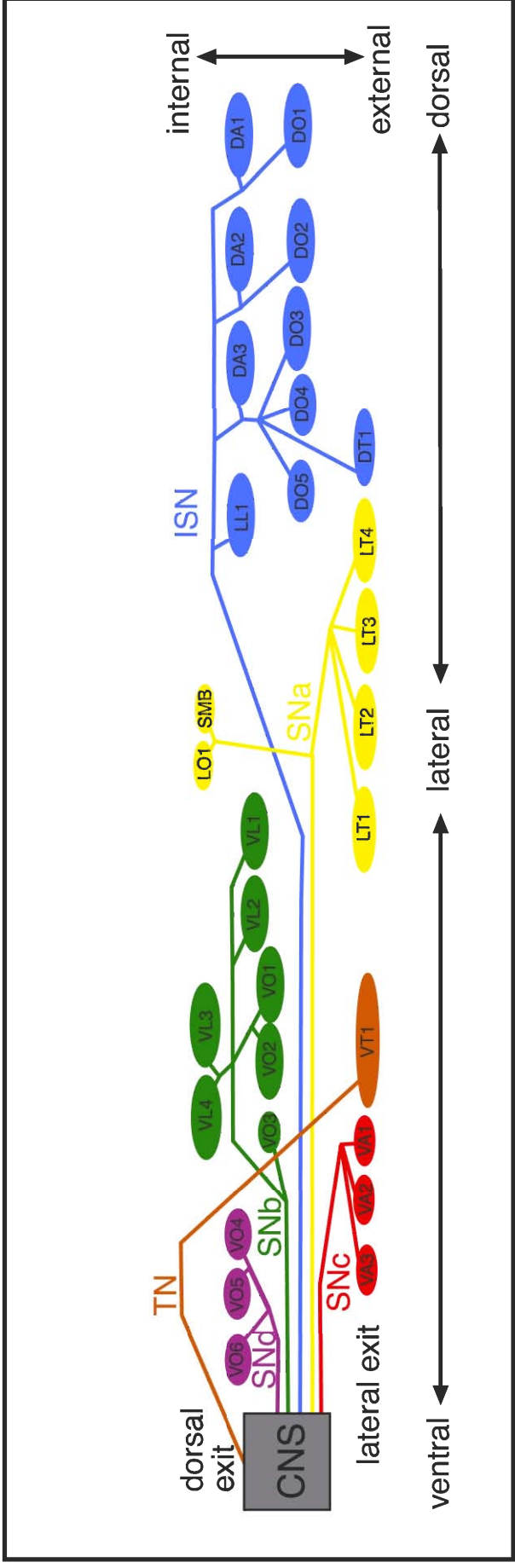


Fig. 5. Schematic representation of the motoneuron projections and target muscles in the *Drosophila* larva in a cross-section through an abdominal segment (A2 - A7). Each major nerve branch is shown in a different colour as it exits the central nervous system (CNS). The target muscles are shown in the same colour. Muscle names are indicated inside the cell bodies. The inter-segmental nerve (ISN, in blue) projects mainly to dorsal muscles (to LL1, DA3, DA2, DA1, DO5, DO4, DO3, DO2, DO1, DT1). The segmental nerve a (SNa, yellow) projects mainly to lateral muscles (to LO1, SMB, LT1, LT2, LT3 and LT4). The SNb (in green) projects mainly to ventral lateral muscles (to VL4, VL3, VL2, VL1, VO1, VO2 and VO3). Nerve branches SNC and SNa (in red and purple, respectively) innervate ventral muscles (VA1, VA2, VA3, VO4, VO5 and VO6). The transverse nerve (TN, in orange) innervates VT1.

Methods

Transgene Expression

Fly stocks were raised on standard cornmeal food under non-crowded conditions. Transgene expression specifically in the nervous system was driven with elav-GAL4 (Lin and Goodman, 1994) using the UAS/GAL4 technique (Brand and Perrimon, 1993). To manipulate the levels of transgene expression we took advantage of the thermosensitivity of GAL4 (Brand and Perrimon, 1993; Entchev *et al.*, 2000). Embryonic and early larval development took place at 16°C to achieve low expression levels during the development. Animals were shifted to 25°C only during the last two days of larval development to increase levels of transgene expression (“25°C protocol”). When 29°C is indicated, the last two days of larval development were at this temperature (“29°C protocol”). In some experiments, the whole development until the third larval stage took place at 16°C (“16°C protocol”). The controls were submitted to the same procedure. Levels of Rab5 expression controlled using the “25°C protocol” represented around 5 fold the levels of endogenous Rab5 as estimated in Western blots using third instar larval CNS extracts. Oregon-R was used as the wildtype strain. Transgene expression in all somatic muscles was performed with the GAL4 enhancer-trap line 24B-GAL4 (flybase), (Baylies and Bate, 1996).

Molecular analysis and mutant strains

The exon/intron organization of Rab5 (Accession number AY081179) was based on 11 cDNAs as well as on genomic sequence information from the Berkeley *Drosophila* Genome Project (BDGP). We sequenced 2 cDNAs, GM02432 and LD03788 (Accession numbers AY081180, AY081181), and used 5' and 3' sequence information from BDGP for 9 other cDNAs (LD39028, GH28628, GH22603, LD05288, LD22469, GH26712, GH21777, GH15713, and GH28615). Alternative splicing generates two major Rab5 mRNA size classes of around 1.0 and 1.8 kb, consistent with two bands in Northern blot

experiments using the open reading frame (ORF) as a probe (Rocio Fernández de la Fuente, personal communication). The genes flanking Rab5 are a zinc finger transcription factor (CG4272) and a Heparansulphate proteoglycan (CG7245) (Fig. 11A). One of the Rab5 splicing forms overlaps by 28 bp with the 5' end of the CG4272 transcript (Fig. 11A).

shibire^{ts1}, *UAS-DRab5* and *UAS-DRab5S43N* have been previously described (Entchev *et al.*, 2000). In *UAS-GFP-Rab5*, EGFP was cloned N-terminal to the ORF of *Drosophila* Rab5 (DRab5). In the chimera, GFP remains attached to Rab5 as shown by colocalization of anti-DRab5 and anti-GFP antibodies in NMJs expressing GFP-Rab5. *UAS-GFP-Rab5S43N* was generated by *in vitro* mutagenesis. The *myc-2xFYVE* sequence was PCR cloned from pGEM-myc-2xFYVE^{Hrs} (Gillooly *et al.*, 2000) into pUAST. *GFP-myc-2xFYVE* is an N-terminal EGFP fusion to the same *myc-2xFYVE* chimera. The *P(w⁺)DRab5⁺* rescue construct was generated by PCR cloning of a genomic fragment amplified from a wildtype fly extract using primers from the 5' and 3' ends of the CG4272 and CG7245 flanking genes into the pCaSpeR4 vector, respectively.

Rab5¹ is a P-element lethal insertion from the Kiss collection, *P{lacw}Rab5^{K08232}*. If raised under "intensive care" conditions (Loewen *et al.*, 2001) very few *Rab5¹* larvae developed into adult flies, which display a flightless phenotype. *Rab5¹* homozygous adults are extremely poor fertile. *Rab5¹* phenotype and lethality were reverted by precise excision of the P-element. *Rab5²*, *Rab5³* and *Rab5⁴* were generated by imprecise excision of the P-element and their lesions determined by PCR cloning and sequencing of the Rab5 gene in the different mutants. *Rab5²* is a 4.0 kb deletion of Rab5. Although *Rab5²* also deletes parts of the 5' non-translated leader of CG4272, the lethality and phenotype of *Rab5²* are caused by loss of Rab5 function since both are rescued by *P(w⁺)DRab5⁺*, a rescue construct spanning Rab5 and excluding the two flanking genes (Fig. 11A). *Rab5³* is an 18+210 bp insertion of sequences from the left and right long terminal repeats (LTR) of the P-element, which remained after imprecise excision of the transposon. *Rab5⁴* is a 14 bp insertion of the right LTR of the P-element.

Larval body wall preparation

Preparation of the larval body wall was performed as described (Estes *et al.*, 1996) with some modifications. Wandering third instar larvae were picked from the food and dissected to expose body wall muscles and innervating motoneurons. For dissection, larvae were placed into a drop of ice-cold Ca^{2+} -free normal saline (Jan and Jan, 1976a) in a 35 mm diameter petridish covered with a thin layer of transparent sylgard resin (RTV 615A + RTV 615B, GE Bayer Silicones). The larval head and tail were pinned to the sylgard resin using insect pins (Fine Science Tools) the body was stretched and dissected open along the dorsal midline using a hypodermic needle (BD Microlance 3, Becton Dickinson). Subsequently, the preparation was pinned out flat to the sylgard resin and internal organs were removed to expose the body wall muscles and the innervating motoneurons. If required, brain and ventral nerve cord were carefully removed using micro-dissecting scissors (Fine Science Tools). Analyses were restricted to synapses of muscles 6 and 7 in abdominal segments 2 to 4 (A2 – A4). These synapses are formed by a pair of identified motoneurons and have been used extensively in studies of synapse structure and function (Littleton *et al.*, 1999; Pallanck and Ganetsky, 1999).

Anti-Drosophila Rab5 antibody

The rabbit anti-*Drosophila* Rab5 immune serum was generated by Eurogentec against a C-terminal peptide of *Drosophila* Rab5 with the following sequence: $\text{H}_2\text{N-TSIRPTGTETNRPTNN-CONH}_2$ (Rab5-peptide). The immune serum was affinity chromatography purified using the Rab5-peptide coupled to CNBr-activated Sepharose 4B (Amersham Pharmacia Biotech). 1 g Sepharose was first activated during 15 min with 200 ml of 1 mM HCl, washed once with coupling buffer (0.1 M NaHCO_3 , 0.5 M NaCl, pH 8.3) and incubated with 30 mg Rab5-peptide for 2 h at RT in order to couple the Rab5-peptide to the Sepharose (Rab5-Sepharose). Subsequently, the Rab5-Sepharose was washed with 20 ml coupling buffer. Remaining active groups were blocked with 15 ml blocking buffer (0.1 M Tris-HCl, pH 8.0) at 4°C ON. The Rab5-Sepharose

was then washed during 3 cycles using 20 ml washing buffer 1 (0.1 M Acetate, 0.5 M NaCl, pH 4.0) followed by 20 ml coupling buffer. Then, the Rab5-Sepharose was filled into a column and washed (1.5 ml/min) with 30 ml of 1) 10 mM Tris-HCl, pH 7.5; 2) 100 mM Glycine, pH 2.5; 3) 10 mM Tris-HCl, pH 8.8; 4) 100 mM Triethylamin, pH 11.5 and 5) 10 mM Tris-HCl, pH 7.5. Subsequently, the immune serum was diluted 1:10 with 10 mM Tris-HCl, pH 7.5 and was passed 3 times over the column (1 ml/min, at 4°C). Prior to the elution, the column was washed with 60 ml 10 mM Tris-HCl, pH 7.5 and 60 ml 10 mM Tris-HCl, 0.5 M NaCl, pH 7.5. Elution of the anti-DRab5 antibody was achieved with 30 ml of 100 mM Glycine, pH 2.5 and 30 ml of 100 mM Triethylamine, pH 11.5. This step was repeated twice. Eluates were immediately neutralized with 1 M Tris-HCl, pH 8.0. Finally, the elution buffer was exchanged against PBS containing protease inhibitor (Complete Mini, EDTA-free, protease inhibitor cocktail tablets, Boehringer) and the anti-DRab5 containing eluates were concentrated using centrifugal filter devices (Centriprep YM-10, Millipore) according to the manufacturers instructions. The antibody detected a single band of the expected size of 24 kDa in Western blot experiments using extracts of *Drosophila* whole larvae, larval CNSs or embryos. The antibody specificity was also tested by a peptide preincubation assay. The purified antibody was incubated with 100 µg/ml Rab5-peptide for 30 min at room temperature (RT) followed by a centrifugation for 10 min 13000 rpm. After this procedure, no Rab5 immunostaining was detected in GFP-Rab5 overexpressing NMJs. Preincubation with a control peptide did not affect the staining.

Immunohistochemistry

Immunofluorescence of third instar larvae NMJs was performed as described in (González-Gaitán and Jäckle, 1997) with some modifications. Larvae were dissected as described above and fixed in fresh 4% paraformaldehyde (PFA) in PEM (80 mM PIPES, 5 mM EGTA, 1 mM MgCl₂, pH 7.4) for 90 - 120 min at RT. The subsequent incubation steps were performed on a rocking platform. The preparation was first permeabilized in PEM containing 0.1% IGEPAL (Sigma) for 3x20 min at RT. The incubation with the primary antibodies was over night at

4°C, with the secondary antibodies for 2 h at RT. Antibodies were diluted in PEM containing 0.1% IGEPAL and 0.1% BSA (bovine serum albumin). Specimens were embedded in MOWIOL antifade embedding medium (Boehringer) and imaged on a Zeiss confocal microscope (LSM-510). Polyclonal primary and all secondary antibodies were preabsorbed using an excess of fixed *Drosophila* embryos prior to use in order to reduce the background. Antibody preabsorption was performed as follows: Antibodies were diluted 1:10 in BBT (10 mM Tris, 55 mM NaCl, 40 mM KCl, 7 mM MgCl₂, 5 mM CaCl₂, 20 mM glucose, 50 mM sucrose, 0.1% Tween 20, 0.1% BSA, pH 6.95) and were incubated at 4°C ON with 200 µl embryos.

Antibodies were used in the following concentrations: Mouse anti-Cystein string protein (CSP) 1:100 (Zinsmaier *et al.*, 1994), rabbit anti- α -Adaptin 1:50 (González-Gaitán and Jäckle, 1997), rabbit anti-Dynamin 1:100, mouse anti-Fasciclin II (1D4) 1:20 (Schuster *et al.*, 1996), mouse anti-nc82 1:100 (Heimbeck *et al.*, 1999) rabbit anti-HRP (Horseradish Peroxidase) 1:50 (Sigma), rabbit anti-DRab5 1:50 (see above). Corresponding secondary Alexa 546-, Alexa 488- or Cy5-conjugated antibodies were used 1:500 diluted (Molecular Probes). Immunofluorescence of embryos was performed exactly as described in (González-Gaitán and Jäckle, 1997). Antibody concentrations were used as described above.

Dextran uptake in Cell culture

Stable lines of *Drosophila* S2 cells containing GFP-Rab5 or GFP-myc-2xFYVE under the control of a metallothionine-inducible promotor were used. Cells were grown for approximately 24 h in 12 well plates in complete Schneider medium (GIBCO) (Schneider medium containing 10% fetal calf serum and 100 IU/ml Penicillin/Streptomycin). GFP-Rab5 or GFP-myc-2xFYVE expression was induced with 500 µM CuSO₄ for 15 – 20 h prior to the dextran internalization experiments. Dextran uptake was performed incubating the cells for 5 min at RT with 375 µl per well of 0.5 mM texas red dextran (3000 MW, lysine fixable, Molecular Probes) in complete Schneider medium. Subsequent washing steps

were performed on ice using ice-cold, complete Schneider medium and incubating 6x2 min, followed by the fixation in 4% PFA in PEM (see above) for 60 min at RT. Specimens were embedded in MOWIOL antifade medium (Boehringer) and imaged on a confocal microscope (TCS SP2, Leica).

Quantification of the NMJ size

For quantifications of the NMJ size only the NMJ of muscles 6/7 in the abdominal segment A2 was used. For the quantification of the active zones only synapses of the NMJ of muscles 6/7 in abdominal segments A2 – A4 were used. For the quantification of the number of boutons per muscle area, preparations were stained with the anti-CSP antibody (Zinsmaier *et al.*, 1994). Subsequently, 6 - 12 z-sections with a spacing of 1 μm were acquired per NMJ with a 40x objective. Individual images were projected using the 3D reconstruction feature of the MetaView software (Visitron Systems GmbH) in order to visualize all boutons from different focal planes. Individual boutons were counted at high magnification using NIH image software. Muscle length and width were measured using NIH software on images acquired with Normarski optics using a 10x objective. The total number of boutons was normalized to the combined rectangular surface area of muscles 6 and 7. For the quantification of the total synaptic area, projections of z-sections acquired after anti-CSP staining as described above were thresholded using the MetaView software. The thresholded area was measured. It corresponds to the total synaptic surface area. The synaptic surface area was subsequently normalized to the combined rectangular surface area of muscle 6 and 7. To quantify the number of active zones per bouton area, preparations were stained with mouse anti-nc82 to label active zones and with rabbit anti-Dynamin or rabbit anti- α -Adaptin to label the centers of endocytosis (González-Gaitán and Jäckle, 1997). Images of individual boutons were acquired with a 100x oil objective on a confocal microscope (LSM-510, Zeiss). Active zones labeled by the nc82 staining were counted on high magnifications and were normalized to the area of the presynaptic terminal determined using the NIH software.

genotype	synaptic area (μm^2)	muscle area ($\mu\text{m}^2 \times 10^4$)	# of boutons	bouton area (μm^2)	# of active zones
WT	356.2 \pm 15.0	8.1 \pm 0.27	102.8 \pm 3.9	28.2 \pm 1.5	24.8 \pm 1.2
<i>R5SN</i>	360.9 \pm 22.9	8.9 \pm 0.24	133.6 \pm 6.6	18.3 \pm 1.0	17.7 \pm 1.0
<i>R5</i>	303.4 \pm 7.9	7.7 \pm 0.23	109.7 \pm 3.9	22.0 \pm 1.1	20.5 \pm 1.0
<i>GFP-R5</i>	317.0 \pm 18.5	8.1 \pm 0.34	109.3 \pm 4.4	19.4 \pm 0.8	19.0 \pm 0.8

Table 1. Data of the NMJ quantification. Summarized are the raw data of wildtype (WT), *w; UAS-Rab5S43N/+; elav-Gal4/+ (R5SN)*, *w; UAS-Rab5/+; elav-Gal4/+ (R5)* and *w; elav-Gal4/UAS-GFP-Rab5 (GFP-R5)* determined as described above.

Western blotting

Western blot experiments were performed according to standard procedures (Towbin *et al.*, 1979). Third instar larvae were dissected in ice-cold Ca^{2+} -free normal saline. 5 CNSs, 3 whole animals or 100 embryos were homogenized in 120 μl HEMG buffer (25 mM HEPES-KOH, 0.1 mM EDTA, 12.5 mM MgCl_2 , 100 mM NaCl, 0.5% Triton X-100 10% glycerol) containing protease inhibitor (Complete Mini, EDTA-free, protease inhibitor cocktail tablets, Boehringer) using an Eppendorf pistill. For solubilization, homogenates were incubated for 30 min on ice, followed by a centrifugation at 13000 rpm for 10 min. The supernatant was MeOH precipitated by adding 1280 μl 100% MeOH incubating for 4 h or ON at -80°C . After centrifugation at 13000 rpm for 15 min proteins were redissolved in 1x sample buffer and boiled for 5 min. Samples were electrophoresed using a 15% SDS polyacrylamid gel (Laemmli, 1970) with the mini protean system (Bio-Rad). Transfer to a nitrocellulose membrane was performed using the Trans-Blot semi-dry system (Bio-Rad) and 25 mM Tris, 192 mM glycine, 20% MeOH, 0.1% SDS as transfer buffer according to Towbin (Towbin *et al.*, 1979). Subsequently, the blot was blocked for 1 h with 10% BSA in PBS (phosphate buffered saline) and incubated with anti-DRab5 (1:200) (see above), anti-GFP (1:200) (SantaCruz), anti-Tubulin (1:400) (Developmental Studies Hybridoma Bank) or anti-Actin antibody (1:200) (Sigma) and subsequently for 1.5 h with HRP-conjugated goat anti-rabbit (1:15000) (Dako) or goat anti-mouse (1:15000) (Jackson) secondary antibodies. The signal was

developed using the ECL+plus Western blot detection system (Amersham Pharmacia Biotech) according to the manufacturers instructions. For the quantifications, the image Gauge software was used (Fuji).

Electron microscopy

For electron microscopy, third instar larvae were dissected in normal saline (Jan and Jan, 1976a), pinned onto sylgard-coated petridishes and processed with some modifications as described (Wu *et al.*, 1998). Preparations were fixed in the pinned state for 15 - 30 min with 1% glutaraldehyde in 0.2 M phosphate buffer (pH 7.2). Then, they were transferred into Eppendorf tubes and washed shortly in 0.2 M phosphate buffer. Larvae were stained en bloc for 1 h at RT in 1% osmiumtetroxide in dH₂O and for 30 min in 2% uranyl acetate in dH₂O. After a short wash they were dehydrated for 5 min in 70% ethanol, 3x5 min in 100% ethanol, 2x3 min in propylene oxide, 30 min in a 1:3-mixture of propylene oxide with araldite and finally overnight in araldite (Serva).

Blocks of muscles 6, 7, 12, 13 were cut out using a razor blade splinter and were embedded for sectioning in araldite. 60 nm sections were cut with a Leica ultramicrotome transferred onto a carbon/formvar-coated slot grid (Plano), post-contrasted 20 min with 1% aqueous uranylacetate and 5 min with lead citrate in a Leica ultrastain and examined on a Phillips TEM.

Salines

Normal saline (Jan and Jan, 1976a) in mM: NaCl 130, KCl 5, HEPES 5, MgCl₂ 2, CaCl₂ 2, sucrose 36, pH 7.3. High K⁺ in mM: NaCl 80, KCl 60, HEPES 5, MgCl₂ 2, CaCl₂ 2, sucrose 36, pH 7.3. Haemolymph-like physiological saline (HL3) (Stewart *et al.*, 1994) in mM: NaCl 70, KCl 5, MgCl₂ 20, NaHCO₃ 10, Trehalose 5, Sucrose 115, HEPES 5, CaCl₂ 0.75 or 1.5, pH 7.2. For Ca²⁺-free normal saline or HL3 CaCl₂ was exchanged against MgCl₂.

Electrophysiology

Current clamp recordings were performed as previously described (Schuster *et al.*, 1996) with some modifications. Wandering third instar larvae were dissected in ice-cold, Ca²⁺-free HL3 (Stewart *et al.*, 1994). Brain and ventral nerve cord were carefully removed using micro-dissecting scissors (Fine Science Tools). Larval fillets were washed twice with fresh HL3 containing the Ca²⁺-concentration used for the subsequent electrophysiological recording. Intracellular recordings were performed at room temperature on muscle 6 in abdominal segments 2 – 4 (A2 – A4). Muscle cells were impaled using sharp microelectrodes (recording electrodes) pulled on a Flaming/Brown micropipette puller P-97 (Sutter Instruments) from filament-containing borosilicate glass with 1 mm outer diameter (OD) (Science Products). The recording electrodes were filled with 3 M KCl and had a resistance of 15 – 25 MΩ. To elicit excitatory junction potentials (EJPs) the appropriate segmental nerve was drawn into a fire-polished suction electrode pulled from filament-containing borosilicate glass with 1.5 mm OD. Stimulation electrodes were filled with extracellular saline. EJPs were evoked by a brief, 0.2 msec stimulation of the nerve with positive current applied using a stimulation-isolation unit A360 (World Precision Instruments). The stimulation strength necessary to recruit both motoneurons innervating muscle 6 was determined by gradually increasing the stimulus strength until the second threshold EJP was seen. Only recordings with resting membrane potentials of at least –60 mV and input resistances of at least 6 MΩ were used for data acquisition.

Voltage signals were amplified with a SEC-0.5L amplifier (npi), filtered at 2 kHz, digitized using a DIGIDATA1320A (Axon Instruments), recorded and analyzed with the Axograph Software (Axon Instruments). The mean EJP amplitude of a muscle was determined by averaging 30 single EJPs evoked at a low frequency of 0.5 Hz. The quantal content reflecting the number of vesicles fused to elicit a certain EJP was calculated by dividing the mean EJP amplitude of a certain muscle by the mean miniature EJP (mEJP) amplitude recorded in the same muscle. Correction for nonlinear summation was performed according to Martin

(Martin, 1955) using a reversal potential of +12 mV as described (Nishikawa and Kidokoro, 1995).

mEJPs were recorded for 1 min immediately after recording EJPs at 0.5 Hz. They were analyzed using the event detection feature of the Axograph Software. For comparison of the mEJPs between different mutant strains, mEJPs recorded in HL3 containing 0.75 mM Ca^{2+} were used. The groups were closely matched concerning their mean resting potentials (in mV: WT: 71.2 ± 1.5 ; *R5SN*: 66.3 ± 1.3 ; *R5*: 69.3 ± 1.8 ; *GFP-R5*: 68.1 ± 1.6 ; *GFP-R5(29°C)*: 67.9 ± 1.8) and mean input resistances (in $\text{M}\Omega$: WT: 7.3 ± 0.3 ; *R5SN*: 8.0 ± 0.5 ; *R5*: 7.6 ± 0.3 ; *GFP-R5*: 8.5 ± 0.5 ; *GFP-R5(29°C)*: 7.0 ± 0.3). Paired-pulse facilitation experiments were performed in HL3 containing 0.75 mM Ca^{2+} by delivering two paired stimuli with an interpulse interval of 20 ms. The paired pulses were repeated 20 times separated by 5 sec rests. To measure the amplitude of the second response the trace of the paired pulses was overlaid with the trace of the basal stimulation at 0.5 Hz of the same muscle. The quantal content of the first and second response was calculated as described above. The degree of facilitation was calculated by dividing the quantal content of the second by the quantal content of the first response (Q_2/Q_1). The Ca^{2+} -dependence was determined in a separate set of experiments recording EJPs at 0.5 Hz in HL 3 containing 0.4, 0.6, 1.0 and 1.5 mM Ca^{2+} . More than 10 NMJ were analyzed for each Ca^{2+} -condition.

Dye Imaging

Wandering third instar larvae were dissected in ice-cold, Ca^{2+} -free normal saline or in Ca^{2+} -free HL3, and pinned to a sylgard-coated chamber (1.3 mm inner diameter). Brain and ventral cord were removed and the preparation was rinsed with the same saline used for the dye uptake. Dye uptake was induced by stimulating the segmental nerves at 3 or 30 Hz in the presence of 10 μM FM1-43 (Molecular Probes) in either normal saline or HL3 containing 0.75 or 1.5 mM Ca^{2+} . Stimulation was performed using a fire-polished suction electrode (filament-containing borosilicate glass, 1.5 mm OD) into which 6-10 segmental

nerves had been sucked in. Stimuli were generated using an isolated pulse stimulator (Model 2100, A-M Systems). Immediately after the stimulation, the preparation was washed in either Ca²⁺-free normal saline or Ca²⁺-free HL3 in the dark, rinsing first thoroughly and then superfusing for 20 or 30 min (1ml/min). The recycling pool of SVs was fully labeled after stimulation for 3 min at 30 Hz in normal saline, as an increase in the stimulation time did not increase the fluorescence within the terminals. Release experiments were performed at 3 Hz in normal saline after imaging a single fully loaded NMJ. Stimulation was interrupted after 5, 10, 20, 30, 40 min and the NMJ was imaged again. Stained boutons were visualized on a Zeiss Axioplan 2 microscope using a Zeiss long-distance water objective (Achromplan 40x / 0.80 W) and a conventional FITC filter set (Zeiss filter set 10 excitation: BP 450-490, beamsplitter: FT 510, emission: BP 515-565). Digital images were acquired with an exposure time of 0.1 or 0.2 sec using a CCD camera (Spot RT Monochrome, Diagnostic Instruments inc.), controlled by MetaView imaging software (Visitron Systems GmbH). To guarantee that the illumination of the field was uniform and to control the absolute fluorescence intensity, a homogeneously fluorescent calibration slide was used (Applied Precision). For the quantitative measurements only presynaptic terminals of the NMJ of muscle 6/7 that were clearly in focus were used, measuring the average intensity of each terminal and subtracting background fluorescence of the muscle near the terminal using the MetaView imaging software.

For the FM5-95 uptake experiments, larvae were dissected as described above. Brain and ventral nerve cord were removed for electrophysiological but not for high K⁺ stimulation. Dye loading was performed using 15 μ M FM5-95 (Molecular Probes) either in high K⁺ solution for 1 min or in normal saline stimulating segmental nerves 3 min at 30 Hz. The preparation was washed 30 min in Ca²⁺-free saline prior imaging. In a set of control experiments, we checked that FM5-95 was not internalized in *sh^{ts1}* at the restrictive temperature or in wildtype the absence of stimulation.

shibire^{ts} depletion/recovery experiments

For the “*shibire^{ts}* depletion/recovery” experiments, *shibire^{ts}* third instar NMJs expressing GFP-myc-2xFYVE were imaged in normal saline in resting conditions, or after stimulation at 3 Hz for 30 min or 30 Hz for 10 min. Depletion of the endosome was performed by stimulating the synapse at the restrictive temperature (around 33°C) at 3 or 30 Hz for different time intervals. Recovery was performed in normal saline at RT. For the quantification, fluorescence measured near the endosomes was subtracted.

FRAP and Wortmannin experiments

For FRAP (Fluorescence Recovery After Photobleaching) experiments, third instar larvae expressing GFP-Rab5 in the nervous system with elav-GAL4 were dissected and imaged in ice-cold Ca²⁺-free saline. The GFP fluorescence at the endosome was bleached by specifically illuminating this region (around 2 μm in diameter) with full laser power for 30 - 60 sec using the ROI-option of an LSM-510 confocal microscope (Zeiss). Bleaching was performed in ice-cold Ca²⁺-free saline to prevent movement. For recovery, the preparation was incubated at RT in Ca²⁺-free saline, or in normal saline stimulating at 3 or 30 Hz for 5 min. The recovery times were around 2 min for all conditions used. For the Wortmannin treatment, GFP-Rab5 or GFP-2xFYVE expressing NMJs were imaged *in vivo* using a confocal microscope (LSM-510, Zeiss). The preparations were then incubated in 100 nM Wortmannin (Sigma) in Ca²⁺-free saline for 45 min at RT. After fixation for 90 - 120 min in 4% paraformaldehyde in PEM, the same NMJs were imaged again using the same imaging conditions as before. No change was seen in the control containing DMSO without Wortmannin. The GFP-Rab5 pattern was not affected even if Wortmannin was used at 250 nM for 45 min as previously reported for mammalian cells (Sonnichsen *et al.*, 2000).

Statistical Analysis

The statistical data analysis was done with InStat 2.03 software. All data are represented as mean ± SEM. In all figures statistical significance (compared to

wildtype controls) is indicated as one asteriks $p < 0.05$, two asteriks $p < 0.01$ and was determined using ANOVA.

Results

Characterization of an early endosomal compartment at the *Drosophila* presynaptic terminal

Rab5 defines an endosomal compartment at the synapse

In cultured mammalian cells, two markers have been used to define the early endosomal compartment (Bucci *et al.*, 1992; Gillooly *et al.*, 2000). One is the small GTPase Rab5 (Bucci *et al.*, 1992; Chavrier *et al.*, 1990). Rab5 regulates the first step within the endosomal pathway, the trafficking from the PM to the early endosome. Activated, GTP-bound Rab5 accumulates at the endosome and initiates there the formation of a membrane domain, the Rab5 domain. This domain is characterized by the accumulation of different Rab5 effector proteins and by the presence of the lipid PI(3)P. The second endosomal marker is based on the specific binding of the FYVE zinc finger protein domain to PI(3)P. It has been found that a myc-tagged tandem repeat of the FYVE domain is specifically localized to the early endosome in cultured fibroblasts (Gillooly *et al.*, 2000).

Rab5 and myc-2xFYVE appear in cultured mammalian cells in a punctuate pattern reflecting the distribution of early endosomes within the cell. Dye internalization and transferrin uptake experiments have been established to functionally define different endosomal compartments in cultured cells (Bucci *et al.*, 1992; Chavrier *et al.*, 1990; Ullrich *et al.*, 1996). In such experiments, labeled transferrin or fluorescent dyes are internalized for different time intervals. After 5 min, these probes accumulated in distinct punctuate structures. The structures correspond to early endosomes because they can also be labeled with Rab5 or 2xFYVE. Therefore, in cultured mammalian cells the early endosome is defined as a structure where internalized probes accumulate after 5 min and which is labeled by Rab5 and 2xFYVE.

In order to monitor endosomes within the presynaptic terminal, we generated several probes: GFP-2xFYVE, myc-2xFYVE and GFP-Rab5 fusions and we produced a specific anti-*Drosophila* Rab5 antibody (see methods). We first

compared the localization of these probes with respect to the functionally defined early endosomes in *Drosophila* S2 cultured cells and developing wing cells and (Fig. 6 and not shown). We found that endogenous Rab5 as well as the GFP-Rab5 and GFP-2xFYVE fusions colocalize with texas-red dextran internalized for 5 min to label early endosomes. Therefore, as in cultured mammalian cells, in cultured *Drosophila* cells Rab5, GFP-Rab5 and GFP-2xFYVE define the early endosomal compartment.

To address whether there is an endosomal compartment within the presynaptic terminal of third instar *Drosophila* larvae, we first specifically expressed the tagged 2xFYVE fusions in the CNS using the UAS/GAL4 technique (Brand and Perrimon, 1993) and elav-GAL4 (Lin and Goodman, 1994) in transgenic flies (Fig. 7, 8). Both GFP-2xFYVE and myc-2xFYVE appeared as punctuate structures within the presynaptic terminal (Fig. 7A, C, D). At least one 2xFYVE-labeled endosome was detected per presynaptic terminal (Fig. 7A, 8C). The number of endosomes was dependent on the size of the presynaptic terminal and up to 4 were detected in large terminals (Fig. 8C).

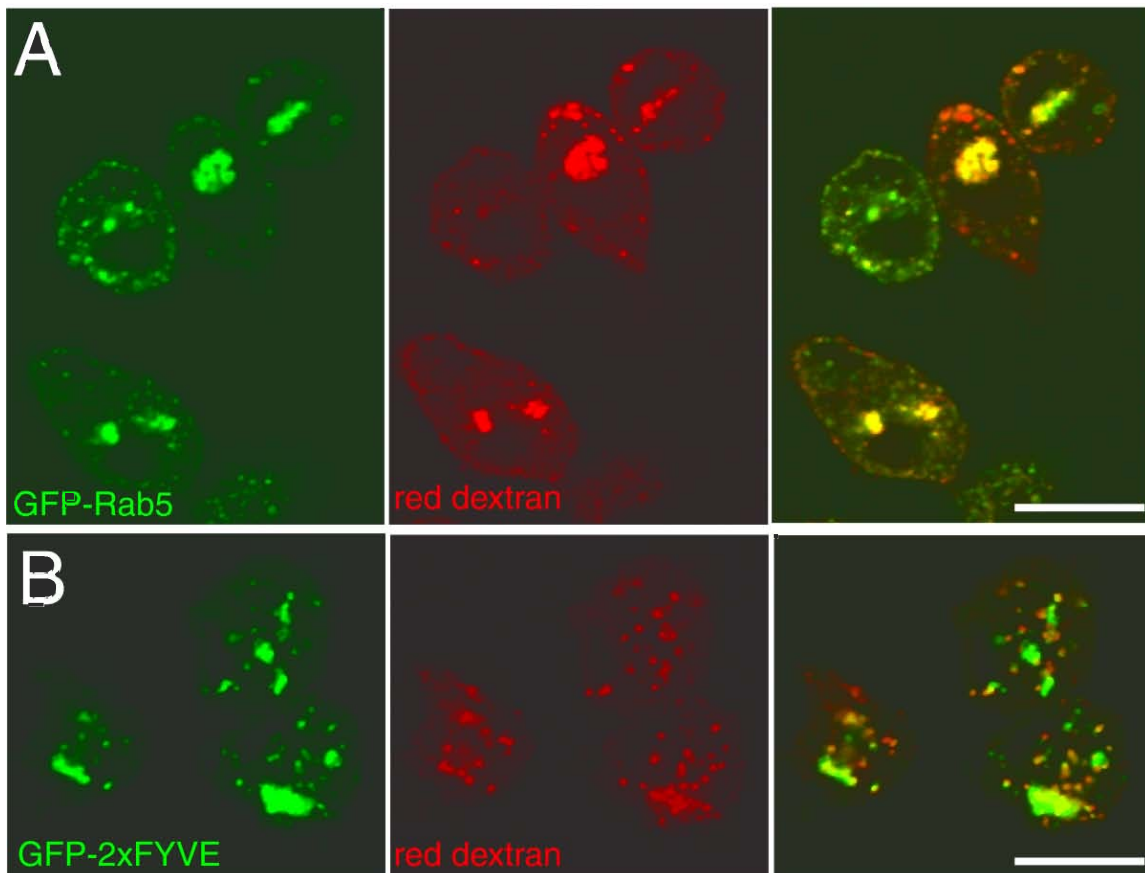


Fig. 6. Early endosomes in *Drosophila* S2 cultured cells. (A) Double labeling showing GFP-Rab5 to label early endosomes (green) and texas red dextran internalized during 5 min at RT (red). Right panel, merge. (B) Double labeling showing GFP-2xFYVE (green) and texas red dextran internalized during 5 min at RT (red). Texas red dextran internalized using a protocol to label early endosomes shows high colocalization with GFP-Rab5 (A) and GFP-2xFYVE (B). Scale bars correspond to 10 μ m.

Furthermore, GFP-Rab5 expressed in the nervous system was detected at punctuate structures within the synapses (Fig. 7B, 8D). Using the anti-DRab5 antibody, we also found endogenous Rab5 in a punctuate pattern at the presynaptic terminal (Fig. 7C). In addition, diffuse Rab5 was found at lower levels (Fig. 7C), which likely corresponds to cytosolic Rab5 and Rab5 associated to vesicles as seen in mammalian cells (Bucci *et al.*, 1992; Chavrier *et al.*, 1990). No overt plasma membrane staining could be detected in a double immunostaining with anti-HRP antibodies (Fig. 7B). Anti-HRP antibodies cross react with the beta subunit of the Na⁺,K⁺-ATPase at the PM (Sun and Salvaterra, 1995) and have thereby been used to visualize the neuronal PM (Fig. 7B).

Both GFP-2xFYVE and myc-2xFYVE colocalize with endogenous Rab5 (Fig. 7C and not shown), indicating that as in cultured mammalian cells and cultured *Drosophila* cells also at the presynaptic terminal 2xFYVE and Rab5 are both diagnostic markers for the early endosome. This was confirmed by the colocalization of a functional GFP-Rab5 fusion (see below) and myc-2xFYVE in transgenic flies coexpressing both markers in the CNS (Fig. 7D).

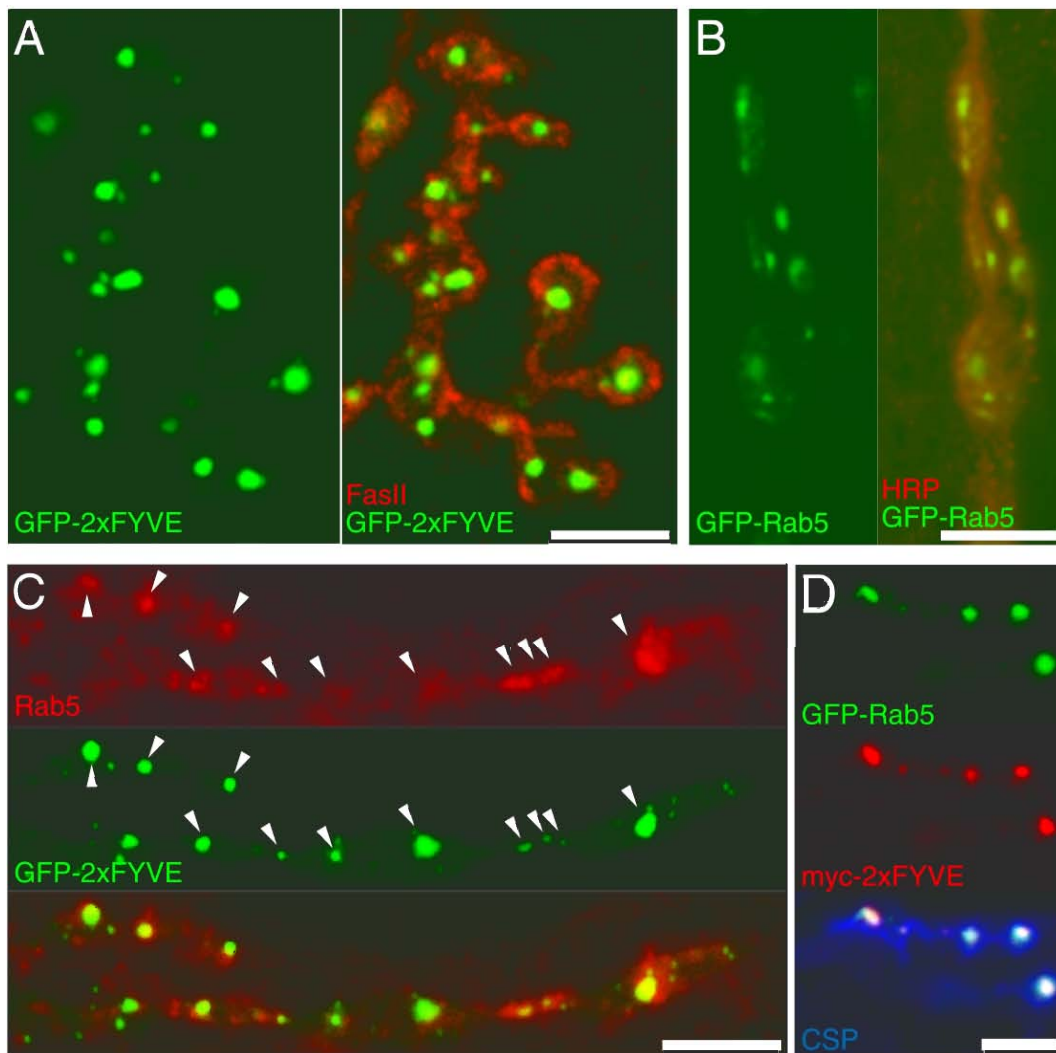


Fig. 7. An endosomal compartment at the presynaptic terminal. (A) Double labeling showing GFP-2xFYVE (green) to monitor the endosomes and Fasciilin II immunostaining to label the NMJ presynaptic terminals (FasII; red). (B) Double immunostaining showing GFP-Rab5 (green) to monitor the endosomes and HRP immunostaining to label the presynaptic terminals (red). (C) Double labeling showing endogenous Rab5 immunostaining (red) and GFP-2xFYVE (green). Lower panel, merge. Arrowheads indicate Rab5 punctuate structures colocalizing with GFP-2xFYVE positive endosomes. (D) Triple labeling showing GFP-Rab5 (green), myc-2xFYVE immunostaining using an anti-cmyc antibody (red) and Cystein string protein immunostaining (CSP; blue) to label the presynaptic terminals in a muscle 6/7 NMJ. Lower panel, merge of the three channels. GFP-Rab5 and myc-2xFYVE show a complete colocalization. Genotypes: (A, C) *w; UAS-GFP-myc-2xFYVE; elav-GAL4*. (B) *w; UAS-GFP-Rab5/elav-GAL4*. (D) *w; UAS-myc-2xFYVE/elav-GAL4 UAS-GFP-Rab5*. Bars correspond to 5 μ m. NMJs from late third instar larvae are shown.

2xFYVE localization at the endosome is PI(3)P dependent

We next addressed whether at the presynaptic terminal the specific localization of GFP-2xFYVE and myc-2xFYVE to the endosome was dependent on the presence of PI(3)P as described in cultured mammalian cells (Gillooly *et al.*, 2000). We blocked PI(3)P-kinase activity with Wortmannin and monitored the tagged 2xFYVE fusions. As in cultured mammalian cells, GFP-2xFYVE loses its punctate pattern and becomes dispersed into the cytosol upon blockage of PI(3)-kinase activity (Fig. 8A). Therefore, as in cultured mammalian cells the endosomal localization of 2xFYVE in the presynaptic terminal depends on PI(3)P.

The endosome is localized within the pool of recycling vesicles

Where is the endosome localized with respect to the SVs within the presynaptic terminal? To address this question recycling vesicles were labeled by the red FM5-95 styryl dye (Fig. 8B). Like the green FM1-43, which was introduced in 1992 by Betz and colleagues (Betz and Bewick, 1992), FM5-95 is an amphipathic dye containing a fluorescent head group and a lipid tail. Styryl dyes have several features making them very useful for internalization experiments in neurons. *First*, when present in the aqueous, extracellular solution surrounding a cell the dye spontaneously inserts into the outer leaflet of the PM. *Second*, dye inserted into the membrane shows a much stronger fluorescence than dye in aqueous solution. *Third*, styryl dyes cannot cross the membrane, and are therefore internalized only during compensatory endocytosis. *Fourth*, FM-dyes can be washed off easily from the membrane.

In a typical experiment, exocytosis is stimulated in the presence of the FM-dye. Dye is internalized together with the membrane during compensatory endocytosis. The internalized dye therefore labels the pool of vesicles that were internalized during synaptic activity, called the recycling pool of SVs. We stimulated synaptic activity and thereby internalized the red FM5-95 into presynaptic terminals of GFP-2xFYVE and GFP-Rab5 expressing NMJs (see

methods). Endosomes labeled with either GFP-2xFYVE (Fig. 8C) or GFP-Rab5 (Fig. 8D) are located within the pool of recycling vesicles. This indicates the presence of a distinct endosomal compartment located within the pool of recycling vesicles. The location of the endosome prompts the possibility that the endocytic vesicles internalized during synaptic transmission traffic through the endosome during their recycling.

The endosome size is stable during synaptic transmission

To study the endosome *in vivo*, we monitored GFP-Rab5 and GFP-2xFYVE in resting terminals or while stimulating the synapse under basal, 3 Hz or more demanding, tetanic, 30 Hz electrophysiological conditions (Fig. 9). Figures 9A and 9B show that neither the location nor the size or the intensity of GFP-2xFYVE was substantially changed under these conditions. This observation indicates that the endosomal size is stable both in the resting terminal and during synaptic transmission. Therefore, if SV recycling involves trafficking through the endosome, then endocytic vesicle fusion to the endosome is balanced with SV budding from the endosome to ensure the constant endosomal size.

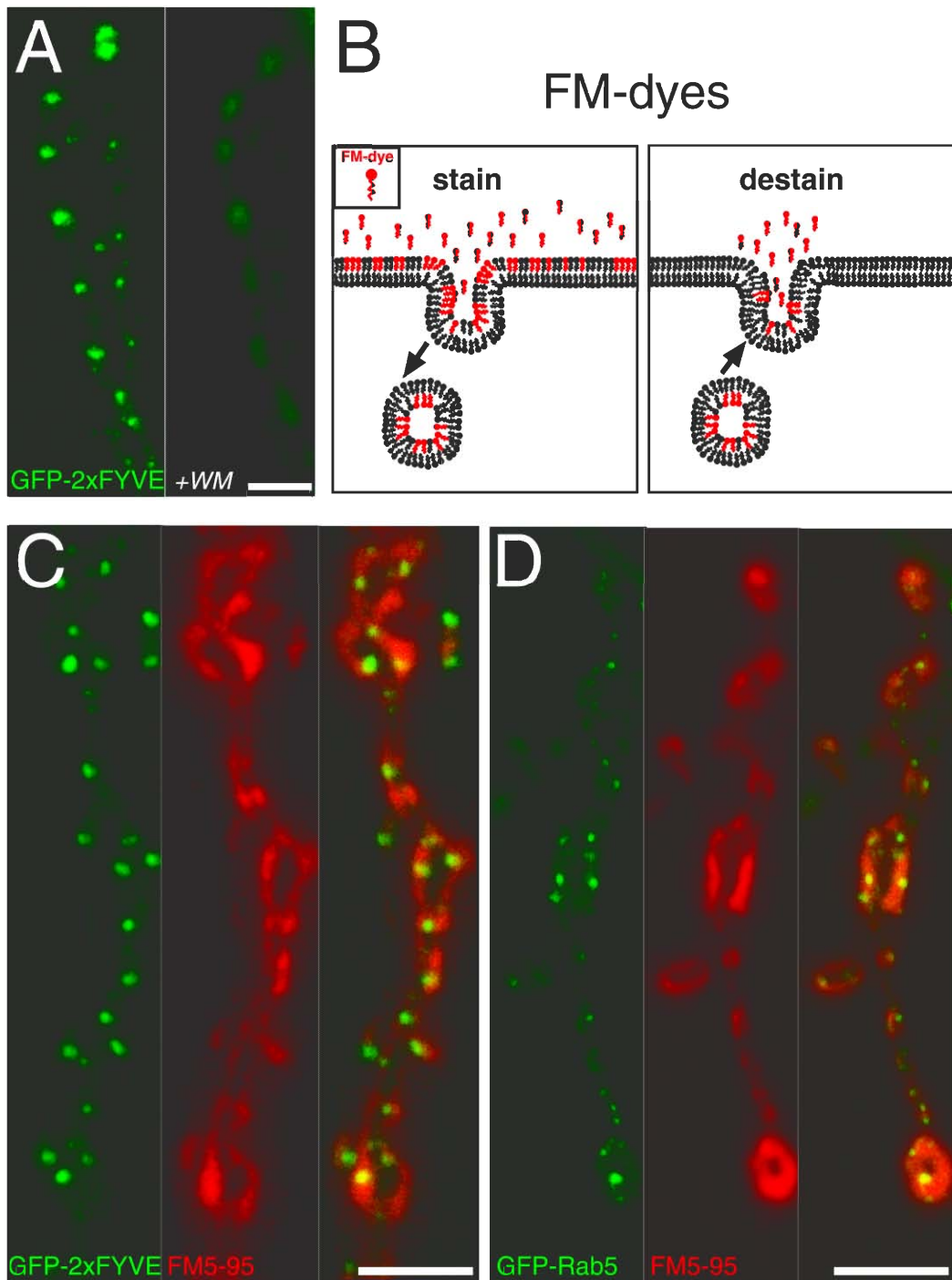


Fig. 8. Endosomes contain PI(3)P and are localized embedded in the pool of SVs. (A) GFP-2xFYVE fluorescence in an abdominal muscle 6/7 NMJ before (left) and after (right) 45 min of treatment with 100 nM of the PI(3)-kinase inhibitor Wortmannin *in vivo* (+WM). Note that, upon Wortmannin treatment, GFP-2xFYVE loses the punctuate pattern and becomes dispersed into the cytosol. Untreated controls retained the punctuate pattern. (B) Scheme of FM-dye experiments. FM-dye inserts into the outer leaflet of the PM and is internalized during endocytosis (left). Upon exocytosis, dye-loaded SVs are destained, due to dye-loss into the surrounding medium (right). (C, D) Double labelings showing in green GFP-2xFYVE (C) or GFP-Rab5 (D) and in red FM5-95 styryl dye internalized into the presynaptic terminal upon 1 min of stimulation with 60 mM K^+ to label the pool of recycling vesicle in two different NMJs of muscle 6/7. Right panels, merge. Note that the endosomes are embedded within the pool of recycling vesicles. Genotypes: (A, C) *w; UAS-GFP-myc-2xFYVE; elav-GAL4*. (D) *w; UAS-GFP-Rab5/elav-GAL4*. Bars correspond to 5 μ m. NMJs are from late third instar larvae.

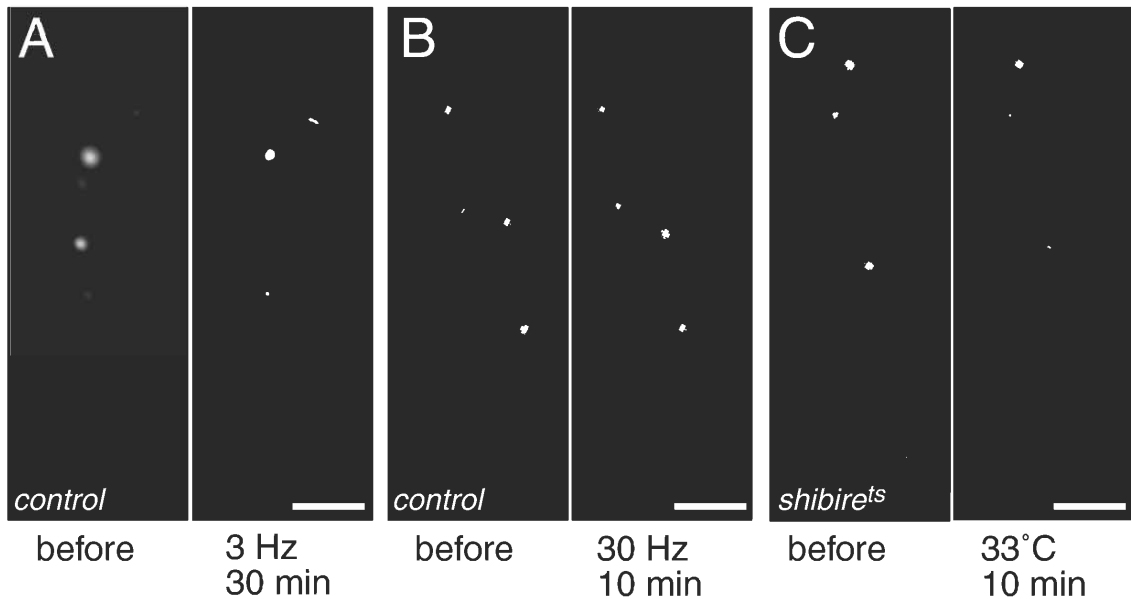


Fig. 9. The endosomal size is stable during synaptic transmission. (A, B) GFP-2xFYVE labeling before (left panel) and after (right panel) stimulation at 3 Hz for 30 min (A) or at 30 Hz for 10 min in normal saline (B). No difference was observed in the number, position, size or intensity of the endosomes upon stimulation, indicating that the endosomal size is stable. Position changes are due to stretching of the muscle. Genotype: *w; UAS-GFP-myc-2xFYVE; elav-GAL4*. (C) GFP-2xFYVE labeling in a *shibire^{ts1}* mutant terminal before (left panel) and after (right panel) 10 min incubation at the restrictive temperature (33°C) without stimulation in Ca^{2+} -free saline. No differences in the endosomal number, size, position or intensity were observed. Note that occasionally, due to muscle movements, endosomes are moved out of the plane. Genotype: *shibire^{ts1}; elav-GAL4 UAS-GFP-myc-2xFYVE*. Bars correspond to 5 μ m. NMJs of late third instar larvae are shown.

SV recycling involves membrane trafficking through the endosome

To address directly whether the endosome is involved in the recycling of SVs we used the *Drosophila* mutant *shibire^{ts}*, named after the Japanese word meaning “paralyzed”. *Shibire^{ts}* is a temperature-sensitive mutation in the GTPase domain of Dynamin (Grant *et al.*, 1998; van der Blik and Meyerowitz, 1991) that allows to specifically and reversibly block endocytosis (Koenig and Ikeda, 1989). At the restrictive temperature, Dynamin becomes nonfunctional immediately causing the complete arrest of endocytosis at a very specific step as demonstrated by Kosaka and Ikeda in 1983 (Kosaka and Ikeda, 1983a). Nascent endocytic vesicles cannot be pinched off from the PM and therefore accumulate in the form of “collared pits” (Estes *et al.*, 1996; Kosaka and Ikeda, 1983a). These structures have distinct necks connected to the PM that are surrounded by an electron-dense collar, presumably containing components of the membrane fission machinery. Therefore, stimulating SV exocytosis in the synapse while blocking endocytosis with *shibire^{ts}* causes a complete depletion of SVs. SV depletion can be directly seen at the ultrastructural level (Koenig and Ikeda, 1989; Koenig *et al.*, 1989; Kosaka and Ikeda, 1983a; Poodry and Edgar, 1979). In addition, measuring neurotransmitter release using standard electrophysiological techniques shows the complete SV depletion by the complete loss of NT release (Koenig and Ikeda, 1999). The phenotype in adult flies is quite striking: within seconds after exposure to the restrictive temperature they become completely paralyzed (Grigliatti *et al.*, 1973). Lowering the temperature releases the endocytosis block and leads within few minutes to a complete recovery as observed by the recovery of paralyzed flies and the reformation of the SV pool detected at the ultrastructural level and in electrophysiological experiments (Koenig and Ikeda, 1999).

We used *shibire^{ts1}* (*shi^{ts}*) to uncouple exo- and endocytosis and thereby to address three questions: *First*, do SVs bud from the endosome? *Second*, do endocytic vesicles fuse to the endosome? *Third*, is endosomal trafficking temporally coupled to synaptic activity? We first excluded a direct effect of *shibire^{ts}* on endosome morphology. Endosomes visualized by GFP-2xFYVE

were monitored in *sh^{ts}* mutant synapses in resting terminals at the permissive and at the restrictive temperature (Fig. 9C and not shown) as well as at the permissive temperature while stimulating at 3 or 30 Hz (not shown). Under these conditions the endosomal size, intensity and position remained stable. Therefore, as in the *sh⁺* controls (Fig. 9A, B) the endosomal size is stable in *shibire^{ts}* at the permissive temperature in resting terminals or during synaptic activity as well as at the restrictive temperature when the terminal is not stimulated, excluding a direct effect of *shibire^{ts}* on endosome morphology.

In order to address whether SVs bud from the endosome, we performed a “*sh^{ts}*/depletion” experiment in the following way: We blocked endocytosis with *shibire^{ts1}* at the restrictive temperature (Koenig and Ikeda, 1989; Koenig and Ikeda, 1999) and depleted the SV pool by electrophysiologically stimulating SV release for 5, 10 and 15 minutes as previously described (Koenig and Ikeda, 1999). At the same time, endosomes labeled by GFP–2xFYVE were monitored. If SVs bud from the endosome, in *sh^{ts}* there will be membrane output (budding) from the endosome upon stimulation, but no membrane input (fusion) because of the absence of newly formed endocytic vesicles that could fuse to the endosome. Consequently, the endosome should be reduced in size or even be depleted together with the SV pool in this “*sh^{ts}*/depletion” experiment.

Figures 10A-C show, that the punctuate endosomal staining disappears during the “*sh^{ts}*/depletion” experiment: GFP-2xFYVE becomes diffuse. This suggests that synaptic vesicles budded from the endosome, depleting the compartment. The kinetics of endosome disappearance depends on the frequency of stimulation with $t_{1/2}$ of 5 minutes during the basal stimulation at 3 Hz (10D) and approximately ten fold faster during the more demanding, tetanic stimulation at 30 Hz (Fig. 10A-C).

We next studied whether endocytic vesicles fuse to the endosome by monitoring endosomal recovery after release of the *sh^{ts}* endocytic block by lowering the temperature. We first depleted the endosome by performing a “*sh^{ts}*/depletion” experiment as described above (Fig. 10E–G). Figure 10G

shows that in contrast to control synapses (Fig. 10J-L) the endosome is depleted. Subsequently, larvae were returned to the permissive temperature to release the *shl^{ts}* endocytosis block. After 15 minutes, we observed fluorescence recovery at the endosome (Fig. 10H, I), suggesting that recovery of the endosome involves dynamin-dependent endocytosis. Furthermore, if we first depleted the endosome by stimulating the synapse at the restrictive temperature as described above (Fig. 10M, N) and then maintained the animals at the restrictive temperature after stimulation no endosomal recovery was observed (Fig. 10O). Afterwards, returning the animals to the permissive temperature and thereby releasing the endocytosis block, led to the recovery of the endosome (Fig. 10P). Therefore, the endosome recovers only when the *shl^{ts}* endocytosis block is released. This indicates that the endosome recovers at the expense of endocytic vesicles that form after release of the endocytosis block. In summary, these results show that endocytic vesicles fuse with the endosome and that synaptic vesicles bud from the endosome. This in turn implies that SV recycling indeed involves trafficking through the Rab5 endosomal compartment.

We next addressed the question of whether endosomal trafficking is coupled to synaptic activity. The fact that the depletion of the endosome in *shl^{ts}* only occurred when the synapse was stimulated (compare Fig. 9C vs. Fig. 10A-C), suggested that SV budding from the endosome only occurs during synaptic activity and is therefore coupled to synaptic transmission. In contrast, when the *shl^{ts}* endocytic block was released, the endosome recovered in a resting terminal (Fig. 10H, I, P). This indicates that endocytic vesicles can fuse to the endosome also in the absence of synaptic activity.

To investigate whether endosomal trafficking is coupled to synaptic activity, we performed FRAP experiments (Cole *et al.*, 1996) in resting and stimulated GFP-Rab5 expressing synapses (Fig. 10Q-S). We first bleached selectively the GFP fluorescence at the endosome in GFP-Rab5 expressing terminals with a confocal microscope (Fig. 10Q, R). Then, we monitored the recovery of the GFP fluorescence at the endosome in resting (Fig. 10S), or in stimulated NMJs (not shown). Recovery of fluorescence occurred within 2 minutes after

bleaching in both resting (Fig. 10Q-S) and stimulated terminals (not shown). These results indicate that vesicles containing GFP-Rab5 can fuse with the endosome also in the absence of synaptic activity.

In summary, SV recycling involves trafficking through an endosomal compartment. Endocytic vesicles internalized after Ca^{2+} -triggered exocytosis fuse with the endosome independent of synaptic activity. Subsequently, SVs bud from the endosome and are eventually released upon arrival of an action potential. The fact that SV recycling involves traffic through a Rab5 positive endosomal compartment prompted us to study the possible role of Rab5 during the process of recycling using Rab5 mutants.

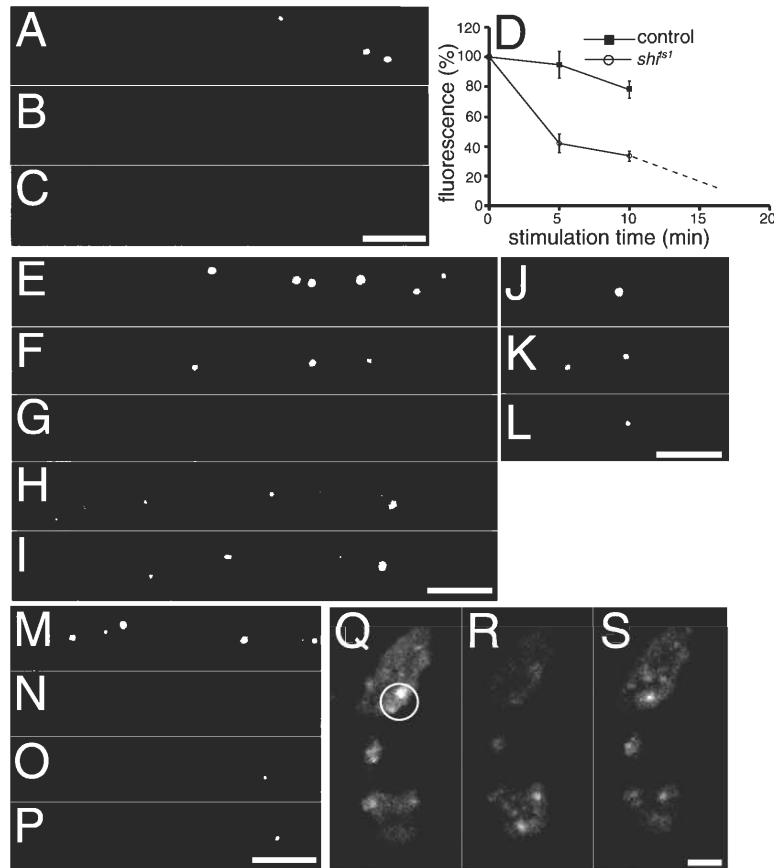


Fig. 10. SVs recycle through the endosome. (A-C) GFP-2xFYVE labeling in a *shi^{ts}* mutant terminal at 25°C (A) and after 5 min of stimulation at 30 Hz in normal saline at 33°C (B, C). (C) same image as in (B), with increased brightness and contrast to show diffuse GFP fluorescence at the terminal. The endosome is depleted together with the pool of SVs, indicating that SVs bud from the endosome. (D) Kinetics of endosome disappearance. Time course of the changes in the GFP fluorescence in *shi^{ts1}; elav-GAL4 UAS-GFP-myc-2xFYVE* (*shi^{ts1}*; n = 5 NMJs) and *w; elav-GAL4 UAS-GFP-myc-2xFYVE* (control; n = 4 NMJs) during 3 Hz at 33°C. Fluorescence in ordinates refers to mean pixel brightness at the punctuate structures normalized to the mean brightness before stimulation. After 10 min of stimulation at 33°C in *shi^{ts1}*, GFP fluorescence at the endosome cannot be distinguished (dashed line). (E-G) GFP-2xFYVE labeling in a *shi^{ts1}* mutant terminal at 25°C (E) and after stimulation at 33°C for 5 (F) and 10 min at 3 Hz in normal saline (G). (H, I) GFP-2xFYVE fluorescence recovery at the endosomes in the same synapse upon downshift to 25°C for 15 (H) and 30 min (I). Fluorescence recovers after releasing the endocytosis block, implying that endocytic vesicles fuse with the endosome and replenish it. (J-L) Control synapses showing the GFP-2xFYVE fluorescence upon 3 Hz stimulation in normal saline during the same time intervals (J, 0 min; K, 5 min; L, 10 min). Genotype: *w; elav-GAL4 UAS-GFP-myc-2xFYVE*. (M, N) GFP-2xFYVE fluorescence in a *shi^{ts}* mutant terminal at 25°C (M) and after stimulation at 33°C for 10 min at 3 Hz in normal saline (N), showing endosome depletion. (O, P) GFP-2xFYVE fluorescence in the same synapses maintained at 33°C for 15 min after stimulation (O), followed by downshift to 25°C for 15 min (P). In the resting terminal fluorescence at the endosome recovered only if the endocytosis block is released, indicating that endosomal recovery involves endocytic vesicle fusion to the endosome. (Q-S) FRAP experiments in a GFP-Rab5 expressing synapse. Fluorescence before (Q) and after bleaching (R). Circle, bleached area. Fluorescence recovery after photobleaching (FRAP) was observed after 5 min without stimulation in Ca²⁺-free saline (S). The same result was observed in stimulated terminals. Genotype: *w; elav-GAL4/UAS-GFP-Rab5*. Changes in the fluorescence in the lower terminal in (R) are due to changes in the focal plane caused by muscle movements. Genotype: (A-C, E-I, M-P) *shi^{ts1}; elav-GAL4 UAS-GFP-myc-2xFYVE*. In (A-P) NMJs belong to A2 - A4 abdominal muscles 6/7, in (Q-S) to an abdominal ventral oblique muscle. Bars correspond to 5 μm (A-P) and 2 μm (Q-S). Error bars are standard errors.

Analysis of Rab5 function using Rab5 mutants and the dominant negative version of Rab5, Rab5S43N

Genomic organization of *Drosophila* Rab5

In *Drosophila*, we found a single Rab5 gene with multiple splicing variants (Fig. 11A). The gene has 7 alternative 5' leader exons and 2 alternative 3' untranslated regions (UTRs) (Fig. 11A) and encodes for a single open reading frame (Fig. 11A; see methods). Consistently, a single band of around 24 kDa was detected in Western blot experiments using the anti-*Drosophila* Rab5 antibody against larval or embryonic extracts (Fig. 11B, C). The size of 24 kDa is consistent with the predicted molecular weight of Rab5 containing 219 amino acids. The presence of a single Rab5 gene and protein isoform in *Drosophila* is in contrast to the situation in yeast and mammals where three Rab5 genes coding for different isoforms were found (Novick and Zerial, 1997). As in *Drosophila*, a single Rab5 gene has been described in *C. elegans* (Grant and Hirsh, 1999). The genes flanking Rab5 are a zinc finger transcription factor (CG4272) and a Heparansulphate proteoglycan (CG7245). One of the splicing forms of Rab5 overlaps by 28 bp with the 5' end of the CG4272 transcript (Fig. 11A).

We identified 2 P-element insertions from the Berkeley genome project inserted in the Rab5 gene (Fig. 11A), $P\{lacw\}Rab5^{k08232}$ and $P(PZ^+)00231$. $P\{lacw\}Rab5^{k08232}$ ($Rab5^1$) is a P-element insertion within the 5' leader coding region (Fig. 11A). $Rab5^2$, $Rab5^3$ and $Rab5^4$ were generated by imprecise excision of $Rab5^1$. $Rab5^2$ is a 4 kb deletion of the promoter region, the 5' non-translated leader and the first exon of the open reading frame (Fig. 11A). This exon encodes the PM1-3 Phosphate/Mg²⁺-binding motifs and the G1 Guanine base-binding motif of the GTPase domain (Fig. 3A) (Olkkonen and Stenmark, 1997). Therefore, $Rab5^2$ is a Rab5 null mutation. $Rab5^3$ contains an insertion of 18 bp from the left and 210 bp from the right LTR of the P-element remaining after imprecise excision of the transposon. In $Rab5^4$ 14 bp from the right LTR remained after the imprecise excision of the P-element.

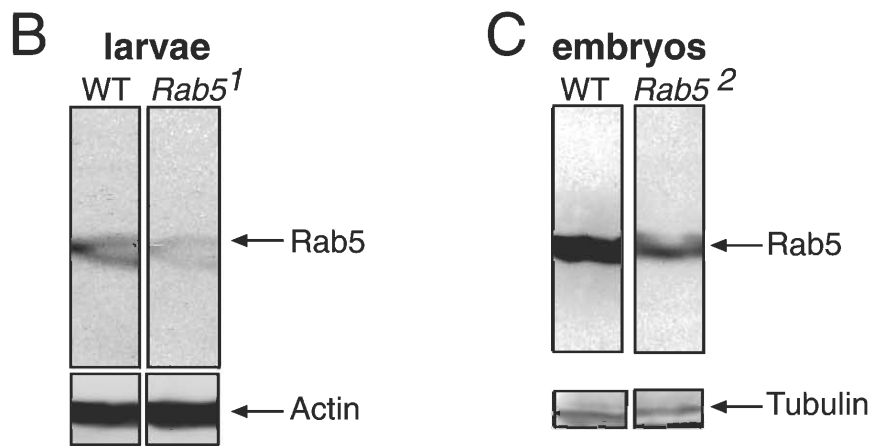
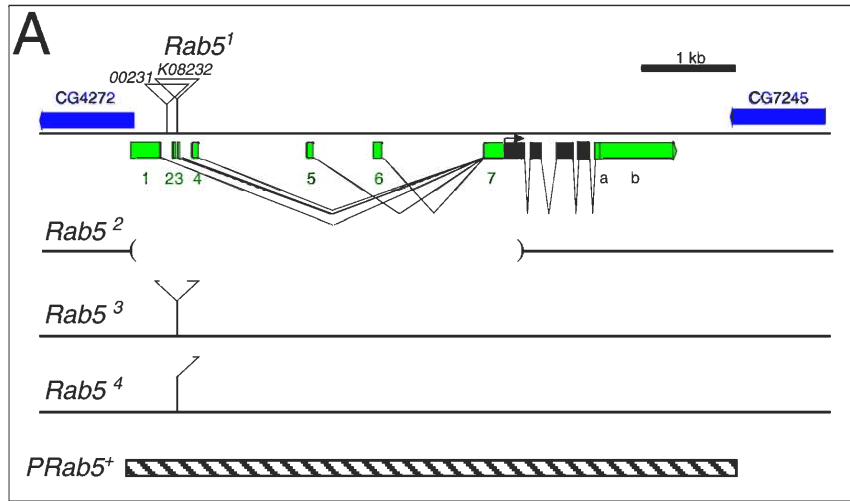


Fig. 11. Rab5 loss of function mutants have reduced Rab5 levels. (A) genomic organization of Rab5. Green/black bars, Rab5 exons. 1-7, alternative 5' leader exons. a, b, alternative 3' UTRs. Black bars, open reading frame. Blue arrows, Rab5 flanking genes (CG4272 and CG7245). I(2)00231 and I(2)k08232, P-element insertions. We renamed I(2)k08232 as Rab5¹. Rab5², 4 kb deletion generated by imprecise excision of Rab5¹. Rab5³ and Rab5⁴ are imprecise excisions where P-element long terminal repeat (LTR) sequences remained. PRab5⁺ (dashed bar), region contained in the genomic Rab5 rescue. (B) Western blot experiment with larval extracts showing the reduction to 30% in the Rab5 proteins level in Rab5¹ compared to wildtype, detected with the anti-DRab5 antibody. The Actin staining serves as loading control. (C) Western blot experiment with extracts from 0 - 2 h embryos, showing low Rab5 protein levels (13% of wildtype) in the early Rab5² mutant embryos, indicating the maternal Rab5 contribution. The Tubulin staining serves as loading control. Note that the anti-DRab5 antibody detects a single band of around 24 kDa.

Rab5 mutants show locomotion defects, paralytic phenotypes and defective endosomes

The level of Rab5 expression in the homozygous mutants was determined by Western blot experiments using the anti-DRab5 antibody. In *Rab5¹* mutants, the level of Rab5 expression was reduced to around 30% compared to the Rab5 protein level in wildtype (Fig. 11B; see methods). Homozygous *Rab5¹* mutant animals die during late second and early third instar larval stages. They show only a light locomotion phenotype when compared to wildtype larvae. When *Rab5¹* mutants were raised under “intensive care” conditions as described (Loewen *et al.*, 2001), very few homozygous adults were observed (around 14% of the homozygous larvae developed to adults). They are extremely poor fertile and show a flightless phenotype. However, no obvious physiological differences were detected in *Rab5¹* mutants when compared to wildtype: *First*, the recycling SV pool size was determined by an FM1-43 internalization assay (see below and methods), in which FM1-43 was internalized during 3 min of stimulation at 30 Hz in normal saline. The recycling SV pool size in *Rab5¹* was $90.6 \pm 3.3\%$ ($n = 14$ NMJs) compared to wildtype. *Second*, synaptic transmission monitored by standard electrophysiological recordings (see below and methods) was normal in the *Rab5¹* mutant. We observed a mean EJP size of $115.2 \pm 0.7\%$ ($n = 14$ muscle 6) in HL3 containing 0.75 mM Ca^{2+} compared to wildtype.

Rab5¹ was rescued by $P(w^+)DRab5^+$, a genomic rescue construct spanning Rab5 and excluding the two flanking genes (Fig. 11A; see methods) as well as by the restricted expression of GFP-Rab5 in the nervous system using elav-GAL4. Therefore, *Rab5¹*-lethality is caused by reduced Rab5 levels in the nervous system. This also indicates that GFP-Rab5 is a functional Rab5 fusion and that Rab5 function is essential during the physiology or development of the nervous system. The two other weaker Rab5 alleles, *Rab5³* and *Rab5⁴* (Fig. 11A; see methods) displayed decreased Rab5 proteins levels of 46% and 35% compared to wildtype respectively (not shown). Homozygous adults show poor fertility and a flightless phenotype in 88% and 63% of adults, respectively.

The null mutant *Rab5²* shows a more severe phenotype. Embryos fail to hatch and when dissected out of their eggshell they are unable to move and don't react to tactile stimuli, such as touching with a brush or poking with a needle. Therefore, *Rab5²* causes embryonic lethality with a paralytic phenotype. Western blot experiments with *Rab5²* homozygous mutant embryos (0 - 22 h) however showed a faint Rab5 band corresponding to 13% of the wildtype Rab5 protein level (Fig. 11C). As *Rab5²* is a null mutation, the protein detected is likely to correspond to Rab5 translated from maternal mRNA. In *Drosophila*, mRNAs transcribed from the maternal genome, called maternal mRNAs, are deposited into the egg and are transcribed during early development. Therefore, during the early development most if not all proteins are translated from maternal mRNAs. Consistently, the Rab5 protein was also detected by Western blot experiments in early embryonic stages (0 - 2 hours) (not shown). This implies that the zygotic loss of Rab5 is partially rescued by the maternal Rab5 contribution in *Rab5²* homozygous mutants.

We next investigated the effect of zygotic loss of Rab5 on the endosomes. We expressed GFP-2xFYVE in the nervous system using elav-GAL4 and monitored the GFP-2xFYVE labeled endosomes in the mutant background. In control embryos the GFP-2xFYVE labeled endosomes appeared as punctuate structures within the neurons of the CNS (Fig. 12A) and the peripheral nervous system (PNS) (Fig. 12B). Zygotic loss of Rab5 caused the disruption of the endosomes in the embryonic CNS and PNS (Fig. 12A, B) as shown by the diffuse GFP fluorescence. Furthermore, at the presynaptic terminals of control NMJs from late embryos (stage 17) GFP-2xFYVE-positive endosomal punctuate structures were observed (Fig. 12C). In contrast, GFP-2xFYVE was dispersed in the cytosol in the *Rab5²* mutant embryonic NMJs (Fig. 12D), indicating that, at the *Rab5²* mutant NMJs, endosomes are disrupted. In summary, these data indicate that Rab5 is essential for the integrity of the endosomes and is required for the development and/or function of the nervous system, since homozygous *Rab5²* mutants die as embryos, probably when the maternally derived Rab5 is exhausted.

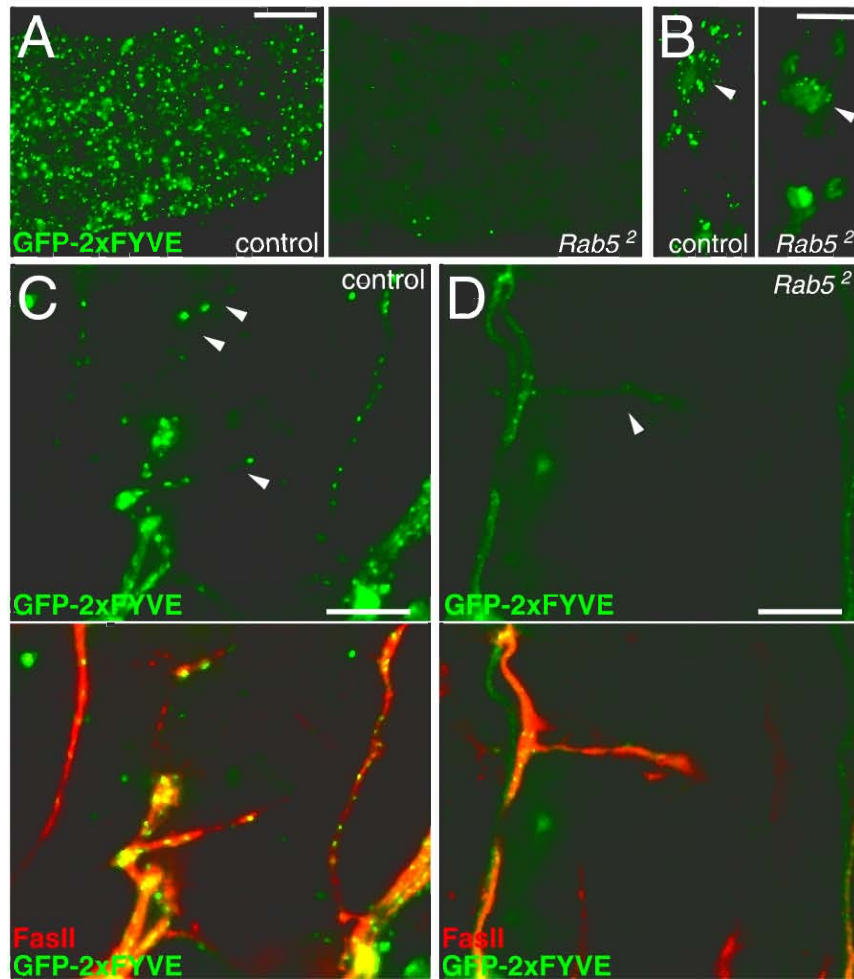


Fig. 12. Rab5 loss of function mutants show disrupted endosomes. (A) GFP-2xFYVE labeling in the CNS of control (left, genotype: *w; elav-GAL4 UAS-GFP-myc-2xFYVE*) and *Rab5*² mutant embryos stage 17 (right, genotype: *Rab5*²; *elav-GAL4 UAS-GFP-myc-2xFYVE*). Note in the control, the punctuate appearance of endosomes labeled by GFP-2xFYVE in the soma of the CNS neurons and in the *Rab5*² mutant embryos the diffuse GFP-2xFYVE fluorescence dispersed in the cytosol, indicating that the endosomal compartments are severely affected. (B) GFP-2xFYVE labeling in the PNS of control (left) and *Rab5*² mutant embryos (right). Genotypes as in (A). Arrowheads, pentachordotonal sensory neurons. (C, D) Double labeling showing GFP-2xFYVE marked endosomes (green) and Fasciilin II immunostainings (red) to monitor the motoneurons at the NMJ (arrowheads) of control and *Rab5*² mutant embryos. Lower panels, merges of the two channels. Genotypes as in (A). Note that few remnant GFP-2xFYVE punctuate structures can be observed occasionally in the *Rab5*² mutant embryos, probably due to the rescue by the maternal contribution. Scale bars correspond to 20 μ m in (A) and 10 μ m in (B-D).

Specific interference of Rab5 during presynaptic physiology does not cause a developmental phenotype

The Rab5 mutants described above represent a deficit of Rab5 function both at the presynaptic (neuron) and postsynaptic (muscle) side of the NMJ. We wanted to study the specific role of Rab5 in the physiology of the presynaptic terminal without affecting other tissues or the nervous system development. To achieve this, we expressed a dominant negative, GDP-bound Rab5 mutant (Rab5S43N) (Entchev *et al.*, 2000; Stenmark *et al.*, 1994) exclusively in the nervous system with *elav*-GAL4 using the UAS/GAL4 technique (Brand and Perrimon, 1993). As GAL4 shows thermosensitivity in *Drosophila* (Brand *et al.*, 1996; Entchev *et al.*, 2000), this allows controlling the expression level using different temperatures. To study the specific effect of the Rab5 mutant during synaptic physiology, we kept expression low during neural development: Rab5S43N was expressed at low levels during embryonic and early larval stages at 16°C, and at higher levels at 25°C or 29°C during the last two days of larval development (see methods).

We first addressed whether mutant Rab5S43N has an effect on the development of the nervous system. Figures 13A-E show that Rab5S43N expressed in the CNS as described above did not cause a developmental phenotype of the NMJ. The overall NMJ morphology was normal in the mutant (Fig. 13A). Furthermore, the normalized synaptic surface, which represents the percentage of synaptic surface with respect to the muscle surface (see methods), was normal in Rab5S43N expressing NMJs (Fig. 13D).

We then looked in more detail at the number and distribution of active zones and centers of endocytosis. Active zones are the regions within the presynaptic terminal where exocytosis of the neurotransmitter glutamate occurs. Postsynaptically, active zones are characterized by the accumulation of glutamate receptor clusters.

The centers of endocytosis have been first described in *Drosophila* (González-Gaitán and Jäckle, 1997) and were later found in organisms such as frog and snake (Jarousse and Kelly, 2001; Ringstad *et al.*, 1999; Roos and Kelly, 1998; Roos and Kelly, 1999; Teng and Wilkinson, 2000). Centers of endocytosis surround the active zones and represent specialized regions where clathrin-mediated, compensatory endocytosis takes place. Therefore, proteins involved in clathrin-mediated endocytosis, like α -Adaptin, Dynamin and Clathrin are accumulated at and therefore define the centers of endocytosis. In order to label the active zones, we used the nc82 antibody (Fig. 13B, C). The nc82 antibody colocalizes with the postsynaptic glutamate receptors at the active zones (not shown) and therefore recognizes an unknown antigen associated to the active zones. As expected the nc82 labeling is surrounded by a staining of α -Adaptin or Dynamin monitoring the centers of endocytosis (Fig. 13B, C and not shown).

Rab5S43N expressing motoneurons showed a normal number and morphology of the centers of endocytosis and the active zones of exocytosis as visualized by anti- α -Adaptin, anti-Dynamin (González-Gaitán and Jäckle, 1997; Roos and Kelly, 1999) and nc82 antibodies (Heimbeck *et al.*, 1999), respectively (Fig. 13C, E and not shown). Therefore, the development and morphology of NMJs was normal in Rab5S43N expressing motoneurons. We next analyzed the role of Rab5 during endosomal trafficking and SV recycling.

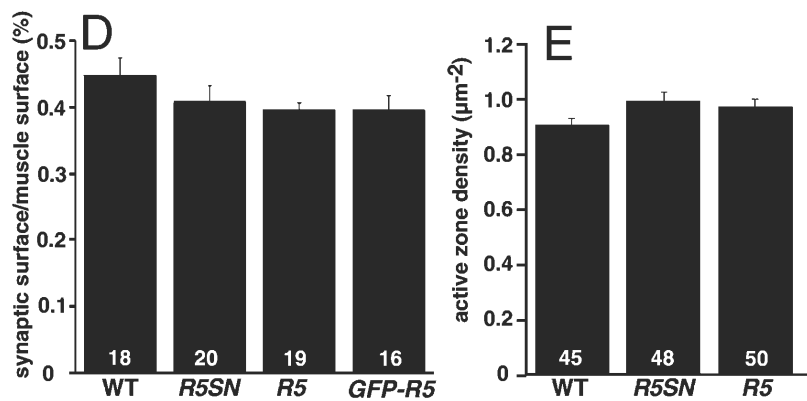
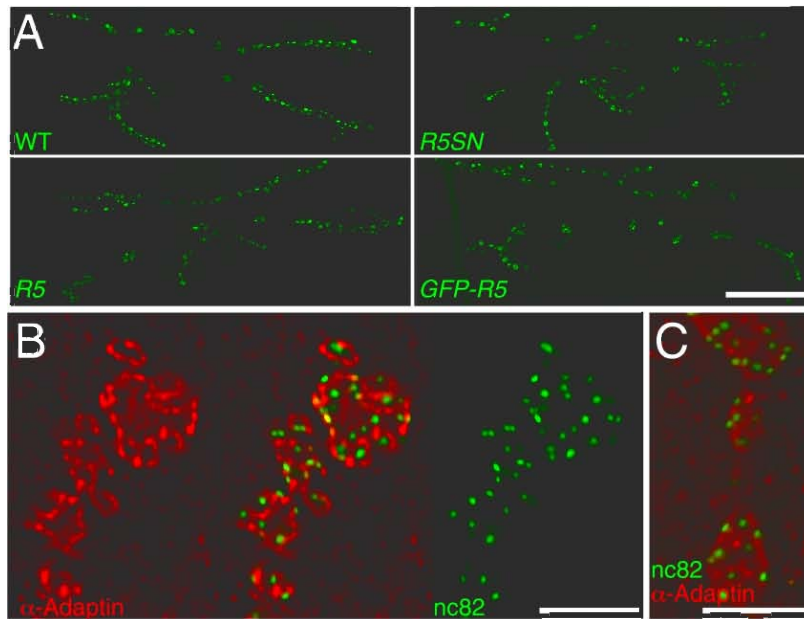


Fig. 13. Normal synaptic morphology in mutant Rab5 expressing presynaptic terminals. (A) CSP immunostaining of the NMJ of muscles 6/7 in the A2 segment of wildtype (WT), *w; UAS-Rab5-S43N/+; elav-GAL4/+* (*R5SN*), *w; UAS-Rab5/+; elav-GAL4/+* (*R5*) and *w; elav-GAL4/UAS-GFP-Rab5* (*GFP-R5*) larvae. (B, C) Double immunostaining showing the centers of endocytosis labeled with α -Adaptin (red) and the active zones of exocytosis labeled with nc82 antibodies (green) in a wildtype (B) and a *w; UAS-Rab5S43N/+; elav-GAL4/+* presynaptic terminal (C). In (B) central panel is the merge. (D, E) Mean synaptic surface area (D) and mean active zone density (E) in muscle 6/7 of A2 in wildtype and the different mutants. Active zone density is the number of nc82 active zones per terminal area. Genotypes as in (A). Bars are standard errors. Numbers in the columns are the number of NMJs (D) and presynaptic terminals quantified (E). Neither the synaptic area nor the active zone density is significantly different in the mutants, implying that the total number of active zones is normal in the mutants. Scale bars correspond to 50 μm in (A) and 5 μm in (B, C). Error bars are standard errors. In this and the following figures, when wildtype or mutant Rab5 was expressed using the UAS/GAL4 system, embryonic and early larval development took place at 16°C and animals were shifted to 25°C only during the last two days of larval development. When 29°C is indicated, the last two days of development took place at 29°C.

Endosomes are disrupted in Rab5S43N mutant presynaptic terminals

The dominant negative, GDP-bound Rab5 mutant impairs the fusion of endocytic vesicles with the endosome in cultured mammalian cells (Bucci *et al.*, 1992). In the mutants, endocytic vesicles accumulate and the endosomes fragment (Bucci *et al.*, 1992). Therefore, the Rab5 mutant protein is dispersed in the cytosol instead of being accumulated at the endosome in a punctuate pattern (Bucci *et al.*, 1992).

GFP-Rab5S43N was expressed using elav-GAL4 as described above and its localization was monitored. Consistent with the phenotypes in cultured mammalian cells, the Rab5S43N mutant protein appeared as a diffuse staining filling the entire presynaptic terminal of the larval NMJ (Fig. 14B). This is in contrast to the punctuate pattern observed when GFP-Rab5 was monitored (cf. Fig. 14A and 14B). This indicates, that the GDP-bound mutant form of Rab5 is largely in the cytosol and not associated to the endosomal compartment at the synapse.

To address whether the expression of the dominant negative Rab5S43N affects the endosomal compartment we coexpressed Rab5S43N with GFP-2xFYVE (Fig. 14C) or GFP-Rab5 (not shown) to monitor the endosomes. Instead of a punctuate GFP appearance associated to endosomes as shown before (Fig. 7A, 8C, 14A), we observed a diffuse GFP localization at the presynaptic terminal in synapses expressing Rab5S43N (Fig. 14C). This result suggests that the Rab5 and PI(3)P containing endosome was severely affected. Therefore, Rab5 function is required for the integrity of the endosomal compartment and the traffic through the endosome at the presynaptic terminal.

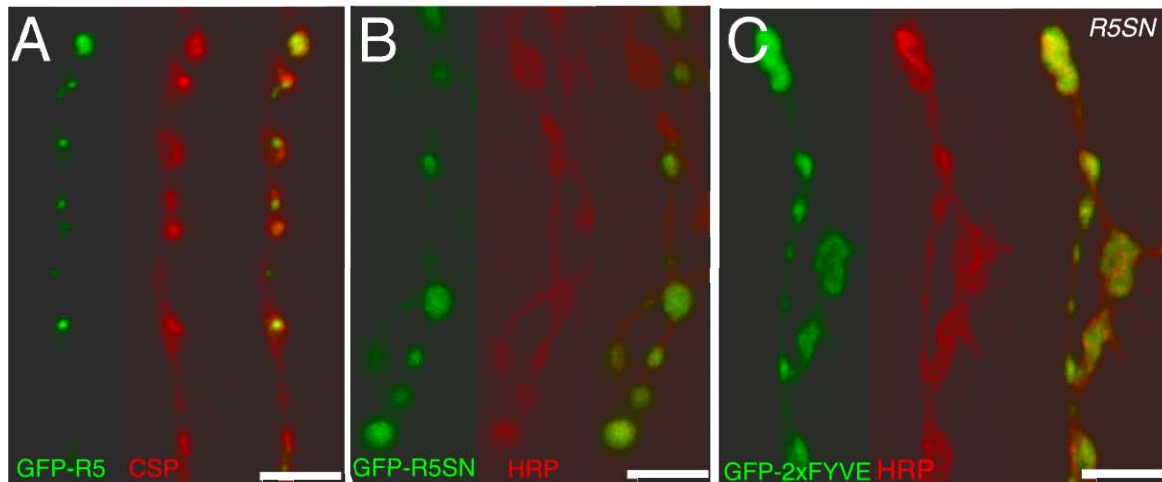


Fig. 14. Endosomes are disrupted in Rab5 mutant expressing presynaptic terminals. (A) Double labeling showing GFP-Rab5 (green) and CSP immunostaining to label the presynaptic terminal (red) in a *w; UAS-GFP-Rab5/elav-GAL4* NMJ. Note the punctuate staining of GFP-Rab5 associated to the endosomes. (B) Double labeling showing GFP-Rab5S43N (green) and HRP immunostaining to monitor the NMJ (red) in a *w; UAS-GFP-Rab5S43N/+; elav-GAL4/+* NMJ. GFP-Rab5S43N is not associated to endosomes and appears dispersed in the cytosol of the presynaptic terminal. (C) Double labeling showing GFP-2xFYVE to label the endosomes (green) and HRP immunostaining to monitor the presynaptic terminal (red) in a *w; UAS-GFP-myc-2xFYVE; elav-GAL4/UAS-Rab5S43N* NMJ. The GFP-2xFYVE labeled endosomal compartment is disrupted upon expression of the dominant negative Rab5S43N mutant as indicated by the cytosolic appearance of GFP-2xFYVE. NMJs of third instar larvae are shown. Bars correspond to 5 μ m.

Endocytic intermediates accumulate in Rab5 mutant presynaptic terminals

We then analyzed the effect of Rab5S43N at the ultrastructural level of type I boutons. In wildtype, type I boutons are surrounded by a prominent subsynaptic reticulum (SSR), which corresponds to the highly folded muscle membrane (Fig. 15A). The presynaptic terminal of type I boutons is filled with small, clear SVs (Fig. 15A-D). In addition, mitochondria required for local energy generation are found in variable numbers (Fig. 15A). The active zones of neurotransmitter release are characterized by an electron dense membrane and the presence of an electron dense T-bar (Fig. 15A). T-bars are unique to *Drosophila* NMJs, however their function is not yet known. We also observed bigger cisternal and tubular structures of around 150 nm, which have been suggested to correspond to endosomal structures (Koenig *et al.*, 1993) (Fig. 15B-D).

In wildtype presynaptic terminals, we could distinguish the two types of vesicles that have been previously reported (Fergestad *et al.*, 1999; Kosaka and Ikeda, 1983a). Synaptic vesicles with a diameter of 35 nm (35.9 ± 0.11 nm, $n = 1991$ vesicles) (Fig. 16A) and a second type of vesicles with a diameter of 70 nm (73.6 ± 2.5 nm, $n = 36$ vesicles) (Fig. 16A, solid arrowheads), previously described as recycling intermediates (Fergestad *et al.*, 1999; Kosaka and Ikeda, 1983a). In *sh^{ts}* mutants, early stages of endocytosis are blocked, causing the accumulation of nascent endocytic vesicles in the form of collared pits at the plasma membrane. Since the 70 nm vesicles have a very similar diameter to these collared pits (Kosaka and Ikeda, 1983a), we suggest that they represent newly formed endocytic vesicles. In addition, endocytic vesicles are probably transient structures since only 2.1 ± 0.5 ($n = 26$ sections) were observed in each EM section.

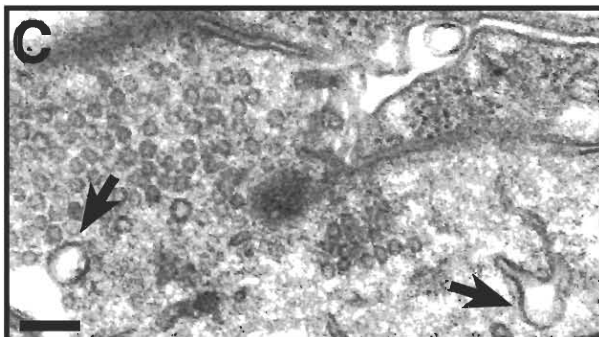
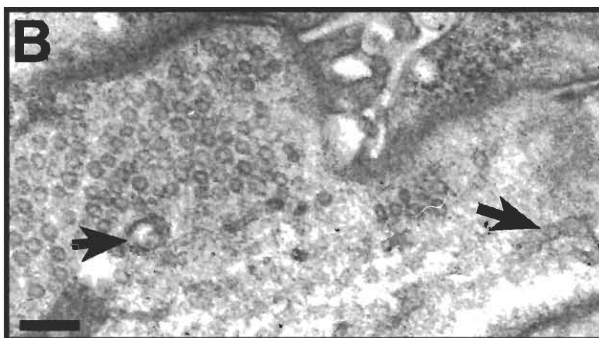
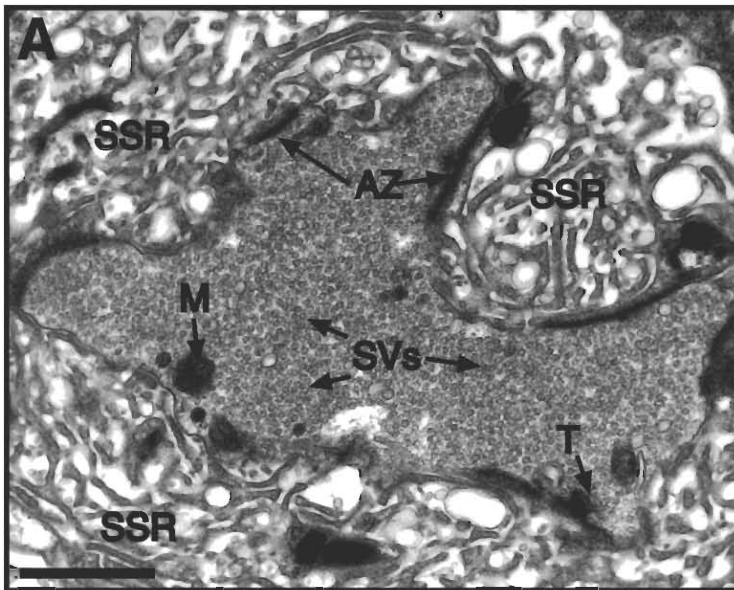


Fig. 15. Morphology of wildtype presynaptic terminals at the ultrastructural level. (A) electron micrograph showing a wild-type synapse surrounded by highly folded muscle membrane, called subsynaptic reticulum (SSR). Wildtype synapses contain mitochondria (M), active zones of neurotransmitter release (AZ), that are characterized by an electron-dense membrane and the presence of an electron-dense T-bar (T). Synapses are filled with synaptic vesicles (SVs). (B-D) electron micrographs corresponding to serial sections from a wild-type synapse showing cisternal (solid arrows) and tubular (empty arrows) endosomal structures. Cisternal structures are frequently detected in serial sections, but are not present in each section through the synapse. Bars correspond to 1 μ m in (A) and 200 nm in (B-D).

Synapses expressing Rab5S43N, showed an accumulation of the 70 nm vesicles (70.6 ± 1.1 nm, $n = 148$ vesicles). 5.9 ± 1.2 ($n = 25$ sections) were observed on average per EM section (Fig. 16B, solid arrowheads). This phenotype suggests that the recycling intermediates (Fergestad *et al.*, 1999; Kosaka and Ikeda, 1983a) indeed correspond to endocytic vesicles, which accumulate in the mutant synapses where Rab5 function is impaired (Fig. 16B, solid arrowheads). These results are consistent with the *Rab5SN* phenotype reported in cultured mammalian cells, where endocytic vesicles accumulate due to their inability to fuse efficiently with the early endosome (Bucci *et al.*, 1992).

We did not observe major changes in other synaptic features in Rab5S43N expressing terminals including the number and structure of the T-bars, the number of docked vesicles as defined as vesicles touching the plasma membrane at the T-bar (Table 2), the overall appearance of the presynaptic terminal and the subsynaptic reticulum postsynaptically. In summary, blocking Rab5 function at the presynaptic terminal using the dominant negative Rab5S43N mutant causes the accumulation of endocytic vesicles, implying that Rab5 regulates the fusion of endocytic vesicles with the endosome.

	WT	<i>Rab5SN</i>	<i>Rab5</i>	<i>GFP-Rab5</i>
docked vesicles	1.31 ± 0.24	1.67 ± 0.20	1.29 ± 0.22	1.22 ± 0.18
n	17	30	14	10

Table 2. Quantification of docked vesicles at the T-bar in wildtype and the different mutants. Docked vesicles were defined as vesicles touching the PM at the T-bar. n corresponds to the number of T-bars analyzed. Genotypes: wildtype (WT), *w*; *UAS-Rab5S43N/+*; *elav-GAL4/+* (*Rab5SN*), *w*; *UAS-Rab5/+*; *elav-GAL4/+* (*Rab5*), *w*; *elav-GAL4/UAS-GFP-Rab5* (*GFP-Rab5*).

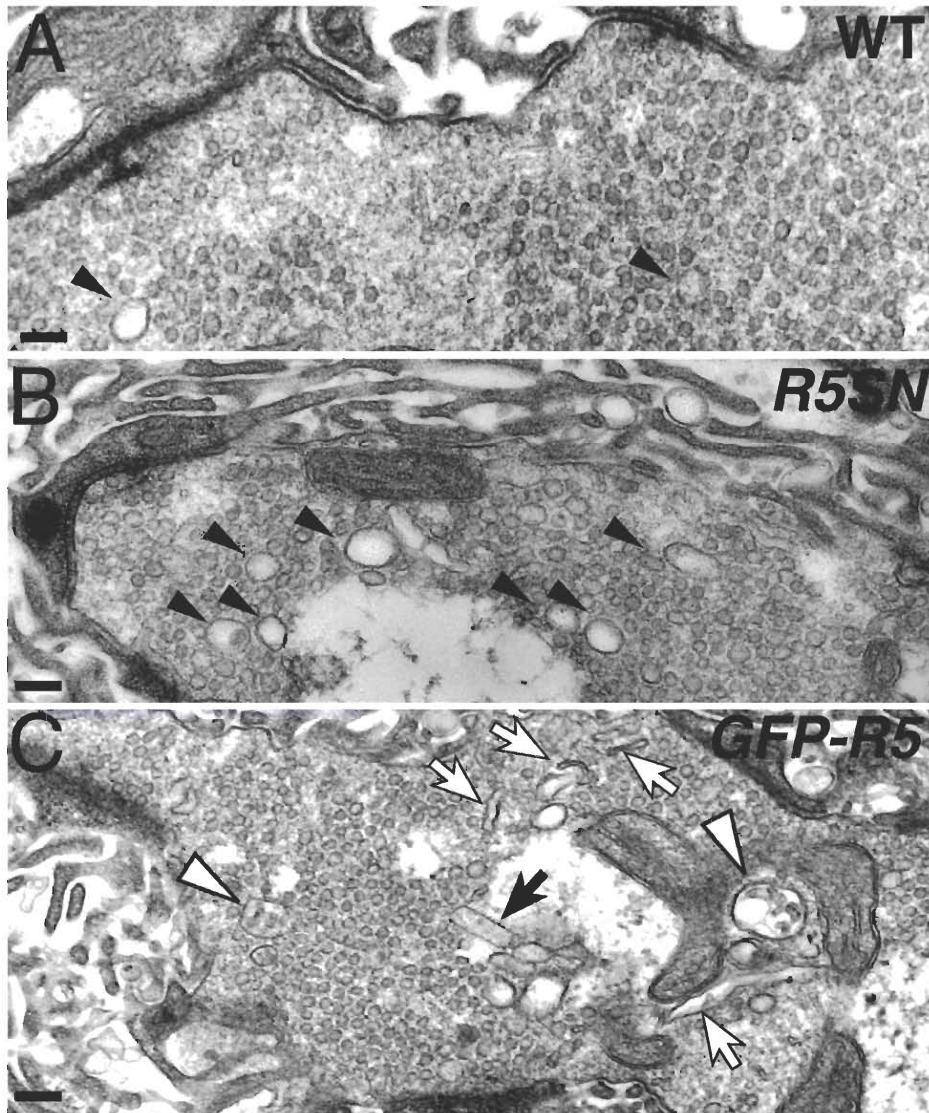


Fig. 16. Endocytic intermediates are affected in Rab5 mutant presynaptic terminals. Ultrastructure of presynaptic terminals of wildtype (A), *w; UAS-Rab5S43N/+; elav-GAL4/+* (B) and *w; UAS-Rab5/+; elav-GAL4/+* third instar larvae (C). Solid arrowheads, endocytic intermediates with an average diameter of 70 nm. (B) In Rab5S43N expressing terminals an accumulation of the 70 nm vesicles was observed. In Rab5 overexpressing terminals (C) tubules (empty arrows), cisternae (solid arrows), and multivesicular bodies (empty arrowheads) can be found in each section through the synapse, indicating an expansion of the endosomal compartment. No major change was observed in other synaptic features neither in Rab5S43N nor in Rab5 overexpressing synapses, including the number and structure of T-bars and number of docked vesicles as defined as vesicles touching the plasma membrane at the T-bar. Bars correspond to 100 nm.

Endocytic trafficking during SV recycling involves Rab5 function

In order to study the role of Rab5 during SV recycling, we performed FM1-43 internalization and release experiments (Betz and Bewick, 1992) (Fig. 17, 18). We monitored three parameters: *first*, the rate of endocytosis, *second*, the size of the vesicle pool and *third*, the recycling rate. The styryl dye FM1-43 is internalized only during endocytosis and the FM1-43 fluorescence is directly proportional to the number of vesicles internalized. Therefore, FM1-43 fluorescence can be used to quantify endocytosis, recycling and the SV pool size.

The rate of internalization was assayed first. FM1-43 uptake was monitored in electrophysiologically stimulated synapse (see methods) at 3 Hz for 3, 5 and 10 minutes in HL3 containing 1.5 mM Ca^{2+} (Stewart *et al.*, 1994) (Fig. 17A-C). In wildtype synapses, FM1-43 fluorescence increased rapidly during the first 3 minutes (Fig. 17C). After the first 3 minutes, the fluorescent increase was slowed down. This phenomenon has been previously reported and was interpreted to be caused by the release of dye-loaded vesicles (Betz and Bewick, 1992; Betz and Bewick, 1993; Kuromi and Kidokoro, 2000; Ryan and Smith, 1995): During the first few minutes FM-dye is only internalized, progressively filling the SV pool with FM1-43 labeled vesicles causing a rapid increase in the fluorescence. Then, after few minutes a mixture of FM1-43 loaded and unloaded vesicles is released. Therefore, the increase in the fluorescence is slowed down due to the release of previously internalized and consequently dye-loaded vesicles. We therefore estimated the rate of dye-internalization by the fluorescence uptake rate during the first 3 minutes. In Rab5S43N expressing presynaptic terminals, the rate of FM1-43 internalization was 2.5 fold slower compared to wildtype (Fig. 17B, C). This result indicates that endocytosis is reduced when Rab5 function is impaired.

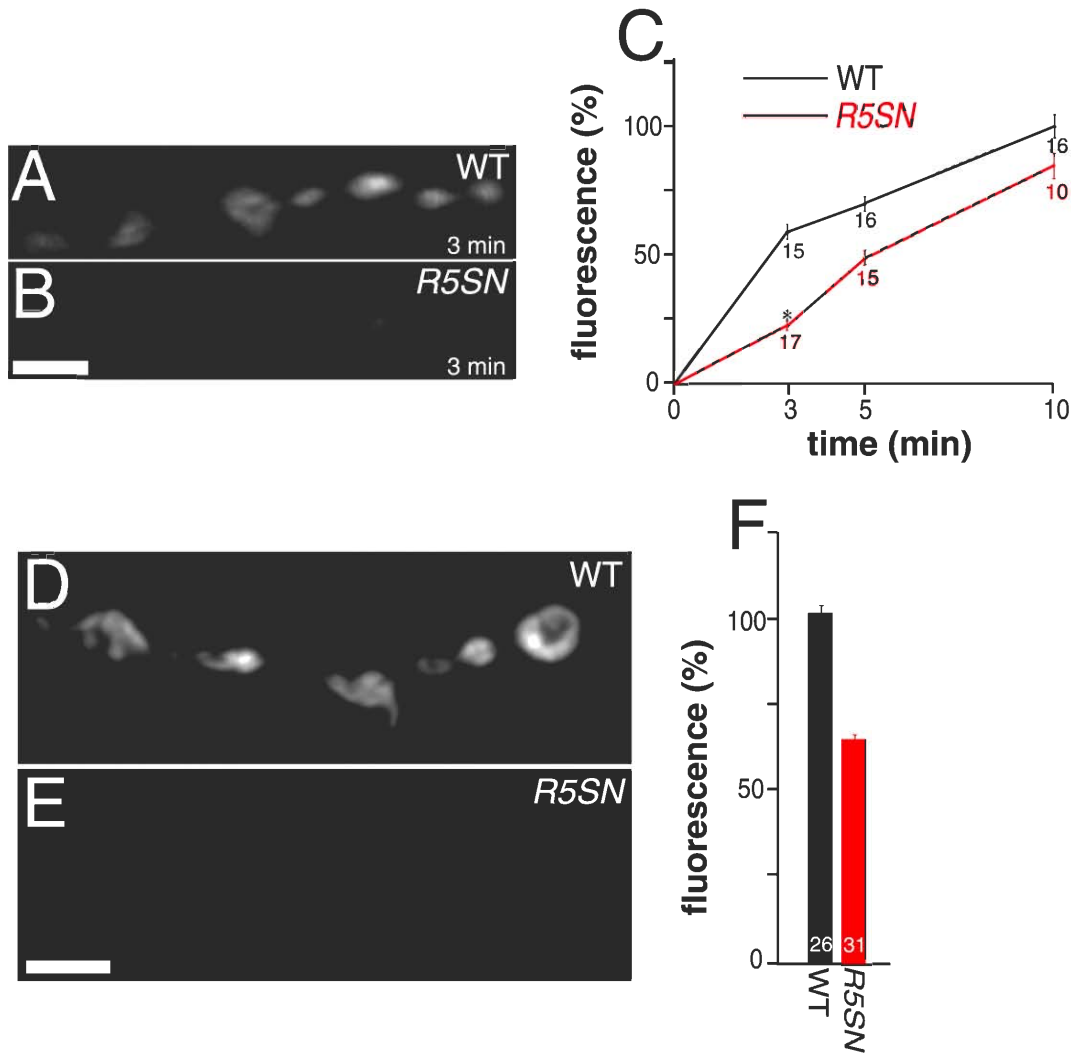


Fig. 17. Rab5 mutants affect SV pool size and kinetics of uptake. (A-C) FM1-43 uptake. (A, B) FM1-43 staining after dye internalization for 3 min at 3 Hz in HL3 containing 1.5 mM Ca^{2+} in wildtype (A) and *w; UAS-Rab5S43N/+; elav-GAL4/+* mutant presynaptic terminals (B). (C) Time course of FM1-43 uptake during stimulation at 3 Hz (HL3, 1.5 mM Ca^{2+}) for 3, 5 and 10 min in wildtype (black) and *w; UAS-Rab5S43N/+; elav-GAL4/+* (red). Fluorescence refers to average pixel brightness values at the terminal normalized as percentage with respect to the average fluorescence in wildtype after 10 min. In the case of *Rab5S43N*, for the uptake quantification after 3 min (asteriks), the terminals were counterstained with the red FM5-95 dye in order to visualize the terminals and quantify the low levels of uptake. Numbers in each time point correspond to the number of NMJs quantified. (D-F) Recycling SV pool size. (D, E) FM1-43 staining in wildtype (D) and *w; UAS-Rab5S43N/+; elav-GAL4/+* terminals after 3 min at 30 Hz in normal saline (2 mM Ca^{2+}) (E). (F) Quantification of FM1-43 internalization upon dye uptake as in (D, E) in wildtype (black) and *w; UAS-Rab5S43N/+; elav-GAL4/+* mutant presynaptic terminals (red). Fluorescence is normalized as percentage with respect to the average fluorescence in wildtype. Numbers in the columns, number of NMJs analyzed. the amount of internalized FM1-43 reaches equilibrium after 3 min. Note the highly significant reduction to $64.15 \pm 2.9\%$ ($p < 0.001$; ANOVA) in the mutant. Error bars correspond to standard errors. Scale bars correspond to 5 μm . Only presynaptic terminals of abdominal A2 - A4 muscle 6/7 NMJs were analyzed.

We next studied the size of the SV pool. The terminal was first loaded by stimulating the synapse at 30 Hz for 3 minutes in normal saline (Jan and Jan, 1976a) (Fig. 17D-F). To test whether the entire recycling pool of vesicles was labeled under these conditions, we increased the stimulation time to 5 minutes at 30 Hz. This increase in the stimulation time did however not further increase the amount of internalized fluorescence at the presynaptic terminal of wildtype or *Rab5S43N* (not shown). This indicates that after 3 min of stimulation at 30 Hz in normal saline, the entire pool of recycling vesicles is labeled with FM1-43, in both wildtype and *Rab5S43N* mutant presynaptic terminals (Fig. 17D-F). We therefore estimated the relative SV recycling pool size by maximally loading the terminal using this protocol. Figure 17F shows that blocking Rab5 function with *Rab5S43N* causes a significant decrease to $64.15 \pm 2.9\%$ ($n = 31$, $p < 0.001$, ANOVA) in the SV recycling pool size.

We then studied the kinetics of FM1-43 release in the mutant synapses (Fig. 18). The terminal was first maximally loaded as described above and subsequently stimulated at 3 Hz for various periods of time in normal saline. The amount of dye released was measured by quantifying the fluorescence remaining within the terminal at each time point (Fig. 18; see methods). We could distinguish three phases during the FM1-43 release in wildtype (Fig. 18G): *first*, a fast release phase during the first 5 minutes, *second*, a slower phase between 5 and 30 minutes and *third*, a third phase, after 30 minutes, when no more dye could be released and $14.5 \pm 1.2\%$ of FM1-43 remained unreleasable. The kinetics of dye release has been previously reported (Betz and Bewick, 1993; Betz *et al.*, 1992). It was shown that during the first phase dye release exactly parallels the amount of neurotransmitter released, because neurotransmitter and dye are released from the same SVs. However, during the second phase significantly less FM-dye than neurotransmitter is released, because the pool of fluorescently labeled SVs becomes increasingly diluted by newly recycled vesicles that do not contain FM1-43.

In the *Rab5S43N* mutant synapses, dye release occurred 2.5 times slower during the first 5 minutes (Fig. 18G; also cf. 18A, B vs. 18D, E), indicating that impaired Rab5 function affects SV release. In addition, the fraction of unreleasable dye was increased to $38.0 \pm 3.3\%$ in Rab5S34N expressing synapses (Fig. 18G). In summary, these data indicate that SV recycling is impaired in *Rab5S43N* mutant synapses. This is consistent with a role of Rab5 in the formation of clathrin-coated vesicles (McLauchlan *et al.*, 1998) and their subsequent fusion to the early endosome (Bucci *et al.*, 1992; Stenmark *et al.*, 1994).

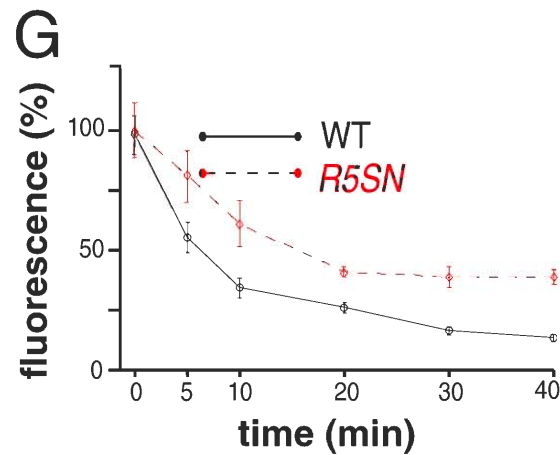
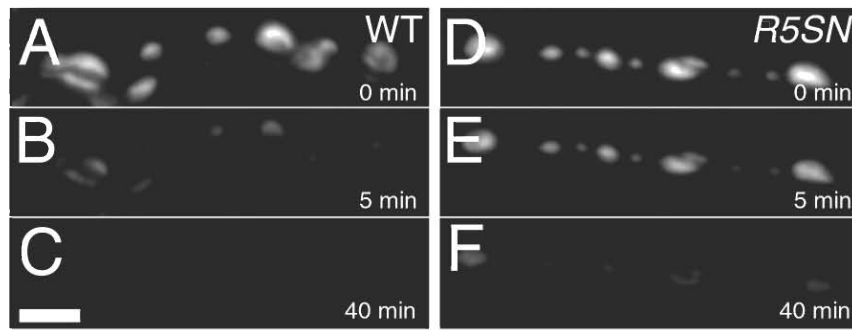


Fig. 18. Rab5 mutations affect the FM1-43 release kinetics. (A-F) FM1-43 fully loaded SV pool stained during 30 Hz stimulation for 3 min in normal saline containing 2 mM Ca^{2+} in wildtype (A) and *w; UAS-Rab5S43N/+; elav-GAL4/+* mutant presynaptic terminals (D). Staining of the same wildtype (B, C) and mutant NMJs (E, F) after 5 min (B, E) and 40 min (C, F) of release by stimulation at 3 Hz (normal saline, 2 mM Ca^{2+}). Brightness in (A) and (D) was adjusted for the best contrast of the signal and the imaging conditions were maintained in (B, C) and (E, F) respectively. (G) Time course of FM1-43 release in wildtype (black, $n = 6$ NMJs) and *w; UAS-Rab5-S43N/+; elav-GAL4/+* (red, $n = 7$ NMJs) presynaptic terminals. Terminals were first fully loaded (3 min stimulation at 30 Hz in normal saline containing 2 mM Ca^{2+}) and fluorescence was quantified. Afterwards, synapses were stimulated at 3 Hz (in normal saline, 2 mM Ca^{2+}) during 5, 10, 20, 30 and 40 min to study the release kinetics. Fluorescence refers to average pixel brightness values at the terminals normalized as percentage with respect to the average fluorescence of the fully loaded SV pool before release. Error bars correspond to standard errors. Scale bars correspond to 5 μm . Only presynaptic terminals of A2 - A4 muscle 6/7 NMJs were analyzed.

Rab5-dependent recycling determines the SV fusion efficacy

How does recycling through the endosome affect the performance of SVs during Ca^{2+} -triggered exocytosis? To address this question, we performed current clamp electrophysiological recordings, a method to measure in the muscle the postsynaptic response caused by presynaptic neurotransmitter release (Fig.19). Under physiological conditions, in the absence of synaptic activity, the membrane potential of the muscle is negative, around -60 mV. It can be measured with a glass electrode (recording electrode) inserted into the muscle. Synaptic activity is then induced by stimulating the segmental nerve with a stimulation electrode. This is achieved by sucking a segmental nerve into the stimulation electrode and applying a short, positive current to induce APs. The APs travel along the axon to the presynaptic terminal. At the presynaptic terminal, each action potential causes the opening of voltage-gated Ca^{2+} -channels. Ca^{2+} -ions enter the presynaptic terminal and trigger the fusion of primed SVs with the plasma membrane. Glutamate is released into the synaptic cleft. Subsequently, the neurotransmitter binds and opens ligand-gated cation-channels located within the postsynaptic membrane causing an influx of cations into the muscle fiber. The influx of cations in turn elicits a very rapid and transient increase in the muscle membrane potential. This increase can be measured with the recording electrode as an excitatory junction potential (EJP).

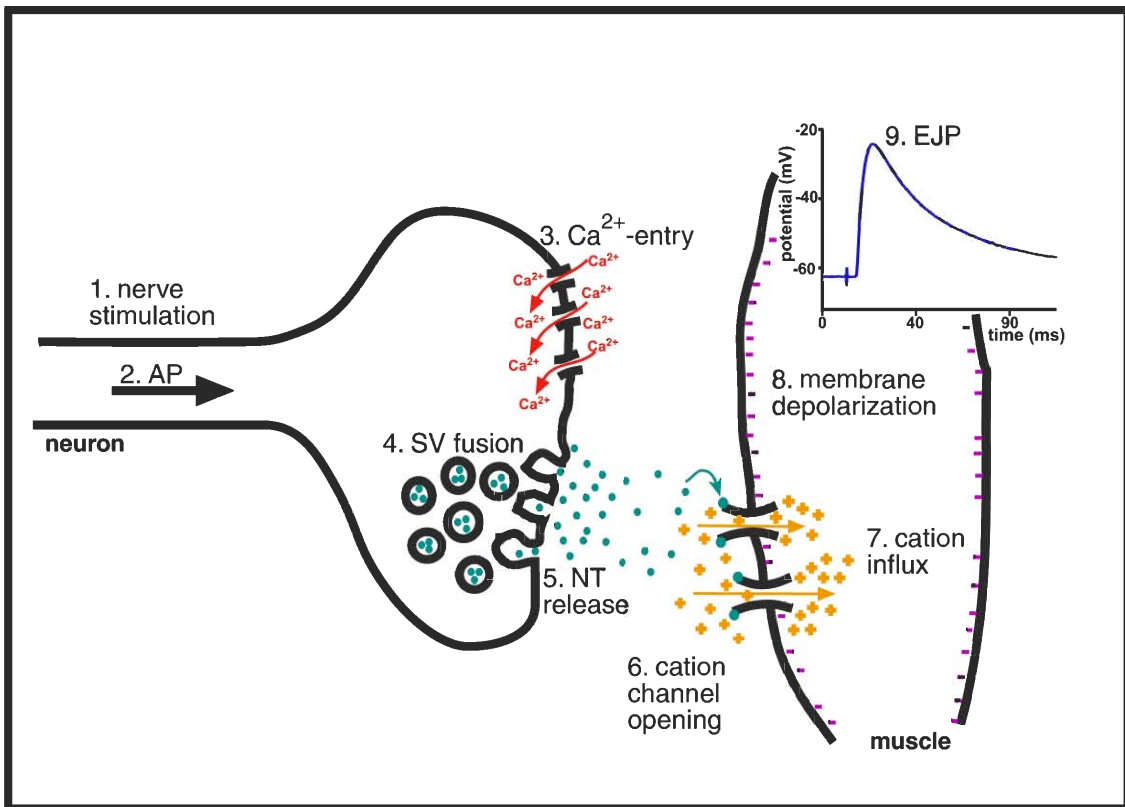


Fig. 19. Measuring synaptic transmission. Indicated are the main steps causing an excitatory junction potential (EJP). Nerve stimulation (1.) induces an action potential (AP, 2.), which travels along the axon to the presynaptic terminal. Within the presynaptic terminal, the AP causes the opening of Ca²⁺-channels (3.). Ca²⁺ enters the presynaptic terminal and triggers the fusion of synaptic vesicles (SVs) with the PM (4.). Neurotransmitter (NT) is released (5.), binds to NT-specific cation-channels in the muscle membrane and induces their opening (6.). Cations enter the muscle (7.) causing a membrane depolarization (8.), which can be measured as EJP with a recording electrode inserted into the muscle (9.).

SVs do not only fuse to the presynaptic membrane after the action potential induced influx of Ca^{2+} into the presynaptic terminal. Single SVs also fuse spontaneously with the membrane, however with a relatively low frequency. The change in the muscle membrane potential caused by neurotransmitter released from single vesicle is called spontaneous or miniature EJP (mEJP) (Katz, 1969). Its size reflects the amount of neurotransmitter stored within a single vesicle, called the quantal size. In addition, the mEJP size depends on the number and sensitivity of the postsynaptic glutamate receptors. By knowing the EJP and the mEJP amplitude it is possible to calculate the quantal content of the response, which reflects the number of SVs that fused after a single action potential. The quantal content is calculated by dividing the EJP amplitude by the mEJP amplitude measured in the same muscle and correcting for nonlinear summation according to Martin (Martin, 1955).

To address whether synaptic transmission is affected in *Rab5S43N* we recorded mEJPs and nerve-evoked EJPs in muscle 6 of third instar larvae (Fig. 20, 21) raised under 3 different conditions (Table 3, 4). Changes in the mean mEJP frequency reflect a change in the total number of fusion competent vesicles. Alterations in the mean mEJP amplitude are indicative for changes in the neurotransmitter content or an affected postsynaptic sensitivity to the released neurotransmitter. mEJP recordings from *Rab5S43N* mutant NMJs displayed no significant differences in mean amplitude, variability, frequency or voltage decay kinetics compared to wildtype mEJPs (Table 3, Fig. 20).

This result indicates that presynaptic expression of *Rab5S43N* does not affect the vesicular neurotransmitter content, the number of fusion competent vesicles or the postsynaptic glutamate receptor function or density. This is consistent with the normal synaptic ultrastructure (Fig. 16), mean number of active zones (Fig. 13E) and docked vesicles at the T-bar (Table 2, Fig. 16) of the mutant NMJs as shown above.

genotype	16°C		25°C		29°C	
	frequency (Hz)	amplitude (mV)	frequency (Hz)	amplitude (mV)	frequency (Hz)	amplitude (mV)
WT	4.4±0.17	1.5±0.05	3.7±0.17	1.3±0.06	3.1±0.17	1.4±0.06
R5SN	3.9±0.24	1.5±0.06	3.3±0.23	1.3±0.06	2.8±0.19	1.3±0.06
R5	3.4±0.20	1.3±0.05	2.8±0.17	1.3±0.07	1.9±0.16	1.3±0.09
GFP-R5	3.3±0.20	1.2±0.05	3.1±0.18	1.4±0.06	3.0±0.14	1.2±0.05

Table 3. mEJP frequencies and amplitudes. Overview of mEJP frequencies and amplitudes in wildtype and the different mutants. Animals were raised using 3 different temperature protocols: *First*, animals were raised at 16°C until the third larval stage (16°C), *second*, animals were raised at 16°C until early third instar larvae, followed by 25°C during the last two days of larval development (25°C), and *third*, animals were raised at 16°C until early third instar larvae, followed by 29°C during the last two days of larval development (29°C). Note that there were no significant differences in the mEJP amplitudes. The mEJP frequencies were slightly higher in animals raised at 16°C until third instar larvae and were slightly lower in animals raised at 29°C during the last two days of larval development compared to animals raised at 25°C during the last two days of larval development. Differences between different genotypes of animals raised using the same temperature protocol or between animals of the same genotype raised using different temperature protocols were not significant ($p > 0.05$, ANOVA). Between 16 and 37 muscles 6 were analyzed per condition. Genotypes: wildtype (WT), *w; UAS-Rab5S43N/+; elav-GAL4/+* (R5SN), *w; UAS-Rab5/+; elav-GAL4/+* (R5), *w; elav-GAL4/UAS-GFP-Rab5* (GFP-R5).

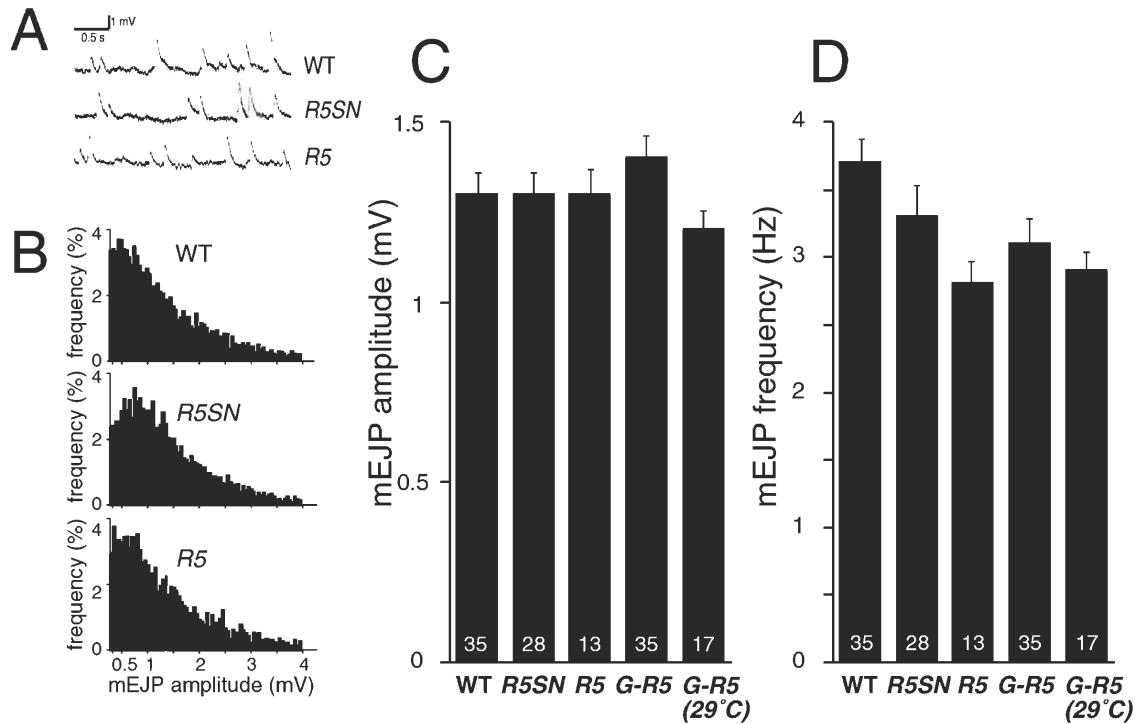


Fig. 20. Spontaneous release is normal in Rab5 mutant synapses. (A) Spontaneous mEJP traces from wildtype (WT), *w; UAS-Rab5S43N/+; elav-GAL4/+* (*R5SN*), and *w; UAS-Rab5/+; elav-GAL4/+* (*R5*) mutant muscle 6. (B) mEJP amplitude distribution from WT, (n = 6187 events); *R5SN*, (n = 4395); *R5*, (n = 3391) muscle 6. (C, D) Mean mEJP amplitudes (C) and mean mEJP frequencies (D) of wildtype (WT), *w; UAS-Rab5S43N/+; elav-GAL4/+* (*R5SN*), *w; UAS-Rab5/+; elav-GAL4/+* (*R5*), *w; UAS-GFP-Rab5/elav-GAL4* (*G-R5*) and *w; UAS-GFP-Rab5/elav-GAL4* raised at 29°C during the last two days of larval development (*G-R5(29°C)*). In the different genotypes studied, there were no significant differences in the mean mEJP amplitude (C) (in mV, WT: 1.3 ± 0.06 , n = 35; *R5SN*: 1.3 ± 0.06 , n = 28; *R5*: 1.3 ± 0.07 , n = 13; *G-R5*: 1.4 ± 0.06 , n = 35; *G-R5(29°C)*: 1.2 ± 0.05 , n = 17 muscle 6) or mean mEJP frequency (D) (in Hz, WT: 3.7 ± 0.17 , n = 35; *R5SN*: 3.3 ± 0.23 , n = 28; *R5*: 2.8 ± 0.17 , n = 13; *G-R5*: 3.1 ± 0.18 , n = 35; *G-R5(29°C)*: 3.0 ± 0.14 , n = 17 muscle 6). Error bars correspond to standard errors. Muscles 6 in abdominal segments A2 - A4 from late third instar larvae were analyzed.

We next addressed the efficacy of the evoked synaptic transmission (Table 4, Fig. 21). EJPs were evoked by stimulating the segmental nerve at 0.5 Hz and the voltage response in the muscle was measured using standard intracellular recording conditions (see methods).

genotype	16°C		25°C		29°C	
	amplitude (mV)	% quantal content	amplitude (mV)	% quantal content	amplitude (mV)	% quantal content
EJP						
WT	23.2±1.7	100.0±11.0	23.5±1.4	100.0± 7.2	19.0±0.8	100.0± 5.9
R5SN	15.5±1.4	52.8± 6.1	12.9±1.2	49.8± 7.8	10.5±1.1	44.2± 6.5
R5	29.9±1.7	170.7±12.2	28.0±1.5	137.6±12.1	25.5±1.1	132.7±11.9
GFP-R5	31.3±1.9	194.3±19.9	30.0±1.1	137.3± 9.8	33.0±1.2	208.8±11.1

Table 4. Mean EJP amplitudes and mean quantal contents. Overview of the mean EJP amplitudes and mean quantal contents in wildtype and the different mutants measured in HL3 containing 0.75 mM Ca²⁺. Animals were raised using 3 different temperature protocols: *First*, animals were raised at 16°C until the third larval stage (“16°C protocol”, 16°C), *second*, animals were raised at 16°C until early third instar larvae, followed by 25°C during the last two days of larval development (“25°C protocol”, 25°C), and *third*, animals were raised at 16°C until early third instar larvae, followed by 29°C during the last two days of larval development (“29°C protocol” 29°C). Note that the reduction of the quantal content in *Rab5S43N* compared to wildtype increases from a reduction to 52.8% using the 16°C protocol to a reduction to 44.2% using the 29°C protocol. Between 16 and 37 muscles 6 were analyzed per condition. Genotypes as in Table 3.

The EJP measured in HL3 containing 0.75 mM Ca²⁺ in wildtype was 23.5 ± 1.4 mV (n = 35) and was significantly reduced in *Rab5S43N* expressing NMJs to 12.9 ± 1.2 mV (n = 28) using the “25°C protocol” (Table 4, Fig. 21A, B). We next calculated the number of vesicles fusing upon arrival of a single action potential, the quantal content, from the mean EJP amplitude and from the mean mEJP amplitude measured in the same muscle (see methods; (Martin, 1955)). We observed that the mean quantal content was drastically reduced to 49.8 ± 7.8% (n = 28) in *Rab5S43N* expressing terminals when compared to wildtype larvae using the “25°C protocol” (Table 4, Fig. 21C), consistent with a decreased FM1-43 release rate in the mutant (Fig. 18). Since the number of docked vesicles (Table 2) and the spontaneous release rate were normal in *Rab5S43N* expressing synapses (Table 3, Fig. 20), these data indicate that impaired *Rab5*

function led to a reduced probability of the Ca^{2+} -triggered release of synaptic vesicles.

We next studied the paired-pulse behavior, a form of synaptic short-term plasticity (Fig. 22A) (Zucker, 1989; Zucker, 1999). This was performed by applying two stimuli with only a short interpulse interval, the second stimulus following the first stimulus within 20 msec. The paired-pulse behavior usually correlates with the size of the first EJP. Synapses with a high release probability and therefore with a large first EJP usually show depression. This is observed as a decrease in the size of the second EJP compared to the first EJP. In contrast, synapses with a low release probability and therefore with a small first EJP usually show paired-pulse facilitation, as indicated by an increased EJP to the second stimulus. According to the residual Ca^{2+} -hypothesis, Ca^{2+} levels are still elevated after the first stimulus, when the second AP arrives. This leads to a further increase in the intracellular Ca^{2+} -concentration (Zucker, 1999). Synapses with low release probabilities respond to the further elevated Ca^{2+} -levels with an increased number of SVs fusing, causing an increased second EJP. In contrast, synapses with high release probabilities, release most of their fusion competent SVs already upon the first stimulus, depleting the pool of primed SVs. Therefore, the second stimulus rather causes a decreased EJP as less fusion-competent vesicles are available than during the first stimulus.

Consistent with the reduced release probability, *Rab5S43N* synapses show stronger paired pulse facilitation than wildtype synapses (Fig. 22A). In wildtype synapses, responses show a slightly facilitated paired-pulse ratio (Q_2/Q_1) of 1.3 ± 0.1 ($n = 26$) at a 20 ms interpulse interval in 0.75 mM $[\text{Ca}^{2+}]_e$ (Fig. 22A). In contrast, *Rab5S43N* expressing terminals show a significantly stronger facilitation and exhibited a Q_2/Q_1 ratio of 2.0 ± 0.2 ($n = 15$, $p < 0.05$). Therefore, *R5S43N* expressing presynaptic terminals show an altered paired-pulse behavior, consistent with a reduced release probability of the SVs.

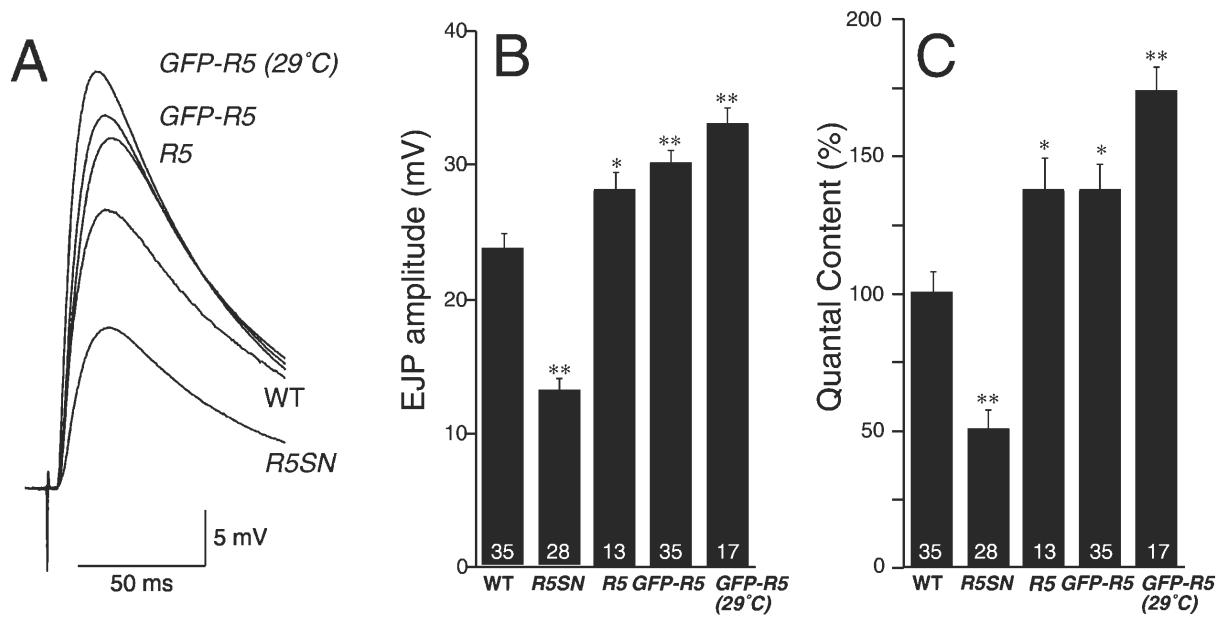


Fig. 21. Neurotransmitter release probability is affected in Rab5 mutant synapses. (A) Nerve-evoked EJP traces from wildtype (WT) and different Rab5 mutants. Genotypes in (A-C): wildtype (WT), *w; UAS-Rab5S43N/+; elav-GAL4/+ (R5SN)*, *w; UAS-Rab5/+; elav-GAL4/+ (R5)*, *w; UAS-GFP-Rab5/elav-GAL4 (GFP-R5)*, *w; UAS-GFP-Rab5/elav-GAL4 raised at 29°C during the last two days of larval development (GFP-R5(29°C))*. (B) Mean EJP amplitudes of wildtype and the different mutants. The mean amplitudes were (in mV) WT: 23.5 ± 1.4 ; *R5SN*: 12.9 ± 1.2 ; *R5*: 28.0 ± 1.5 ; *GFP-R5*: 30.0 ± 1.1 ; *GFP-R5(29°C)*: 33.0 ± 1.2 . Number in columns, number of muscle 6 analyzed. (C) Mean quantal content in wildtype and different Rab5 mutants. Quantal content is normalized as percentage of wildtype. The quantal content was (in %) *R5SN*: 49.8 ± 7.8 ; *R5*: 137.6 ± 12.1 ; *G-R5*: 137.3 ± 9.8 ; *G-R5(29°C)*: 173.7 ± 9.4 . Number in columns, numbers of muscle 6 analyzed. Error bars correspond to standard errors. One asteriks denotes $p < 0.05$ significance value with respect to wildtype and two asteriks, $p < 0.01$ (ANOVA). No significant differences in the EJP and quantal contents were observed in controls submitted to the 29°C treatment when compared to animals at 25°C.

Since the Ca^{2+} -triggered release probability was reduced in *R5S43N* expressing synapses, we next examined the Ca^{2+} -sensitivity and Ca^{2+} -cooperativity during neurotransmitter release. The Ca^{2+} -cooperativity reflects the Ca^{2+} -binding to the Ca^{2+} -sensor of the release machinery, which likely corresponds to the vesicle protein Synaptotagmin (Brose *et al.*, 1992; Desai *et al.*, 2000; Fernandez-Chacon *et al.*, 2001; Geppert and Sudhof, 1998; Littleton and Bellen, 1995; Littleton *et al.*, 1999; Perin *et al.*, 1990). In order to study the Ca^{2+} -sensitivity and Ca^{2+} -cooperativity we systematically examined the quantal content as a function of the external Ca^{2+} -concentration ($[\text{Ca}^{2+}]_e$) (Fig. 22B). The slope of the Ca^{2+} -dependency of the mean quantal content was not affected in the mutant synapses (Fig. 22B), reflecting a normal Ca^{2+} -cooperativity and indicating that Ca^{2+} -binding to the Ca^{2+} -sensor was not affected.

However, for all $[\text{Ca}^{2+}]_e$ examined, the release probability in *Rab5S43N* was significantly reduced (Fig. 22B) indicating that the defect induced by the impaired Rab5 function is likely to be Ca^{2+} -independent and probably affects the efficacy of the evoked SV fusion process itself. This can be either due to a reduced number of fusion competent vesicles or due to a reduced efficacy of vesicular release. The fact that the mEJP frequency (Table 3, Fig. 20D) as well as the number of active zones and docked vesicles (Table 2, Fig. 13C, E, 16B) is normal in *Rab5S43N* implies that it is the probability of SV fusion, which is affected in the mutant. Furthermore, the change in the paired-pulse behavior (Fig. 22A) also indicates that the effect is not simply due to a change in the number of synapses, but is rather due to a change in synaptic performance. In summary, Rab5-dependent endosomal trafficking determines the efficacy of Ca^{2+} -triggered exocytosis at the presynaptic terminal. Impaired Rab5 function causes a reduction in the release probability of SVs.

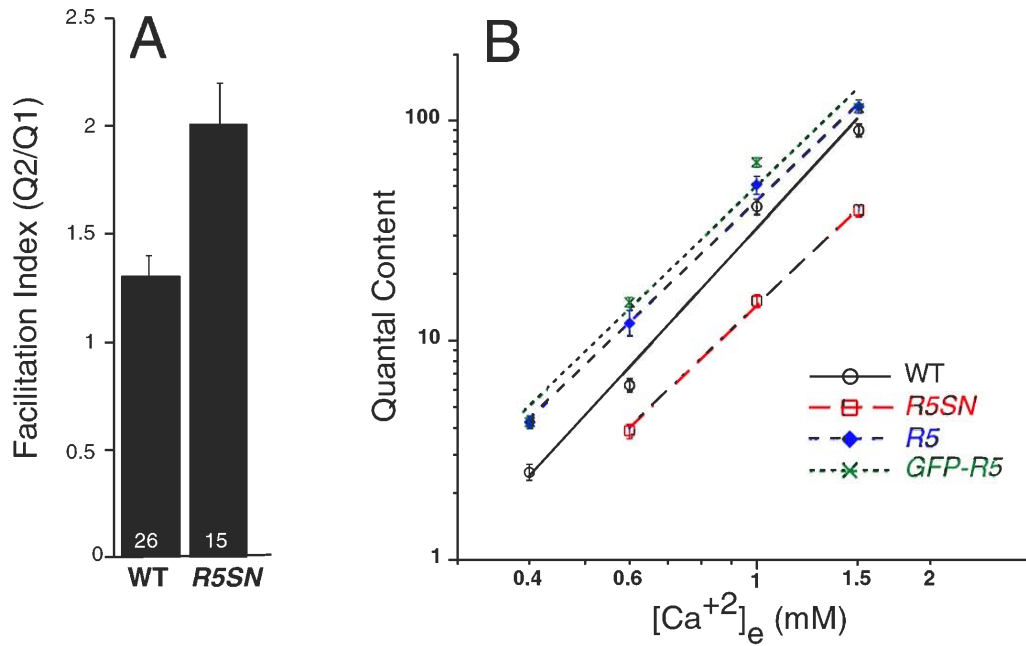


Fig. 22. Short-term plasticity and Ca²⁺-cooperativity in wildtype and the Rab5 mutants. (A) Paired-pulse facilitation. Facilitation index (Q2/Q1) calculated as mean ratio of the quantal contents of the second vs. the first response in a paired-pulse stimulation protocol with a 20 ms interpulse interval. Q2/Q1 was significantly higher ($p < 0.05$) in *Rab5S43N* with respect to wildtype (WT: 1.3 ± 0.1 ; R5SN: 2.0 ± 0.2). Numbers in columns, number of muscles 6 analyzed. (B) Ca²⁺-dependency of the quantal content in WT (black o), *R5SN* (red □), *R5* (blue ◆) and *GFP-R5* (green x). Genotypes: wildtype (WT), *w; UAS-Rab5S 43N/+; elav-GAL4/+* (*R5SN*), *w; UAS-Rab5/+; elav-GAL4/+* (*R5*), *w; UAS-GFP-Rab5/elav-GAL4* (*GFP-R5*). Note, there are no differences in the slope of the Ca²⁺-dependency of the quantal content. More than 10 muscle 6 were analyzed per Ca²⁺-condition. Error bars correspond to standard errors.

Analysis of Rab5 gain of function

Rab5-mediated endosomal trafficking is rate-limiting during SV recycling and synaptic transmission

We have shown above that Rab5 is required during SV recycling and synaptic transmission. Expression of the dominant negative version of Rab5, Rab5S43N causes a reduction in both the rate of endocytosis and the size of the recycling SV pool. Furthermore, Rab5S43N causes the accumulation of endocytic vesicles and a decrease in the fusion efficacy of SVs, while synaptic morphology was normal.

What happens if Rab5 is overexpressed? It has been shown in cultured mammalian cells that Rab5 is rate-limiting in the regulation of the kinetics of endocytic vesicle fusion with the early endosome (Bucci *et al.*, 1992) and in the homotypic fusion between early endosomes (Rybin *et al.*, 1996). The level of available active Rab5 regulates the degree of recruitment of tethering and fusion factors to the Rab5 subdomain at the early endosome and thereby the extent of the subsequent fusion. If Rab5-dependent trafficking is also rate-limiting in the synapse, Rab5 overexpression should cause an increase in the SV recycling efficacy and thereby an improved synaptic performance.

To address this issue we overexpressed Rab5 in the CNS and monitored synaptic development, the kinetics of recycling, synaptic transmission and the ultrastructure of the synapse. As with Rab5S43N, Rab5 and GFP-Rab5 were expressed specifically in the CNS with elav-GAL4. The expression levels were controlled using to the thermosensitivity of GAL4 in *Drosophila* (Brand *et al.*, 1996; Entchev *et al.*, 2000) (see methods). Expression was kept low during embryonic and early larval development at 16°C and was increased during the last to two days of larval development at either 25°C or 29°C.

Overexpression of Rab5 does not cause a developmental phenotype of the NMJ but causes an enlargement of endosomes

Rab5 or GFP-Rab5 expressed as described above did not cause a developmental phenotype of the NMJ. The overall NMJ morphology was normal (Fig. 13A). In addition, no change in the synaptic surface (Fig. 13D) and in the density of active zones was detected (Fig. 13E). As the development was normal, we next studied the ultrastructure of Rab5-overexpressing presynaptic terminals (Fig. 16). We observed no difference in the overall synaptic morphology or structure of the postsynaptic SSR. In addition, the number of docked vesicles at the T-bar was normal (Table 2). In wildtype, we observed 1.31 ± 0.24 docked vesicles at the T-bar ($n = 17$ T-bars), in *Rab5* 1.29 ± 0.22 ($n = 14$) and in *GFP-Rab5* 1.22 ± 0.18 ($n = 10$). However, endosomal structures were enlarged in the Rab5 overexpressing terminals. In wildtype, cisternal structures were only occasionally found. In contrast, in each random EM section through the overexpressing terminals, we observed large tubular structures (Fig. 16C; empty arrows), cisternal structures (Fig. 16C; solid arrows) and multivesicular bodies (Fig. 16C; empty arrowheads). Therefore, as in cultured mammalian cells (Bucci *et al.*, 1992) Rab5 overexpression at the *Drosophila* NMJ causes enlarged endosomal structures.

Rab5 overexpression enhances synaptic performance

Rab5 overexpression in cultured mammalian cells causes an increase in the rates of endocytosis as measured by dye internalization and transferrin uptake assays (Bucci *et al.*, 1995; Bucci *et al.*, 1992). Consistently, FM1-43 internalization rates were significantly increased up to $118.0 \pm 4.4\%$ ($n = 14$ NMJs; $p < 0.05$; 3 Hz 10 min) in HL3 containing 1.5 mM Ca^{2+} and up to $158.82 \pm 4.5\%$ ($n = 16$ NMJs, $p < 0.0001$; 3 Hz 15 min) in HL3 containing 0.75 mM Ca^{+2} in Rab5 overexpressing terminals with respect to control (not shown). Therefore, like in mammalian cells (Bucci *et al.*, 1992), Rab5 overexpression causes an increase in the endocytic rate, as reflected by the internalization rate.

We next studied the size of the recycling SV pool by FM1-43 internalization for 3 min at 30 Hz in normal saline (as described above) and observed an average fluorescence intensity in the Rab5 overexpressing terminals of $102 \pm 2.6\%$ ($n = 25$ NMJs) compared to wildtype. Using this dye uptake protocol the entire pool of recycling SVs was labeled in Rab5 overexpressing synapses, because an increase in the stimulation time to 5 min did not further increase the amount of internalized fluorescence (as described above). Therefore, we observed no difference between wildtype and Rab5 overexpressing terminals in the size of the recycling SV pool, indicating that Rab5 overexpression did not increase the size of the recycling SV pool at the synapse. We then studied SV recycling by first loading the entire SV pool as described above and then stimulating at 3 Hz for different periods of time in normal saline. We observed no differences in the FM1-43 release kinetics when compared to wildtype (not shown). This indicates that Rab5 overexpression does not affect SV release kinetics.

To address the effect of Rab5 overexpression on the efficacy of vesicular release we recorded mEJPs and EJPs and calculated the quantal content upon basal stimulation at 0.5 Hz as described above (Table 3, 4, Fig. 20, 21). mEJPs of Rab5 overexpressing synapses displayed no significant difference in the mean amplitude, variability, frequency or voltage decay kinetics compared to wildtype (Table 3, Fig. 20). This indicates that the vesicular neurotransmitter content, the number of fusion competent SVs and the postsynaptic glutamate receptor function and density are normal in the overexpressing terminals. These observations are consistent with the normal NMJ morphology (Fig. 13A, D, E) and normal number of docked SVs as observed at the ultrastructural level (Table 2, Fig. 16C).

The mean EJP was significantly increased from 23.5 ± 1.4 mV ($n = 35$ muscles 6) in wildtype to 28.0 ± 1.5 mV ($n = 13$ muscles 6) in Rab5 overexpressing terminals and to 30.0 ± 1.1 mV ($n = 35$ muscles 6) in GFP-Rab5 overexpressing terminals (Table 4, Fig. 21B). This phenotype was even further increase in GFP-Rab5 overexpressing NMJs in animals raised at 29°C during the last two days of larval development (see methods) to an EJP of 33.0 ± 1.2 ($n = 17$

muscles 6) (Table 4, Fig. 21B). Consistently, the quantal content was significantly increased up to 1.74 fold with respect to wildtype (Table 4, Fig. 21C). The phenotype caused by Rab5 and GFP-Rab5 is the same, supporting the finding, that GFP-Rab5 is a functional Rab5 fusion. Since the number of docked vesicles (Table 2) and the mEJP frequency were normal (Table 3, Fig. 20), the higher quantal content indicates that elevated levels of Rab5 function led to an increased probability of the Ca^{2+} -triggered SV release. Consistently, Rab5 overexpressing synapses showed a slightly depressed paired-pulse behavior. The Q2/Q1 ratio was 1.0 ± 0.4 ($n = 17$ muscle 6) for Rab5 overexpressing presynaptic terminals and 0.8 ± 0.3 ($n = 19$ muscle 6) in the case of GFP-Rab5 overexpressing terminals compared to a Q2/Q1 ratio of 1.3 ± 0.1 ($n = 26$ muscles 6) in wildtype (not shown).

We finally examined the Ca^{2+} -cooperativity and the Ca^{2+} -dependency of the quantal content (Fig. 22B). We observed no change in the slope of the Ca^{2+} -dependency of the quantal content (Fig. 22B), indicating that the Ca^{2+} -binding to the Ca^{2+} -sensor of the release machinery was normal. Therefore, overexpression of Rab5 or GFP-Rab5 causes an increase in the efficacy of the Ca^{2+} -triggered SV exocytosis. We conclude that Rab5-mediated endosomal trafficking affects in a rate-limiting manner a Ca^{2+} -independent step during the SV fusion process.

Discussion

Synaptic vesicle recycling

At the presynaptic terminal, SVs are regenerated through a local recycling process after Ca^{2+} -triggered exocytosis. However, the mechanism of SV recycling is largely unknown. Two models for SV retrieval have been proposed: “kiss-and-run” and clathrin-mediated endocytosis (Ceccarelli *et al.*, 1973; Fesce *et al.*, 1994; Heuser and Reese, 1973; Valtorta *et al.*, 2001). Recent evidence suggests that both models are valid and that two or more recycling pathways might operate simultaneously and/or in different systems. Why should a neuron use different recycling mechanisms, and how does it control which pathway is used? It has been proposed that the molecular composition of the vesicles influences their competence for “kiss-and-run” (Burgoyne *et al.*, 2001; Valtorta *et al.*, 2001). Furthermore, the “kiss-and-run” mode might be used under high frequency stimulation conditions, when fast SV recycling is required (Alés *et al.*, 1999).

“kiss-and-run” recycling ensures a stable composition of SVs and PM, since no mixing of the two membranes occurs. However, this also implies that the same molecular SV components including proteins and lipids are used repeatedly. This raises the question of how turned over proteins and lipids are sorted out and are replaced. The second SV recycling pathway, clathrin-mediated endocytosis, might provide a mechanism to control the SV membrane composition: Endocytic vesicles derived by clathrin-mediated endocytosis could fuse to early endosomes, where sorting can occur. Although endosome-like structures have been observed in nerve terminals (de Hoop *et al.*, 1994; Parton *et al.*, 1992; Sulzer and Holtzman, 1989; Teichberg and Holtzman, 1975), it is controversial whether SV recycling involves trafficking through endosomal compartments (de Wit *et al.*, 1999; Hannah *et al.*, 1999; Jarousse and Kelly, 2001; Murthy and Stevens, 1998; Takei *et al.*, 1996; Zenisek *et al.*, 2000).

This study established the presence of an early endosomal compartment characterized by Rab5 and PI(3)P at the presynaptic terminal of the *Drosophila* NMJ. Furthermore, it was shown that SV recycling involves trafficking through the endosome and that this recycling pathway is controlled by the small GTPase Rab5. Finally, endosomal recycling is relevant during neurophysiology: it regulates the synaptic performance.

SVs recycle through an endosomal compartment at the *Drosophila* NMJ

In cultured mammalian cells, the small GTPase Rab5 regulates the fusion of endocytic vesicles to the early endosome (Bucci *et al.*, 1992; Mukherjee *et al.*, 1997; Stenmark *et al.*, 1994). Rab5 accumulates at the endosome (Bucci *et al.*, 1992; Fialka *et al.*, 1999; Roberts *et al.*, 1999; Sonnichsen *et al.*, 2000) and induces the formation of the Rab5 domain. The Rab5 domain is enriched in Rab5-GTP and the lipid PI(3)P, to which several Rab5 effector molecules bind through their FYVE domain. Therefore, Rab5 and a tandem repeat of the FYVE domain have been used as markers to visualize the early endosomal compartment in mammalian cultured cells (Bucci *et al.*, 1992; De Renzis *et al.*, 2002; Fialka *et al.*, 1999; Gillooly *et al.*, 2000; Roberts *et al.*, 1999; Sonnichsen *et al.*, 2000).

Using the same markers, we detected early endosomal compartments within the presynaptic terminal at the *Drosophila* NMJ. As in cultured mammalian cells (Bucci *et al.*, 1992), they appear in a punctuate pattern and contain PI(3)P. In addition, the early endosomes are located within the pool of SVs. Are early endosomes involved in the recycling of SVs? We established that the SV recycling pathway involves trafficking through early endosomes. *First*, SVs bud from the endosome as shown using *shibire*^{ts}. Blocking endocytosis while stimulating SV release causes endosomal depletion, observed by the redistribution of the endosomal markers GFP-2xFYVE and GFP-Rab5 from the punctuate endosome into the cytosol. *Second*, endocytic vesicles fuse to the endosome, since endosomal recovery was observed only after releasing the

shibire^{ts} block. This indicates that newly formed endocytic vesicles reestablished the endosomal compartment.

This result also raises the question of how the compartment is reestablished. Are endosomes generated *de novo*, or from preexisting early endosomes? After the depletion, no endosome could be observed at the light microscopical level. This however, does not prove that the compartment disappeared completely during the “*shibire^{ts}/depletion*” experiment. Thus, small endosomal fragments might have remained, to which endocytic vesicles fuse to reestablish the endosome. To ultimately determine whether endosomes disappear completely or if small “seeds” remain will be addressed by immunoelectron microscopy.

Different pathways to recycle synaptic vesicles

Is endosomal recycling the only recycling pathway for vesicles derived by clathrin-mediated endocytosis, or are there other routes to recycle SVs? This study cannot exclude that two recycling pathways coexist within the presynaptic terminal, the Rab5-dependent endosomal pathway and one bypassing this compartment. To address the issue of endosome-independent SV regeneration, it is necessary to study the recycling of clathrin-coated vesicles in a situation where endosomal trafficking is completely blocked.

In this study, we have expressed the dominant negative mutant of Rab5 Rab5S43N to interfere with the Rab5-dependent, endosomal recycling pathway. In the mutant presynaptic terminals, no endosome was observed. However, this does not exclude that some Rab5 function and thereby residual endosomal structures might remain in Rab5S43N expressing synapses. It would therefore be interesting to study SV recycling in the complete absence of Rab5 function. This experiment is however hampered by the maternal Rab5 contribution in the *Rab5²* null mutant. Furthermore, the loss of maternal contribution for several endocytic factors, including Dynamin (Swanson and Poodry, 1981), as well as α -Adaptin and Rab5 (Marcos González-Gaitán, personal communication) causes an early arrest of embryogenesis during cellularization, long before

nervous system differentiation. This makes it difficult, if not impossible, to study SV recycling in a complete (maternal and zygotic) null situation for Rab5.

Another possibility to study Rab5-independent SV recycling is to use conditional Rab5 mutants. In yeast, several Rab-homologs with distinct amino-acid changes known to cause rapid thermosensitivity have been used (Jedd *et al.*, 1995; Salminen and Novik, 1987; Yoo *et al.*, 1999). It should be thereby possible to generate an analogous mutation in the *Drosophila* Rab5 gene, designing a protein with a comparable thermosensitivity. This would allow studying SV recycling immediately after Rab5 function has been completely blocked by raising the temperature.

How important is endosomal SV recycling? Since we cannot determine how many SV recycling pathways exist, the question about the importance of the endosomal recycling route arises. For example, we don't know what percentage of SVs is regenerated through endosomal trafficking. However, this study demonstrated that the Rab5-dependent endosomal SV recycling route is relevant for synaptic transmission. Interfering with Rab5 function as well as overexpression of Rab5 caused strong phenotypes both in synapse structure and function. Therefore, Rab5-dependent endosomal SV recycling is important for synapse function.

In summary, different SV recycling pathways might coexist in neurons. Membrane retrieval might be achieved by "kiss-and-run" and/or by clathrin-mediated endocytosis, generating endocytic vesicles. This study showed that one SV recycling route involves trafficking through an intermediate endosomal compartment. In addition, other SV recycling pathways bypassing the endosome may exist.

Is endosomal trafficking activity-dependent?

A special feature of compensatory, clathrin-mediated endocytosis at the synapse is its temporal coupling to the process of exocytosis, i.e. there is no

endocytosis without exocytosis. Exocytosis is triggered by the action potential-induced Ca^{2+} -influx. Endocytosis is also Ca^{2+} -dependent, which might explain the exo/endo temporal coupling. The Ca^{2+} -activated phosphatase Calcineurin has been suggested to be the endocytic Ca^{2+} -sensor, initiating endocytosis by the dephosphorylation of Dynamin, Amphiphysin 1 and 2 and Synaptojanin (Lai *et al.*, 1999; Marks and McMahon, 1998). Is the next step, namely endosomal trafficking, also coupled to synaptic activity, or does it occur independent of synaptic transmission?

In the “*shibire^{ts}/depletion*” experiment, disappearance of the endosome was only observed when the synapse was stimulated at the restrictive temperature. This prompts the possibility that vesicle budding from the endosome is activity-dependent. This observation however does not exclude an alternative scenario, in which vesicles bud constitutively (also in the resting terminal) from the endosome but also fuse back to it again. This model requires a dynamic equilibrium between vesicle budding from - and vesicle fusion to the endosome in order to achieve the constant endosomal size observed in this study.

How can the “*shibire^{ts}/depletion*” experiment be explained by the “dynamic equilibrium” model of the resting terminal? In the “*shibire^{ts}/depletion*” experiment, exocytosis was stimulated while endocytosis was blocked, first causing the depletion of the SV pool. The depletion of the SV pool shifted the dynamic equilibrium toward vesicle budding from the endosome. In addition, because endocytosis was blocked, there was no membrane input into the endosome by the fusion of endocytic vesicles. Consequently, the endosome was depleted. Furthermore, the result from the FRAP experiment is also consistent with the concept of a dynamic vesicle budding/fusion equilibrium at the endosome in the resting terminal. After bleaching of the fluorescence associated to the endosome, endosomal recovery was observed even in the absence of synaptic activity, suggesting that vesicle fusion with the endosome is independent of synaptic transmission. Therefore, it is possible that a resting terminal is not “resting” but is rather “heavily active” to constantly improve its SVs by repeated rounds of sorting and quality control at the endosome.

The role of Rab5 in endosomal trafficking

Structural phenotypes in Rab5 mutants

In cultured mammalian cells blocking Rab5 function by expressing the dominant negative version, Rab5SN, causes the fragmentation of early endosomes and the accumulation of endocytic vesicles in the cytosol (Bucci *et al.*, 1992). Consistently, we observed the disruption of the endosomes in presynaptic terminals expressing Rab5S43N, indicated by the cytosolic appearance of the endosomal markers Rab5 and GFP-2xFYVE. Furthermore, in Rab5S43N expressing terminals larger vesicles accumulated as seen at the ultrastructural level.

Several features indicate that the large vesicles correspond to endocytic vesicles. *First*, they are not abnormal structures of Rab5S43N expressing synapses, since they are also present in wildtype. *Second*, as in cultured mammalian cells, they accumulate when Rab5 functions is impaired. *Third*, their size is comparable to the size of collared pits, nascent endocytic vesicles that accumulate in *shibire*^{ts} at the restrictive temperature when endocytosis is blocked. However, the ultimate proof that the large vesicles are endocytic vesicles requires a specific labeling of endocytic vesicles for visualization at the ultrastructural level. There are two possibilities to achieve this. One is to shortly internalize HRP, followed by a DAB (diaminobenzidine) reaction, which produces an electron-dense precipitate visible at the electron microscope (de Hoop *et al.*, 1994; Ichimura *et al.*, 1997). This approach might be difficult in the case of the *Drosophila* NMJ, since HRP is a relatively large molecule (44 kDa) (Welinder, 1979) and the presynaptic membrane is rather inaccessible due to the surrounding SSR. Alternatively, internalized FM1-43 dye could be photoconverted into an electron-dense precipitate. This method has been successfully applied in a few preparations (Harata *et al.*, 2001; Henkel *et al.*, 1996; Richards *et al.*, 2000; Schikorski and Stevens, 2001), but has not yet been established in *Drosophila*.

The overexpression of Rab5 in cultured cells leads to the formation of enlarged endosomes (Barbieri *et al.*, 1994; Bucci *et al.*, 1992; Gorvel *et al.*, 1991; Roberts *et al.*, 1999; Stenmark *et al.*, 1994), a feature that we also observed at the presynaptic terminal of *Drosophila*. Therefore, interfering with Rab5 function causes structural phenotypes comparable to those observed in cultured mammalian cells.

SV quality control at the endosome and synaptic plasticity

In addition to the structural phenotypes described above, this study showed that the level of Rab5 function regulates synaptic performance. Thus, interfering with Rab5 by expression of Rab5S43N, decreases synaptic efficacy as observed by a reduction in the number of quanta released during synaptic transmission. In contrast, elevated levels of Rab5 increase the quantal content. The size of the quantal content is Ca²⁺-dependent. At a given Ca²⁺-concentration, the quantal content is determined by two parameters: *First*, by the number of vesicles available during Ca²⁺-triggered exocytosis i.e. the size of the readily releasable pool (Delgado *et al.*, 2000; Kuromi and Kidokoro, 1998; Neher and Zucker, 1993) and *second*, by properties of the SVs, which influence their fusion efficacy.

In *Drosophila* larvae, the readily releasable pool size is determined by measuring the mEJP frequency as well as by quantifying the number of docked vesicles at the ultrastructural level. In preparations where whole cell patch-clamp recordings are performed, e.g. cultured hippocampal neurons and the *Drosophila* embryo, the application of hyperosmotic saline is a standard assay to measure the readily releasable pool size (Aravamudan *et al.*, 1999; Rosenmund and Stevens, 1996; Stevens and Tsujimoto, 1995; Suzuki *et al.*, 2002). This assay however cannot be used in current clamp recordings as in the case of *Drosophila* third instar larvae.

In this study, the morphological and electrophysiological analysis of the Rab5 mutants indicates that the changes in synaptic performance are not caused by

alterations in the readily releasable pool size: The overall NMJ morphology, the synaptic area, the number of active zones and docked vesicles at the T-bar is normal. Consistently, the frequency of mEJPs is not altered in Rab5S43N, or Rab5 overexpressing presynaptic terminals. Therefore, since the size of the readily releasable pool is normal in the mutants, differences in the quantal content are likely caused by alterations in SV properties, changing their efficacy during Ca²⁺-triggered exocytosis.

Which step during Ca²⁺-triggered release might be affected? SV exocytosis is thought to be initiated by binding of Ca²⁺ to a putative Ca²⁺-sensor of the release machinery. Ca²⁺-binding is known to occur in a cooperative fashion. The Ca²⁺- and phospholipid-binding protein Synaptotagmin has been suggested as Ca²⁺-sensor (Brose *et al.*, 1992; Geppert and Sudhof, 1998; Littleton and Bellen, 1995; Littleton *et al.*, 1999). However, the Ca²⁺-cooperativity was normal in the Rab mutants, arguing against a change in the Ca²⁺-sensing step of exocytosis. Therefore, the efficacy with which SVs fuse to the PM seems to be affected, i.e. the release probability of SVs.

How can trafficking through the endosome affect the SV release probability? It is well established that in cultured mammalian cells the Rab5 endosome is a primary sorting organelle (Zerial and McBride, 2001). At the presynaptic terminal, the endosome might be used as a general “quality control station”, required to sort out “per default” any turned over protein and lipid. In addition, we suggest that the endosome plays even a more specific role by actively controlling and changing the protein and lipid composition of SV membranes. The precise molecular architecture of the SVs in turn determines their release probability during Ca²⁺-triggered exocytosis.

Which factors could be targets for the sorting? The Rab5-dependent changes in the SV release probability prompt the possibility that components of the SV release machinery such as Synaptotagmin or SNARE proteins might be sorted at the endosome. In this respect, it has been shown that several Synaptotagmin isoforms exist, 13 in mammals. The different isoforms can polymerize into

different hetero-oligomers with different efficacies during Ca^{2+} -triggered exocytosis (Chapman *et al.*, 1998; Fukuda and Mikoshiba, 2000; Osborne *et al.*, 1999; Thomas *et al.*, 1999). Consistently, it has recently been shown in *Drosophila* that Synaptotagmin I/Synaptotagmin IV hetero-oligomers are less efficient during evoked exocytosis and neurotransmission at the NMJ (Littleton *et al.*, 1999).

In summary, we propose a model in which synaptic performance can be controlled by Rab5-dependent endosomal SV recycling (Fig. 23). Therefore, the regulation of endosomal trafficking might be a new molecular mechanism for synaptic plasticity. Since synaptic plasticity is involved in learning and memory processes at the cellular level, it would be interesting to monitor endosomes *in vivo* and to manipulate Rab5 function in well-established learning and memory paradigms in *Drosophila* (Belvin and Yin, 1997; Waddell and Quinn, 2001).

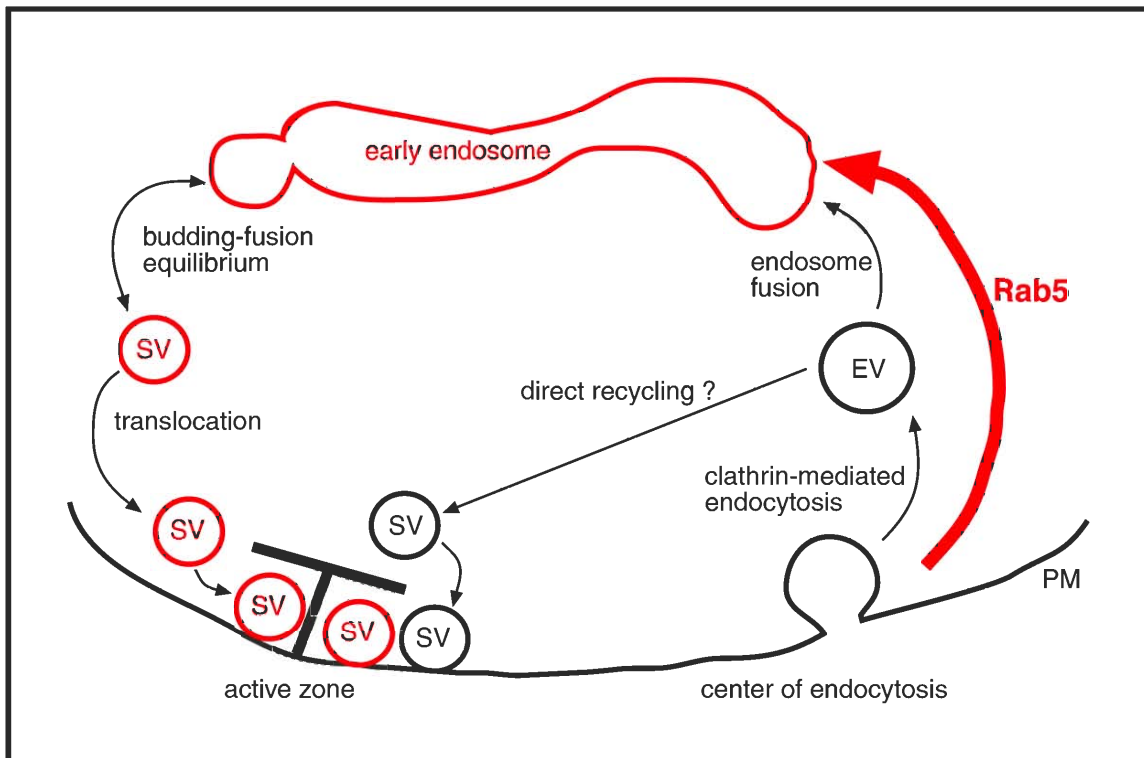


Fig. 23. Model of synaptic vesicle recycling including results from this study. After clathrin-mediated endocytosis from the plasma membrane (PM) at the centers of endocytosis, endocytic vesicles (EV) fuse to early endosomes. This process is mediated by the small GTPase Rab5. Synaptic vesicles (SVs) bud from the endosome, but can also fuse back to it again. Therefore, there is a dynamic equilibrium between vesicle budding from the endosome and vesicle fusion to this compartment. SVs recycled through the Rab5 dependent pathway (shown in red) show a higher efficacy of Ca^{2+} -triggered fusion during synaptic transmission. In addition to the endosomal recycling route, a direct recycling pathway may exist, generating vesicles with a lower efficacy during Ca^{2+} -triggered exocytosis (shown in black).

Summary

During synaptic transmission, NT-filled synaptic vesicles are released by Ca^{2+} -triggered exocytosis at the active zone. Following exocytosis, SV membrane is immediately re-internalized and SVs are regenerated. SV regeneration occurs by a local recycling mechanism within the presynaptic terminal, independent of membrane input from the soma.

Two models for SV recycling have been proposed: “kiss-and-run” and clathrin-mediated endocytosis (Ceccarelli *et al.*, 1973; De Camilli and Takei, 1996; Fesce *et al.*, 1994; Heuser and Reese, 1973; Palfrey and Artalejo, 1998). Both models may be used by different synapses or may even work in parallel within the same synapse. “Kiss-and-run” is thought to take place at the active zone, by the release of NT from SVs through a transient fusion pore. After closure of the fusion pore, SVs are refilled with NT, immediately being available for another round of NT release. According to the other model, SV membrane is internalized by clathrin-mediated endocytosis. At the synapse, clathrin-mediated endocytosis takes place at specialized sites, the centers of endocytosis (González-Gaitán and Jäckle, 1997; Jarousse and Kelly, 2001; Ringstad *et al.*, 1999; Roos and Kelly, 1998; Roos and Kelly, 1999; Teng and Wilkinson, 2000). It is however not known how the SV membrane is subsequently reassembled into SVs. In particular, there is some debate about whether or not an intermediate endosomal compartment is present at the synapse and whether it is involved in the SV recycling process (Blumstein *et al.*, 2001; De Camilli and Takei, 1996; de Wit *et al.*, 1999; Faundez *et al.*, 1998; Fischer von Mollard *et al.*, 1994; Heuser and Reese, 1973; Holtzman *et al.*, 1971; Murthy and Stevens, 1998; Parton *et al.*, 1992; Provoda *et al.*, 2000; Sulzer and Holtzman, 1989; Takei *et al.*, 1996).

In contrast, it is well known from cultured mammalian cells, that endocytic vesicles derived by clathrin-mediated endocytosis fuse to an intracellular endocytic compartment, the early sorting endosome (Bucci *et al.*, 1992; Zerial and McBride, 2001; Zerial and Stenmark, 1993). The early endosome is a major

sorting station of the cell. From there, cargo is sent into the degradative pathway to late endosome and lysosome or towards recycling. There are two recycling routes: directly from the early endosome back to the PM or via another compartment the recycling endosome. Each trafficking step between the different endocytic compartments is mediated by a certain protein of the Rab family (Pfeffer, 1994; Rothman, 1994; Zerial and Stenmark, 1993).

Rab proteins are small GTPases belonging to the Ras superfamily. In the steady state, Rab proteins accumulate at their target compartments and have thereby been used as markers for the different endocytic organelles (Bucci *et al.*, 1992; Chavrier *et al.*, 1990; Daro *et al.*, 1996; Olkkonen *et al.*, 1993; Pfeffer, 1994; Ullrich *et al.*, 1996; van der Sluijs *et al.*, 1992). Rab5 mediates the trafficking step from the PM to the early sorting endosome (Bucci *et al.*, 1992), Rab7 regulates the degradative pathway (Bucci *et al.*, 2000; Feng *et al.*, 1995; Méresse *et al.*, 1995; Vitelli *et al.*, 1997) and Rab4 and Rab11 the recycling route (Daro *et al.*, 1996; Prekeris *et al.*, 2000; Schlierf *et al.*, 2000; Sheff *et al.*, 1999; Ullrich *et al.*, 1996; van der Sluijs *et al.*, 1992; van der Sluijs *et al.*, 1991).

In particular, Rab5 is involved in the formation of endocytic vesicles at the PM (McLauchlan *et al.*, 1998) and their subsequent fusion to the early endosome (Bucci *et al.*, 2000). In addition, Rab5 regulates the homotypic fusion between early endosomes (Barbieri *et al.*, 1994; Gorvel *et al.*, 1991; Li *et al.*, 1994; Roberts *et al.*, 1999; Rybin *et al.*, 1996) and endosome motility along microtubuli (Nielsen *et al.*, 1999). Rab5 has been used as marker for the early endosome in cultured mammalian cells (Bucci *et al.*, 1992; Chavrier *et al.*, 1991). A second early endosomal marker is based on the specific binding of the FYVE zinc finger protein domain to the lipid PI(3)P that is specifically generated at the early endosomal membrane (Gillooly *et al.*, 2000).

This study used the *Drosophila* NMJ as a model system to investigate the SV recycling process. In particular, three questions were addressed: *First*, is an endosomal compartment present at the synapse? *Second*, do SVs recycle through an endosome? *Third*, is Rab5 involved in SV recycling?

We used GFP fusions of Rab5 and 2xFYVE to visualize endosomal compartments at the presynaptic terminal of *Drosophila* third instar larval NMJs. We observed an early endosomal compartment characterized by the localization of Rab5 and the lipid PI(3)P, to which the FYVE zinc finger protein domain binds specifically. Furthermore, the endosomes are located within the pool of recycling SVs, labeled with the styryl-dye FM5-95. Using the temperature-sensitive mutation in Dynamin, *shibire^{ts}*, to uncouple endo- from exocytosis, we showed that endocytic vesicles derived by clathrin-mediated endocytosis fuse to the endosome and that SVs bud from this compartment. Therefore, SV recycling involves trafficking through an intermediate endosomal compartment at the *Drosophila* NMJ.

In cultured mammalian cells, Rab5 is required for the integrity of the endosomal compartment. Interfering with Rab5 function by expressing the dominant negative version, Rab5SN causes the fragmentation of the endosome and the accumulation of endocytic vesicles in the cytosol (Bucci *et al.*, 1992). In contrast, when Rab5 is overexpressed enlarged endosomal compartments were observed (Bucci *et al.*, 1992). In *Drosophila*, Rab5 is also required for endosome integrity and endosomal SV recycling, as shown using loss of function, dominant negative and gain of function Rab5 mutants. In the loss of function and dominant negative mutants, the endosomal compartment was disrupted. In addition, at the ultrastructural we observed an accumulation of endocytic vesicles in Rab5S43N expressing terminals and enlarged endosomes when Rab5 was overexpressed. Furthermore, interfering with Rab5 function using the dominant negative Rab5S43N caused a decrease in the SV recycling kinetics as shown by FM1-43 experiments. In contrast, overexpression of Rab5 or GFP-Rab5 caused an increase in the FM1-43 internalization rate.

Finally, we used standard electrophysiological techniques to measure synaptic function. We found that the Rab5-mediated endosomal SV recycling pathway generates vesicles with a higher fusion efficacy during Ca²⁺-triggered release, compared to SVs recycled when Rab5 function was impaired. We therefore suggest a model in which the endosome serves as organelle to control the SV

fusion efficacy and thereby the synaptic strength. Since changes in the synaptic strength are occurring during learning and memory processes, controlling endosomal SV recycling might be a new molecular mechanism involved in learning and memory.

Zusammenfassung

Synaptische Vesikel werden während synaptischer Transmission durch Ca^{2+} -induzierte Exozytose an der aktiven Zone der Präsynapse freigesetzt. Sofort nach der Exozytose wird die synaptische Vesikelmembran endozytiert. Ein sich daran anschließender Recyclingmechanismus regeneriert die synaptischen Vesikel. Das Recycling synaptischer Vesikel findet somit lokal in der Synapse statt und ist unabhängig von Membranzufuhr aus dem Zellsoma.

Derzeit gibt es zwei Modelle für den Mechanismus des Vesikelrecyclings, genannt "kiss-and-run" und Clathrin-vermittelte Endozytose. (Ceccarelli *et al.*, 1973; De Camilli und Takei, 1996; Fesce *et al.*, 1994; Heuser und Reese, 1973; Palfrey und Artalejo, 1998). Möglicherweise verwenden verschiedene Synapsen unterschiedliche Recyclingmechanismen, oder beide Modelle kommen gleichzeitig innerhalb einer Synapse zum Zuge. Der "kiss-and-run" Mechanismus soll an der aktiven Zone stattfinden. Dem Modell zufolge, wird hier der Neurotransmitter durch eine transiente Fusionspore freigesetzt. Nach dem Wiederverschliessen dieser Fusionspore sollen synaptische Vesikel erneut mit Neurotransmitter befüllt und sofort für eine weitere Runde der Exozytose bereitstehen. Das zweite Modell geht davon aus, dass die synaptische Vesikelmembran durch Clathrin-vermittelte Endozytose reinternalisiert wird.

In der Synapse findet Clathrin-vermittelte Endozytose an spezialisierten Regionen der präsynaptischen Membran statt, den Zentren für Endozytose (González-Gaitán und Jäckle, 1997; Jarousse und Kelly, 2001; Ringstad *et al.*, 1999; Roos und Kelly, 1998; Roos und Kelly, 1999; Teng und Wilkinson, 2000). Es ist jedoch unbekannt wie aus der endozytierten Vesikelmembran neue synaptische Vesikel entstehen. Insbesondere ist unklar, ob endosomale Kompartimente innerhalb der Präsynapse existieren, und wenn ja, ob diese als Zwischenstation im Vesikelrecycling eine Rolle spielen (Blumstein *et al.*, 2001; De Camilli und Takei, 1996; de Wit *et al.*, 1999; Faundez *et al.*, 1998; Fischer von Mollard *et al.*, 1994; Heuser und Reese, 1973; Holtzman *et al.*, 1971;

Murthy und Stevens, 1998; Parton *et al.*, 1992; Provoda *et al.*, 2000; Sulzer und Holtzman, 1989; Takei *et al.*, 1996).

Im Gegensatz dazu ist aus Zellkulturexperimenten bekannt, dass durch Clathrin-vermittelte Endozytose entstandene, endozytische Vesikel mit einem intrazellulären Organell, dem frühen Endosomen, verschmelzen. Der frühe Endosom ist eine Hauptsortierstelle der Zelle (Bucci *et al.*, 1992; Zerial und McBride, 2001; Zerial und Stenmark, 1993). Internalisierte Moleküle werden hier in den Degradationsweg zu spätem Endosom und Lysosom geschickt, oder in die Recyclingroute geleitet. Zwei Recyclingrouten sind bekannt: Die schnelle führt direkt vom frühen Endosom zurück zur Plasmamembran. Der zweite Weg geht durch ein weiteres endosomales Kompartiment, den Recyclingendosom und erst von dort zur Plasmamembran. Jeder dieser unterschiedlichen Transportwege zwischen den verschiedenen Organellen innerhalb der Zelle wird von einem spezifischen Protein der Rab Familie kontrolliert (Pfeffer, 1994; Rothman, 1994; Zerial und Stenmark, 1993).

Rab Proteine sind kleine GTPasen die der Überfamilie der Ras GTPasen angehören. Da sich Rab Proteine an ihren Zielorganellen ansammeln werden sie als Marker für verschiedene Kompartimente verwendet (Bucci *et al.*, 1992; Chavrier *et al.*, 1990; Daro *et al.*, 1996; Olkkonen *et al.*, 1993; Pfeffer, 1994; Ullrich *et al.*, 1996; van der Sluijs *et al.*, 1992). Rab5 kontrolliert den Transportweg von der Plasmamembran zum frühen Endosom (Bucci *et al.*, 1992), Rab7 reguliert den Degradationsweg (Bucci *et al.*, 2000; Feng *et al.*, 1995; Méresse *et al.*, 1995; Vitelli *et al.*, 1997), Rab4 und Rab11 überwachen die Recyclingroute (Daro *et al.*, 1996; Prekeris *et al.*, 2000; Schlierf *et al.*, 2000; Sheff *et al.*, 1999; Ullrich *et al.*, 1996; van der Sluijs *et al.*, 1992; van der Sluijs *et al.*, 1991).

Rab5 kontrolliert die Herstellung endozytischer Vesikel an der Plasmamembran (McLauchlan *et al.*, 1998), sowie deren Fusion mit dem frühen Endosom (Bucci *et al.*, 2000). Zusätzlich reguliert Rab5 die homotypische Fusion zwischen frühen Endosomen (Barbieri *et al.*, 1994; Gorvel *et al.*, 1991; Li *et al.*, 1994;

Roberts *et al.*, 1999; Rybin *et al.*, 1996), sowie die Bewegung von Endosomen entlang der Mikrotubuli (Nielsen *et al.*, 1999). In Zellkultur wird Rab5 als Marker für frühe Endosomen verwendet (Bucci *et al.*, 1992; Chavrier *et al.*, 1991). Ein zweiter endosomaler Marker beruht auf der spezifischen Bindung der FYVE Zinkfinger Proteindomäne an das Lipid Phosphatidylinositol-3-phosphat (PI(3)P), das am frühen Endosomen entsteht (Gillooly *et al.*, 2000).

In dieser Arbeit diente die neuromuskuläre Synapse von *Drosophila* als Modellsystem, um den Mechanismus des Vesikelrecyclings zu untersuchen. Insbesondere wurden drei Fragestellungen bearbeitet. *Erstens*, gibt es in der Präsynapse endosomale Kompartimente? *Zweitens*, haben Endosomen eine Bedeutung beim Recycling synaptischer Vesikel? *Drittens*, spielt Rab5 eine Rolle im Vesikelrecycling?

GFP-Fusionsproteine von Rab5 und 2xFYVE wurden verwendet, um endosomale Kompartimente in der Synapse darzustellen. Auf diese Weise dargestellte Endosomen waren durch Rab5 und das Lipid Phosphatidylinositol-3-phosphat gekennzeichnet. Es wurde weiterhin gezeigt, dass sich die Endosomen innerhalb des Pools synaptischer Vesikel befinden. Die temperaturempfindliche Mutation in Dynamin, *shibire*, wurde eingesetzt, um Endo- und Exozytose zu entkoppeln. So konnte gezeigt werden, dass endozytische Vesikel die durch Clathrin-vermittelte Endozytose entstehen mit Endosomen verschmelzen, und dass synaptische Vesikel von Endosomen abknospen. Endosomale Kompartimente werden somit als Zwischenstufen beim Recycling synaptischer Vesikel in der neuromuskulären Synapse von *Drosophila* verwendet.

Aus Zellkulturexperimenten ist bekannt, dass Rab5 für die Intaktheit der Endosomen notwendig ist. Eine Störung der Rab5 Funktion durch die Expression der dominant negativen Form von Rab5, Rab5SN, führt zur Fragmentation der Endosomen und zur Ansammlung endozytischer Vesikel im Zellplasma (Bucci *et al.*, 1992). Die Überexpression von Rab5 hingegen hat eine Vergrößerung der Endosomen zur Folge (Bucci *et al.*, 1992). Auch in

Drosophila ist Rab5 für die Intaktheit von Endosomen und für endosomales Recycling synaptischer Vesikel notwendig. Dies wurde mit Hilfe von Verlustmutationen, dominant negativen und Gewinnmutationen von Rab5 gezeigt. In den Verlustmutanten und dominant negativen Mutanten war das endosomale Kompartiment zerstört. Des weiteren wurde in Rab5SN exprimierenden Synapsen auf ultrastruktureller Ebene eine Ansammlung endozytischer Vesikel beobachtet. In Rab5 überexprimierenden Synapsen hingegen fanden wir vergrösserte endosomale Kompartimente. FM1-43 Experimente zeigten, dass die Inhibition von Rab5 eine Reduktion der Recyclinggeschwindigkeit synaptischer Vesikel zur Folge hat. Im Gegensatz dazu führte die Überexpression von Rab5 oder GFP-Rab5 zu einer erhöhten FM1-43 Internalisationsrate.

Schliesslich wurde die synaptische Funktion mittels elektrophysiologischer Methoden gemessen. Dabei zeigte sich, dass der durch Rab5 kontrollierte endosomale Recyclingweg synaptische Vesikel erzeugt, die eine höhere Fusionseffizienz während Ca^{2+} -induzierter Exozytose aufweisen, als Vesikel die entstehen wenn die Funktion von Rab5 gestört ist. Aus diesem Grund schlagen wir ein Modell des Vesikelrecyclings vor, in dem Endosomen die Fusionseffizienz synaptischer Vesikel und somit die Stärke synaptischer Verbindungen kontrollieren. Da es auch während Lern- und Gedächtnisvorgängen zur Modulation synaptischer Verbindungen kommt, könnte das endosomale Vesikelrecycling einen neuen molekularen Mechanismus darstellen, der bei der Gedächtnisbildung eine Rolle spielt.

References

- Adams, M. D., Celniker, S. E., Holt, R. A., *et al.* (2000). The genome sequence of *Drosophila melanogaster*. *Science* 287, 2185-2195.
- Adari, H., Lowy, D. R., Willumsen, B. M., Der, C. J. and McCormick, F. (1988). Guanosine triphosphatase activating protein (GAP) interacts with the p21 ras effector binding domain. *Science* 240, 518-521.
- Ahle, S. and Ungewickell, E. (1986). Purification and properties of a new Clathrin assembly protein. *EMBO J* 5, 3143-3149.
- Ahle, S. and Ungewickell, E. (1989). Identification of a Clathrin binding subunit in the AP-2 adaptor protein complex. *J Biol Chem* 264, 20089-20093.
- Albillos, A., Dernick, G., Horstmann, H., Almers, W., Alvarez de Toledo, G. and Lindau, M. (1997). The exocytotic event in chromaffin cells revealed by patch amperometry. *Nature* 389, 509-512.
- Alés, E., Tabares, L., Poyato, J. M., Valero, V., Lindau, M. and Alvarez de Toledo, G. (1999). High calcium concentrations shift the mode of exocytosis to the kiss-and-run mechanism. *Nat Cell Biol* 1, 40-44.
- Alexandrov, K., Horiuchi, H., Steele-Mortimer, O., Seabra, M. C. and Zerial, M. (1994). Rab escort protein-1 is a multifunctional protein that accompanies newly prenylated Rab proteins to their target membranes. *EMBO J* 13, 5262-5273.
- Almers, W. and Tse, F. W. (1990). Transmitter release from synapses: does a preassembled fusion pore initiate exocytosis? *Neuron* 4, 813-818.
- Alvarez de Toledo, G. and Fernandez, J. M. (1990). Compound versus multigranular exocytosis in peritoneal mast cells. *J Gen Physiol* 95, 397-409.
- Anderson, M. S., Halpern, M. E. and Keshishian, H. (1988). Identification of the neuropeptide transmitter proctolin in *Drosophila* larvae: characterization of muscle fiber-specific neuromuscular endings. *J Neurosci* 8, 242-255.
- Andres, D. A., Seabra, M. C., Brown, M. S., Armstrong, S. A., Smeland, T. E., Cremers, F. P. and Goldstein, J. L. (1993). cDNA cloning of component A of Rab geranylgeranyl transferase and demonstration of its role as a Rab escort protein. *Cell* 73, 1091-1099.
- Araki, S., Kikuchi, A., Hata, Y., Isomura, M. and Takai, Y. (1990). Regulation of reversible binding of smg p25A, a ras p21-like GTP-binding protein, to synaptic plasma membranes and vesicles by its specific regulatory protein, GDP dissociation inhibitor. *J Biol Chem* 265, 13007-13015.
- Aravamudan, B., Fergestad, T., Davis, W. S., Rodesch, C. K. and Broadie, K. (1999). *Drosophila* UNC-13 is essential for synaptic transmission. *Nat Neurosci* 2, 965-971.
- Atwood, H. L., Govind, C. K. and Wu, C. F. (1993). Differential ultrastructure of synaptic terminals on ventral longitudinal abdominal muscles in *Drosophila* larvae. *J Neurobiol* 24, 1008-1024.

- Ayad, N., Hull, M. and Mellman, I. (1997). Mitotic phosphorylation of Rab4 prevents binding to a specific receptor on endosome membranes. *EMBO J* 16, 4497-4507.
- Barbieri, M. A., Li, G., Colombo, M. I. and Stahl, P. D. (1994). Rab5, an early acting endosomal GTPase, supports *in vitro* endosome fusion without GTP hydrolysis. *J Biol Chem* 269, 18720-18722.
- Barouch, W., Prasad, K., Greene, L. and Eisenberg, E. (1997). Auxilin-induced interaction of the molecular chaperone Hsc70 with Clathrin baskets. *Biochemistry* 36, 4303-4308.
- Barouch, W., Prasad, K., Greene, L. E. and Eisenberg, E. (1994). ATPase activity associated with the uncoating of Clathrin baskets by Hsp70. *J Biol Chem* 269, 28563-28568.
- Barr, F. A. and Shorter, J. (2000). Membrane traffic: do cones mark sites of fission? *Curr Biol* 10, R141-R144.
- Bate, M. (1990). The embryonic development of larval muscles in *Drosophila*. *Development* 110, 791-804.
- Bate, M. (1993). The mesoderm and its derivatives. The development of *Drosophila melanogaster*. (Cold Spring Harbor, NY., Cold Spring Harbor Laboratory Press).
- Baylies, M. K. and Bate, M. (1996). Twist: A myogenic switch in *Drosophila*. *Science* 272, 1481-1484.
- Belvin, M. P. and Yin, J. C. (1997). *Drosophila* learning and memory: recent progress and new approaches. *Bioessays* 19, 1083-1089.
- Benli, M., Doring, F., Robinson, D. G., Yang, X. and Gallwitz, D. (1996). Two GTPase isoforms, Ypt31p and Ypt32p, are essential for Golgi function in yeast. *EMBO J* 15, 6460-6475.
- Bennett, M. K., Calakos, N. and Scheller, R. H. (1992). Syntaxin: a synaptic protein implicated in docking of synaptic vesicles at presynaptic active zones. *Science* 257, 255-259.
- Betz, W. J. and Bewick, G. S. (1992). Optical analysis of synaptic vesicle recycling at the frog neuromuscular junction. *Science* 255, 200-203.
- Betz, W. J. and Bewick, G. S. (1993). Optical monitoring of transmitter release and synaptic vesicle recycling at the frog neuromuscular junction. *J Physiol* 460, 287-309.
- Betz, W. J., Mao, F. and Bewick, G. S. (1992). Activity-dependent fluorescent staining and destaining of living vertebrate motor nerve terminals. *J Neurosci* 12, 363-375.
- Blumstein, J., Faundez, V., Nakatsu, F., Saito, T., Ohno, H. and Kelly, R. B. (2001). The neuronal form of adaptor protein-3 is required for synaptic vesicle formation from endosomes. *J Neurosci* 21, 8034-8042.
- Bock, J. B., Matern, H. T., Peden, A. A. and Scheller, R. H. (2001). A genomic perspective on membrane compartment organization. *Nature* 409, 839-841.

- Boll, W., Ohno, H., Songyang, Z., Rapoport, I., Cantley, L. C., Bonifacino, J. S. and Kirchhausen, T. (1996). Sequence requirements for the recognition of tyrosine-based endocytic signals by Clathrin AP-2 complexes. *EMBO J* 15, 5789-5795.
- Bourne, H. R. (1988). Do GTPases direct membrane traffic in secretion? *Cell* 53, 669-671.
- Brady, S. T. (1991). Molecular motors in the nervous system. *Neuron* 7, 521-533.
- Braell, W. A., Schlossman, D. M., Schmid, S. L. and Rothman, J. E. (1984). Dissociation of Clathrin coats coupled to the hydrolysis of ATP: role of an uncoating ATPase. *J Cell Biol* 99, 734-741.
- Brand, A., Manoukian, A. S. and Perrimon, N. (1996). Ectopic expression in *Drosophila*. In *Drosophila melanogaster*. Practical Uses in Cell and Molecular Biology. L. S. B. Goldstein, and E. A. Fyrberg, eds. (San Diego, Academic Press), pp. 635-654.
- Brand, A. H. and Perrimon, N. (1993). Targeted gene expression as a means of altering cell fates and generating dominant phenotypes. *Development* 118, 401-415.
- Breckenridge, L. J. and Almers, W. (1987). Final steps in exocytosis observed in a cell with giant secretory granules. *PNAS* 84, 1945-1949.
- Broadie, K. and Bate, M. (1993a). Innervation directs receptor synthesis and localization in *Drosophila* embryo synaptogenesis. *Nature* 361, 350-353.
- Broadie, K. and Bate, M. (1993b). Muscle development is independent of innervation during *Drosophila* embryogenesis. *Development* 119, 533-543.
- Broadie, K. S. and Bate, M. (1993c). Development of the embryonic neuromuscular synapse of *Drosophila melanogaster*. *J Neurosci* 13, 144-166.
- Brodin, L., Low, P. and Shupliakov, O. (2000). Sequential steps in clathrin-mediated synaptic vesicle endocytosis. *Curr Opin Neurobiol* 10, 312-320.
- Brose, N., Petrenko, A. G., Südhof, T. C. and Jahn, R. (1992). Synaptotagmin: a Ca²⁺-sensor on the synaptic vesicle surface. *Science* 256, 1021-1025.
- Brown, S. J., Mahaffey, J. P., Lorenzen, M. D., Denell, R. E. and Mahaffey, J. W. (1999). Using RNAi to investigate orthologous homeotic gene function during development of distantly related insects. *Evol Dev* 1, 11-15.
- Brunger, A. T. (2000). Structural insights into the molecular mechanism of Ca²⁺-dependent exocytosis. *Curr Opin Neurobiol* 10, 293-302.
- Bucci, C., Lutcke, A., Steele-Mortimer, O., Olkkonen, V. M., Dupree, P., Chiariello, M., Bruni, C. B., Simons, K. and Zerial, M. (1995). Co-operative regulation of endocytosis by three Rab5 isoforms. *FEBS Let* 366, 65-71.
- Bucci, C., Parton, R. G., Mather, I. H., Stunnenberg, H., Simons, K., Hoflack, B. and Zerial, M. (1992). The small GTPase Rab5 functions as a regulator factor in the early endocytic pathway. *Cell* 70, 715-728.

- Bucci, C., Thomsen, P., Nicoziani, P., McCarthy, J. and van Deurs, B. (2000). Rab7: a key to lysosome biogenesis. *Mol Biol Cell* 11, 467-480.
- Budnik, V. (1996). Synapse maturation and structural plasticity at *Drosophila* neuromuscular junctions. *Curr Opin Neurobiol* 6, 858-867.
- Budnik, V. and Gorczyca, M. (1992). SSB, an antigen that selectively labels morphologically distinct synaptic boutons at the *Drosophila* larval neuromuscular junction. *J Neurobiol* 23, 1054-1065.
- Budnik, V., Zhong, Y. and Wu, C. F. (1990). Morphological plasticity of motor axons in *Drosophila* mutants with altered excitability. *J Neurosci* 10, 3754-3768.
- Burd, C. G. and Emr, S. D. (1998). Phosphatidylinositol(3)-phosphate signaling mediated by specific binding to RING FYVE domains. *Mol Cell* 2, 157-162.
- Burgoyne, R. D., Fisher, R. J. and Graham, M. E. (2001). Regulation of kiss-and-run exocytosis. *Trends Cell Biol* 11, 404-405.
- Burns, M. E. and Augustine, G. J. (1995). Synaptic structure and function: dynamic organization yields architectural precision. *Cell* 83, 187-194.
- Burstein, E. S., Brondyk, W. H. and Macara, I. G. (1992). Amino acid residues in the Ras-like GTPase Rab3A that specify sensitivity to factors that regulate the GTP/GDP cycling of Rab3A. *J Biol Chem* 267, 22715-22718.
- Burton, J., Roberts, D., Montaldi, M., Novick, P. and De Camilli, P. (1993). A mammalian guanine-nucleotide-releasing protein enhances function of yeast secretory protein Sec4. *Nature* 361, 464-467.
- Burton, J. L., Burns, M. E., Gatti, E., Augustine, G. J. and De Camilli, P. (1994). Specific interactions of Mss4 with members of the Rab GTPase subfamily. *EMBO J* 13, 5547-5558.
- Campos-Ortega, J. A. and Hartenstein, V. (1997). The embryonic development of *Drosophila melanogaster*, (Berlin, Springer Verlag).
- Cantera, R. and Nassel, D. R. (1992). Segmental peptidergic innervation of abdominal targets in larval and adult dipteran insects revealed with an antiserum against leucokinin I. *Cell Tissue Res* 269, 459-471.
- Carr, J. F. and Hinshaw, J. E. (1997). Dynamin assembles into spirals under physiological salt conditions upon the addition of GDP and gamma-phosphate analogues. *J Biol Chem* 272, 28030-28035.
- Carthew, R. W. (2001). Gene silencing by double-stranded RNA. *Curr Opin Cell Biol* 13, 244-248.
- Ceccarelli, B., Grohovaz, F. and Hurlbut, W. P. (1979). Freeze-fracture studies of frog neuromuscular junctions during intense release of neurotransmitter. II. Effects of electrical stimulation and high potassium. *J Cell Biol* 81, 178-192.
- Ceccarelli, B., Hurlbut, W. P. and Mauro, A. (1973). Turnover of transmitter and synaptic vesicles at the frog neuromuscular junction. *J Cell Biol* 57, 499-524.

- Chad, J. E. and Eckert, R. (1984). Calcium domains associated with individual channels can account for anomalous voltage relations of Ca²⁺-dependent responses. *Biophys J* 45, 993-999.
- Chapman, E. R., Desai, R. C., Davis, A. F. and Tornehl, C. K. (1998). Delineation of the oligomerization, AP-2 binding, and synprint binding region of the C2B domain of Synaptotagmin. *J Biol Chem* 273, 32966-32972.
- Chappell, T. G., Welch, W. J., Schlossman, D. M., Palter, K. B., Schlesinger, M. J. and Rothman, J. E. (1986). Uncoating ATPase is a member of the 70 kilodalton family of stress proteins. *Cell* 45, 3-13.
- Chavrier, P., Gorvel, J. P., Stelzer, E., Simons, K., Gruenberg, J. and Zerial, M. (1991). Hypervariable C-terminal domain of Rab proteins acts as a targeting signal. *Nature* 353, 769-772.
- Chavrier, P., Parton, R. G., Hauri, H. P., Simons, K. and Zerial, M. (1990). Localization of low molecular weight GTP binding proteins to exocytic and endocytic compartments. *Cell* 62, 317-329.
- Chen, M. S., Obar, R. A., Schroeder, C. C., Austin, T. W., Poodry, C. A., Wadsworth, S. C. and Vallee, R. B. (1991). Multiple forms of Dynamin are encoded by *shibire*, a *Drosophila* gene involved in endocytosis. *Nature* 351, 583-586.
- Chiba, A., Hing, H., Cash, S. and Keshishian, H. (1993). Growth cone choices of *Drosophila* motoneurons in response to muscle fiber mismatch. *J Neurosci* 13, 714-732.
- Christoforidis, S., McBride, H. M., Burgoyne, R. D. and Zerial, M. (1999a). The Rab5 effector EEA1 is a core component of endosome docking. *Nature* 397, 621-625.
- Christoforidis, S., Miaczynska, M., Ashman, K., Wilm, M., Zhao, L. Y., Yip, S. C., Waterfield, M. D., Backer, J. M. and Zerial, M. (1999b). Phosphatidylinositol-3-OH kinases are Rab5 effectors. *Nat Cell Biol* 1, 249-252.
- Cole, N. B., Smith, C. L., Sciaky, N., Terasaki, M., Edidin, M. and Lippincott-Schwartz, J. (1996). Diffusional mobility of Golgi proteins in membranes of living cells. *Science* 273, 797-801.
- Cottrell, J. R., Dube, G. R., Egles, C. and Liu, G. (2000). Distribution, density, and clustering of functional glutamate receptors before and after synaptogenesis in hippocampal neurons. *J Neurophysiol* 84, 1573-1587.
- Cremona, O., Di Paolo, G., Wenk, M. R., *et al.* (1999). Essential role of phosphoinositide metabolism in synaptic vesicle recycling. *Cell* 99, 179-188.
- Crossley, C. A. (1978). The morphology and development of the *Drosophila* musculatur system. In: *The Genetics and Biology of Drosophila*. M. Ashburner, and T. R. F. Wright, eds. (Academic, New York).
- Crowther, R. A. and Pearse, B. M. (1981). Assembly and packing of Clathrin into coats. *J Cell Biol* 91, 790-797.

- Cupers, P., Veithen, A., Kiss, A., Baudhuin, P. and Courtoy, P. J. (1994). Clathrin polymerization is not required for bulk-phase endocytosis in rat fetal fibroblasts. *J Cell Biol* 127, 725-735.
- Daro, E., van der Sluijs, P., Galli, T. and Mellman, I. (1996). Rab4 and Cellubrevin define different early endosome populations on the pathway of transferrin receptor recycling. *PNAS* 93, 9559-9564.
- David, C., McPherson, P. S., Mundigl, O. and de Camilli, P. (1996). A role of Amphiphysin in synaptic vesicle endocytosis suggested by its binding to Dynamin in nerve terminals. *PNAS* 93, 331-335.
- Davis, A. F., Bai, J., Fasshauer, D., Wolowick, M. J., Lewis, J. L. and Chapman, E. R. (1999). Kinetics of Synaptotagmin responses to Ca^{2+} and assembly with the core SNARE complex onto membranes. *Neuron* 24, 363-376.
- De Camilli, P. D. and Takei, K. (1996). Molecular mechanisms in synaptic vesicle endocytosis and recycling. *Neuron* 16, 481-486.
- de Hoop, M. J., Huber, L. A., Stenmark, H., Williamson, E., Parton, R. G. and Dotti, C. (1994). The involvement of the small GTP-binding protein Rab5a in neuronal endocytosis. *Neuron* 13, 11-22.
- De Renzis, S., Sonnichsen, B. and Zerial, M. (2002). Divalent Rab effectors regulate the sub-compartmental organization and sorting of early endosomes. *Nat Cell Biol* 4, 124-133.
- de Wit, H., Lichtenstein, Y., Geuze, H. Y., Kelly, R. B., van der Sluijs, P. and Klumperman, J. (1999). Synaptic vesicles form by budding from tubular extensions of sorting endosomes in PC12 cells. *Mol Biol Cell* 10, 4163-4176.
- Delgado, R., Maureira, C., Oliva, C., Kidokoro, Y. and Labarca, P. (2000). Size of vesicle pools, rates of mobilization, and recycling at neuromuscular synapses of a *Drosophila* mutant, *shibire*. *Neuron* 28, 941-953.
- Der, C. J., Finkel, T. and Cooper, G. M. (1986). Biological and biochemical properties of human rasH genes mutated at codon 61. *Cell* 44, 167-176.
- Desai, R. C., Vyas, B., Earles, C. A., Littleton, J. T., Kowalchuck, J. A., Martin, T. F. and Chapman, E. R. (2000). The C2B domain of Synaptotagmin is a Ca^{2+} -sensing module essential for exocytosis. *J Cell Biol* 150, 1125-1136.
- Dirac-Svejstrup, A. B., Sumizawa, T. and Pfeffer, S. R. (1997). Identification of a GDI displacement factor that releases endosomal Rab GTPases from Rab-GDI. *EMBO J* 16, 465-472.
- Donrunz, L. E. and Stevens, C. F. (1999). Heterogeneity of release probability, facilitation, and depletion at a central synapse. *Neuron* 18, 995-1008.
- Dunn, K. W., McGraw, T. E. and Maxfield, F. R. (1989). Iterative fractionation of recycling receptors from lysosomally destined ligands in an early sorting endosome. *J Cell Biol* 109, 3303-3314.
- Ehlers, M. D., Mammen, A. L., Lau, L. F. and Huganir, R. L. (1996). Synaptic targeting of glutamate receptors. *Curr Opin Cell Biol* 8, 484-489.

- Entchev, E. V., Schwabedissen, A. and González-Gaitán, M. A. (2000). Gradient formation of the TGF-beta homolog Dpp. *Cell* 103, 981-991.
- Estes, P. S., Roos, J., van der Blik, A., Kelly, R. B., Krishnan, K. S. and Ramaswami, M. (1996). Traffic of Dynamin within individual *Drosophila* synaptic boutons relative to compartment-specific markers. *J Neurosci* 16, 5443-5456.
- Farnsworth, C. L. and Feig, L. A. (1991). Dominant inhibitory mutations in the Mg²⁺-binding site of RasH prevent its activation by GTP. *Mol Cell Biol* 11, 4822-4829.
- Fasshauer, D., Eliason, W. K., Brunger, A. T. and Jahn, R. (1998a). Identification of a minimal core of the synaptic SNARE complex sufficient for reversible assembly and disassembly. *Biochemistry* 37, 10354-10362.
- Fasshauer, D., Sutton, R. B., Brunger, A. T. and Jahn, R. (1998b). Conserved structural features of the synaptic fusion complex: SNARE proteins reclassified as Q- and R-SNAREs. *PNAS* 95, 15781-15786.
- Faundez, V., Horng, J. T. and Kelly, R. B. (1998). A function for the AP-3 coat complex in synaptic vesicle formation from endosomes. *Cell* 93, 423-432.
- Feig, L. A. and Cooper, G. M. (1988). Relationship among guanine nucleotide exchange, GTP hydrolysis, and transforming potential of mutated ras proteins. *Mol Cell Biol* 8, 2472-2478.
- Feng, Y., Press, B. and Wandinger, N. A. (1995). Rab7: An important regulator of late endocytic membrane traffic. *J Cell Biol* 131, 1435-1452.
- Fergestad, T., Davis, W. S. and Broadie, K. (1999). The stoned proteins regulate synaptic vesicle recycling in the presynaptic terminal. *J Neurosci* 19, 5847-5860.
- Fernandez-Chacon, R., Königstorfer, A., Gerber, S. H., *et al.* (2001). Synaptotagmin I functions as a calcium regulator of release probability. *Nature* 410, 41-49.
- Ferro-Novick, S. and Novick, P. (1993). The role of GTP-binding proteins in transport along the exocytic pathway. *Annu Rev Cell Biol* 9, 575-599.
- Fesce, R., Grohovaz, F., Valtorta, F. and Meldolesi, J. (1994). Neurotransmitter release: fusion or "kiss-and-run"? *Trends Cell Biol* 4, 1-4.
- Fialka, I., Steinlein, P., Ahorn, H., *et al.* (1999). Identification of Syntenin as a protein of the apical early endocytic compartment in Madin-Darby canine kidney cells. *J Biol Chem* 274, 26233-26239.
- Fischer von Mollard, G., Stahl, B., Walch-Solimena, C., Takei, K., Daniels, L. and Jahn, R. (1994). Localization of Rab5 to synaptic vesicles identifies endosomal intermediates in synaptic vesicle recycling pathway. *Eur J Cell Biol* 65, 319-326.
- Fogelson, A. L. and Zucker, R. S. (1985). Presynaptic calcium diffusion from various arrays of single channels. Implications for transmitter release and synaptic facilitation. *Biophys J* 48, 1003-1017.

- Fukuda, M. and Mikoshiba, K. (2000). Calcium-dependent and -independent hetero-oligomerization in the Synaptotagmin family. *J Biochem* 128, 637-645.
- Gaidarov, I., Chen, Q., Falck, J. R., Reddy, K. K. and Keen, J. H. (1996). A functional phosphatidylinositol-3,4,5-trisphosphate/phosphoinositide binding domain in the Clathrin adaptor AP-2 alpha subunit. Implications for the endocytic pathway. *J Biol Chem* 271, 20922-20929.
- Gaidarov, I. and Keen, J. H. (1999). Phosphoinositide-AP-2 interactions required for targeting to plasma membrane clathrin-coated pits. *J Cell Biol* 146, 755-764.
- Gallusser, A. and Kirchhausen, T. (1993). The beta 1 and beta 2 subunits of the AP complexes are the Clathrin coat assembly components. *EMBO J* 12, 5237-5244.
- Gallwitz, D., Donath, C. and Sander, C. (1983). A yeast gene encoding a protein homologous to the human c-ha/bas proto-oncogene product. *Nature* 306, 704-707.
- Garrett, M. D., Kabcenell, A. K., Zahner, J. E., Kaibuchi, K., Sasaki, T., Takai, Y., Cheney, C. M. and Novick, P. J. (1993). Interaction of Sec4 with GDI proteins from bovine brain, *Drosophila melanogaster* and *Saccharomyces cerevisiae*. Conservation of GDI membrane dissociation activity. *FEBS Lett* 331, 233-238.
- Gaullier, J. M., Ronning, E., Gillooly, D. J. and Stenmark, H. (2000). Interaction of the EEA1 FYVE finger with phosphatidylinositol-3-phosphate and early endosomes. Role of conserved residues. *J Biol Chem* 275, 24595-24600.
- Gaullier, J. M., Simonsen, A., D'Arrigo, A., Bremnes, B., Stenmark, H. and Aasland, R. (1998). FYVE fingers bind PtdIns(3)P. *Nature* 394, 432-433.
- Geppert, M. and Sudhof, T. C. (1998). Rab3 and Synaptotagmin: the yin and yang of synaptic membrane fusion. *Annu Rev Neurosci* 21, 75-95.
- Ghosh, R. N., Gelman, D. L. and Maxfield, F. R. (1994). Quantification of low density lipoprotein and transferrin endocytic sorting HEp2 cells using confocal microscopy. *J Cell Sci* 107, 2177-2189.
- Ghosh, R. N. and Maxfield, F. R. (1995). Evidence for nonvectorial, retrograde transferrin trafficking in the early endosomes of HEp2 cells. *J Cell Biol* 128, 549-561.
- Gillooly, D. J., Morrow, I. C., Lindsay, M., Gould, R., Bryant, N. J., Gaullier, J. M., Parton, R. G. and Stenmark, H. (2000). Localization of phosphatidylinositol 3-phosphate in yeast and mammalian cells. *EMBO J* 19, 4577-4588.
- Golic, K. G. and Lindquist, S. (1989). The FLP recombinase of yeast catalyzes site-specific recombination in the *Drosophila* genome. *Cell* 59, 499-509.
- González-Gaitán, M. A. and Jäckle, H. (1997). Role of *Drosophila* α -adaptin during synaptic vesicle recycling. *Cell* 88, 767-776.

- Gorczyca, M., Augart, C. and Budnik, V. (1993). Insulin-like receptor and insulin-like peptide are localized at neuromuscular junctions in *Drosophila*. *J Neurosci* 13, 3692-3704.
- Gorvel, J. P., Chavrier, P., Zerial, M. and Gruenberg, J. (1991). Rab5 controls early endosome fusion in vitro. *Cell* 64, 915-925.
- Goud, B. and McCaffrey, M. (1991). Small GTP-binding proteins and their role in transport. *Curr Opin Cell Biol* 3, 626-633.
- Gournier, H., Stenmark, H., Rybin, V., Lippe, R. and Zerial, M. (1998). Two distinct effectors of the small GTPase Rab5 cooperate in endocytic membrane fusion. *EMBO J* 17, 1930-1940.
- Grant, B. and Hirsh, D. (1999). Receptor-mediated endocytosis in the *Caenorhabditis elegans* oocyte. *Mol Biol Cell* 10, 4311-4326.
- Grant, D., Unadkat, S., Katzen, A., Krishnan, K. S. and Ramaswami, N. (1998). Probable mechanisms underlying interallelic complementation and temperature sensitivity of mutations at the *shibire* locus of *Drosophila melanogaster*. *Genetics* 149, 1019-1030.
- Grigliatti, T. A., Hall, L. M., Rosenbluth, R. and Suzuki, D. T. (1973). Temperature-sensitive mutations in *Drosophila melanogaster* - XIV. A selection of immobile adults. *Mol Gen Gen* 120, 107-114.
- Gruenberg, J. and Kreis, T. E. (1995). Membranes and sorting. *Curr Opin Cell Biol* 7, 519-522.
- Gruenberg, J. and Maxfield, F. R. (1995). Membrane transport in the endocytic pathway. *Curr Opin Cell Biol* 7, 552-563.
- Guan, B., Hartmann, B., Kho, Y. H., Gorczyca, M. and Budnik, V. (1996). The *Drosophila* tumor suppressor gene, *dlg*, is involved in structural plasticity at a glutamatergic synapse. *Curr Biol* 6, 695-706.
- Guo, S., Stolz, L. E., Lemrow, S. M. and York, J. D. (1999). SAC1-like domains of yeast SAC1, INP52, and INP53 and of human Synaptojanin encode polyphosphoinositide phosphatases. *J Biol Chem* 274, 12990-12995.
- Halpern, M. E., Chiba, A., Johansen, J. and Keshishian, H. (1991). Growth cone behavior underlying the development of stereotypic synaptic connections in *Drosophila* embryos. *J Neurosci* 11, 3227-3238.
- Hannah, M. J., Schmidt, A. A. and Huttner, W. B. (1999). Synaptic vesicle biogenesis. *Annu Rev Cell Dev Biol* 15, 733-798.
- Hanson, P. I., Roth, R., Morisaki, H., Jahn, R. and Heuser, J. E. (1997). Structure and conformational changes in NSF and its membrane receptor complexes visualized by quick-freeze/deep-etch electron microscopy. *Cell* 90, 523-535.
- Harata, N., Ryan, T. A., Smith, S. J., Buchanan, J. and Tsien, R. W. (2001). Visualizing recycling synaptic vesicles in hippocampal neurons by FM1-43 photoconversion. *PNAS* 98, 12748-12753.

- Harris, T. W., Hartweg, E., Horvitz, H. R. and Jorgensen, E. M. (2000). Mutations in Synaptojanin disrupt synaptic vesicle recycling. *J Cell Biol* 150, 589-600.
- Haucke, V., Wenk, M. R., Chapman, E. R., Farsad, K. and De Camilli, P. (2000). Dual interaction of Synaptotagmin with mu2- and alpha-adaptin facilitates clathrin-coated pit nucleation. *EMBO J* 19, 6011-6019.
- Hay, J. C. and Scheller, R. H. (1997). SNAREs and NSF in targeted membrane fusion. *Curr Opin Cell Biol* 9, 505-512.
- Hayashi, T., McMahon, H., Yamasaki, S., Binz, T., Hata, Y., Sudhof, T. C. and Niemann, H. (1994). Synaptic vesicle membrane fusion complex: action of clostridial neurotoxins on assembly. *EMBO J* 13, 5051-5061.
- Heimbeck, G., Bugnon, V., Gendre, N., Haberland, C. and Stocker, R. F. (1999). Smell and taste perception in *Drosophila melanogaster* larva: toxin expression studies in chemosensory neurons. *J Neurosci* 19, 6599-6609.
- Henkel, A. W., Lubke, J. and Betz, W. J. (1996). FM1-43 dye ultrastructural localization in and release from frog motor nerve terminals. *PNAS* 93, 1918-1923.
- Heuser, J. (1989). The role of coated vesicles in recycling of synaptic vesicle membrane. *Cell Biol Int Rep* 13, 1063-1076.
- Heuser, J. E. and Reese, T. E. (1973). Evidence for recycling of synaptic vesicle membrane during transmitter release at the frog neuromuscular junction. *J Cell Biol* 57, 315-344.
- Hinshaw, J. E. and Schmid, S. L. (1995). Dynamin self-assembles into rings suggesting a mechanism for coated vesicle budding. *Nature* 374, 190-192.
- Hirst, J. and Robinson, M. S. (1998). Clathrin and adaptors. *Biochim Biophys Acta* 1404, 173-193.
- Hoang, B. and Chiba, A. (2001). Single-cell analysis of *Drosophila* larval neuromuscular synapses. *Dev Biol* 229, 55-70.
- Hoffenberg, S., Sanford, J. C., Liu, S., Daniel, D. S., Tuvin, M., Knoll, B. J., Wessling-Resnick, M. and Dickey, B. F. (1995). Biochemical and functional characterization of a recombinant GTPase, Rab5, and two of its mutants. *J Biol Chem* 270, 5048-5056.
- Holstein, S. E., Ungewickell, H. and Ungewickell, E. (1996). Mechanism of Clathrin basket dissociation: separate functions of protein domains of the DnaJ homologue Auxilin. *J Cell Biol* 135, 925-937.
- Holtzman, E., Freeman, A. R. and Kashner, L. A. (1971). Stimulation-dependent alterations in Peroxidase uptake at lobster neuromuscular junctions. *Science* 173, 733-736.
- Hopkins, C. R. (1983). Intracellular routing of Transferrin and Transferrin receptors in epidermoid carcinoma A431 cells. *Cell* 35, 321-330.

- Horiuchi, H., Lippe, R., McBride, H. M., *et al.* (1997). A novel Rab5 GDP/GTP exchange factor complexed to Rabaptin-5 links nucleotide exchange to effector recruitment and function. *Cell* 90, 1149-1159.
- Hubbard, A. L. (1989). Endocytosis. *Curr Opin Cell Biol* 1, 675-683.
- Huber, L. A., Pimplikar, S., Parton, R. G., Virta, H., Zerial, M. and Simons, K. (1993). Rab8, a small GTPase involved in vesicular traffic between the TGN and the basolateral plasma membrane. *J Cell Biol* 123, 35-45.
- Hunter, C. P. (1999). Genetics: a touch of elegance with RNAi. *Curr Biol* 9, R440-R442.
- Ichimura, T., Hatae, T. and Ishida, T. (1997). Direct measurement of endosomal pH in living cells of the rat yolk sac epithelium by laser confocal microscopy. *Eur J Cell Biol* 74, 41-48.
- Ikonen, E. (2001). Roles of lipid rafts in membrane transport. *Curr Opin Cell Biol* 13, 470-477.
- Jahn, R. and Niemann, H. (1994). Molecular mechanisms of clostridial neurotoxins. *Ann N Y Acad Sci* 733, 245-255.
- Jahn, R. and Sudhof, T. C. (1999). Membrane fusion and exocytosis. *Annu Rev Biochem* 68, 863-911.
- Jan, L. Y. and Jan, J. N. (1976a). Properties of the larval neuromuscular junction in *Drosophila melanogaster*. *J Physiol* 262, 189-214.
- Jan, L. Y. and Jan, Y. N. (1976b). L-glutamate as an excitatory transmitter at the *Drosophila* larval neuromuscular junction. *J Physiol* 262, 215-236.
- Jarousse, N. and Kelly, R. B. (2001). Endocytotic mechanisms in synapses. *Curr Opin Cell Biol* 13, 461-469.
- Jedd, G., Richardson, C., Litt, R. and Segev, N. (1995). The Ypt1 GTPase is essential for the first two steps of the yeast secretory pathway. *J Cell Biol* 131, 583-590.
- Jia, X. X., Gorczyca, M. and Budnik, V. (1993). Ultrastructure of neuromuscular junctions in *Drosophila*: comparison of wildtype and mutants with increased excitability. *J Neurobiol* 24, 1025-1044.
- Johansen, J., Halpern, M. E., Johansen, K. M. and Keshishian, H. (1989a). Stereotypic morphology of glutamatergic synapses on identified muscle cells of *Drosophila* larvae. *J Neurosci* 9, 710-725.
- Johansen, J., Halpern, M. E. and Keshishian, H. (1989b). Axonal guidance and the development of muscle fiber-specific innervation in *Drosophila* embryos. *J Neurosci* 9, 4318-4332.
- Jones, A. T. and Clague, M. J. (1995). Phosphatidylinositol 3-kinase activity is required for early endosome fusion. *Biochem J* 311, 31-34.
- Kalidas, S. and Smith, D. P. (2002). Novel genomic cDNA hybrids produce effective RNA interference in adult *Drosophila*. *Neuron* 33, 177-184.

- Kanaseki, T. and Kadota, K. (1969). The "vesicle in a basket". A morphological study of the coated vesicle isolated from the nerve endings of the guinea pig brain, with special reference to the mechanism of membrane movements. *J Cell Biol* 42, 202-220.
- Katz, B. (1969). The release of neural transmitter substances. Liverpool, England: Liverpool University.
- Kelly, R. B. (1993). Storage and release of neurotransmitters. *Cell* 72 *Suppl*, 43-53.
- Keshishian, H., Broadie, K., Chiba, A. and Bate, M. (1996). The *Drosophila* neuromuscular junction: a model system for studying synaptic development and function. *Annu Rev Neurosci* 19, 545-575.
- Keshishian, H., Chiba, A., Chang, T. N., *et al.* (1993). Cellular mechanisms governing synaptic development in *Drosophila melanogaster*. *J Neurobiol* 24, 757-787.
- Kirchhausen, T. (1999). Cell biology. Boa constrictor or rattlesnake? *Nature* 398, 470-471.
- Kirchhausen, T. (2000a). Clathrin. *Annu Rev Biochem* 69, 699-727.
- Kirchhausen, T. (2000b). Three ways to make a vesicle. *Nat Rev Mol Cell Biol* 1, 187-198.
- Kirchhausen, T. and Harrison, S. C. (1981). Protein organization in Clathrin trimers. *Cell* 23, 755-761.
- Klausner, R. D., Donaldson, J. G. and Lippincott-Schwartz, J. (1992). Brefeldin A: insights into the control of membrane traffic and organelle structure. *J Cell Biol* 116, 1071-1080.
- Klenchin, V. A. and Martin, T. F. (2000). Priming in exocytosis: attaining fusion-competence after vesicle docking. *Biochimie* 82, 399-407.
- Klingauf, J., Kavalali, E. T. and Tsien, R. W. (1998). Kinetics and regulation of fast endocytosis at hippocampal synapses. *Nature* 394, 581-585.
- Kneussel, M. and Betz, H. (2000). Clustering of inhibitory neurotransmitter receptors at developing postsynaptic sites: the membrane activation model. *Trends Neurosci* 23, 429-435.
- Koenig, J. H. and Ikeda, K. (1989). Disappearance and reformation of synaptic vesicle membrane upon transmitter release observed under reversible blockage of membrane retrieval. *J Neurosci* 9, 3844-3860.
- Koenig, J. H. and Ikeda, K. (1999). Contribution of active zone subpopulation of vesicles to evoked and spontaneous release. *J Neurophysiol* 81, 1495-1505.
- Koenig, J. H., Kosaka, T. and Ikeda, K. (1989). The relationship between the number of synaptic vesicles and the amount of transmitter released. *J Neurosci* 9, 1937-1942.
- Koenig, J. H., Yamaoka, K. and Ikeda, K. (1993). Calcium-induced translocation of synaptic vesicles to the active site. *J Neurosci* 13, 2313-2322.

- Kosaka, T. and Ikeda, K. (1983a). Possible temperature-dependent blockage of synaptic vesicle recycling induced by a single gene mutation in *Drosophila*. *J Neurobiol* 14, 207-225.
- Kosaka, T. and Ikeda, K. (1983b). Reversible blockage of membrane retrieval and endocytosis in the garland cell of the temperature-sensitive mutant of *Drosophila melanogaster*, *shibire^{ts1}*. *J Cell Biol* 97, 499-507.
- Kreis, T. E. (1992). Regulation of vesicular and tubular membrane traffic of the Golgi complex by coat proteins. *Curr Opin Cell Biol* 4, 609-615.
- Kurdyak, P., Atwood, H. L., Stewart, B. A. and Wu, C. F. (1994). Differential physiology and morphology of motor axons to ventral longitudinal muscles in larval *Drosophila*. *J Comp Neurol* 350, 463-472.
- Kuromi, H. and Kidokoro, Y. (1998). Two distinct pools of synaptic vesicles in single presynaptic boutons in a temperature-sensitive *Drosophila* mutant, *shibire*. *Neuron* 20, 917-925.
- Kuromi, H. and Kidokoro, Y. (1999). The optically determined size of exo/endo cycling vesicle pool correlates with the quantal content at the neuromuscular junction of *Drosophila* larvae. *J Neurosci* 19, 1557-1565.
- Kuromi, H. and Kidokoro, Y. (2000). Tetanic stimulation recruits vesicles from reserve pool via a cAMP-mediated process in *Drosophila* synapses. *Neuron* 27, 133-143.
- Kuznetsov, S. A., Langford, G. M. and Weiss, D. G. (1992). Actin-dependent organelle movement in squid axoplasm. *Nature* 356, 722-725.
- Laemmli, U. K. (1970). Cleavage of structural proteins during the assembly of the head of bacteriophage T4. *Nature* 227, 680-685.
- Lai, M. M., Hong, J. J., Ruggiero, A. M., Burnett, P. E., Slepnev, V. I., de Camilli, P. and Snyder, S. H. (1999). The Calcineurin-Dynamin1 complex as a calcium sensor for synaptic vesicles endocytosis. *J Biol Chem* 274, 25963-25966.
- Lawe, D. C., Patki, V., Heller-Harrison, R., Lambricht, D. and Corvera, S. (2000). The FYVE domain of early endosome antigen 1 is required for both phosphatidylinositol-3-phosphate and Rab5 binding - Critical role of this dual interaction for endosomal localization. *J Biol Chem* 275, 3699-3705.
- Lazar, T., Gotte, M. and Gallwitz, D. (1997). Vesicular transport: how many Ypt/Rab-GTPases make a eukaryotic cell? *Trends Biochem Sci* 22, 468-472.
- Li, C., Ullrich, B., Zhang, J. Z., Anderson, R. G., Brose, N. and Sudhof, T. C. (1995a). Ca²⁺-dependent and -independent activities of neural and non-neural Synaptotagmins. *Nature* 375, 594-599.
- Li, G., Barbieri, M. A., Colombo, M. I. and Stahl, P. D. (1994). Structural features of the GTP-binding defective Rab5 mutants required for their inhibitory activity on endocytosis. *J Biol Chem* 269, 14631-14635.
- Li, G., D'Souza-Schorey, C., Barbieri, M. A., Roberts, R. L., Klippel, A., Williams, L. T. and Stahl, P. D. (1995b). Evidence for phosphatidylinositol-3-

- kinase as a regulator of endocytosis via activation of Rab5. PNAS 92, 10207-10211.
- Li, G. and Stahl, P. D. (1993). Structure-function relationship of the small GTPase Rab5. J Biol Chem 268, 24475-24480.
- Lian, J. P., Stone, S., Jiang, Y., Lyons, P. and Ferro-Novick, S. (1994). Ypt1p implicated in v-SNARE activation. Nature 372, 698-701.
- Lim, N. F., Nowycky, M. C. and Bookman, R. J. (1990). Direct measurement of exocytosis and calcium currents in single vertebrate nerve terminals. Nature 344, 449-451.
- Lin, D. M. and Goodman, C. S. (1994). Ectopic and increased expression of Fasciclin II alters motoneuron growth cone guidance. Neuron 13, 507-523.
- Lin, R. C. and Scheller, R. H. (1997). Structural organization of the synaptic exocytosis core complex. Neuron 19, 1087-1094.
- Lindau, M., Stuenkel, E. L. and Nordmann, J. J. (1992). Depolarization, intracellular calcium and exocytosis in single vertebrate nerve endings. Biophys J 61, 19-30.
- Lippe, R., Miaczynska, M., Rybin, V., Runge, A. and Zerial, M. (2001). Functional synergy between Rab5 effector Rabaptin-5 and exchange factor Rabex-5 when physically associated in a complex. Mol Biol Cell 12, 2219-2228.
- Littleton, J. T. (2000). A genomic analysis of membrane trafficking and neurotransmitter release in *Drosophila*. J Cell Biol 150, F77-F82.
- Littleton, J. T. and Bellen, H. J. (1995). Synaptotagmin controls and modulates synaptic-vesicle fusion in a Ca²⁺-dependent manner. Trends Neurosci 18, 177-183.
- Littleton, J. T., Chapman, E. R., Kreber, R., Garment, M. B., Carlson, S. D. and Ganetzky, B. (1998). Temperature-sensitive paralytic mutations demonstrate that synaptic exocytosis requires SNARE complex assembly and disassembly. Neuron 21, 401-413.
- Littleton, J. T., Serano, T. L., Rubin, G. M., Ganetzky, B. and Chapman, E. R. (1999). Synaptic function modulated by changes in the ratio of Synaptotagmin I and IV. Nature 400, 757-760.
- Liu, S. H., Wong, M. L., Craik, C. S. and Brodsky, F. M. (1995). Regulation of Clathrin assembly and trimerization defined using recombinant triskelion hubs. Cell 83, 257-267.
- Llinas, R., Sugimori, M. and Silver, R. B. (1992). Microdomains of high calcium concentration in a presynaptic terminal. Science 256, 677-679.
- Llinas, R., Sugimori, M. and Simon, S. M. (1982). Transmission by presynaptic spike-like depolarization in the squid giant synapse. PNAS 79, 2415-2419.
- Lnenicka, G. A. and Keshishian, H. (2000). Identified motor terminals in *Drosophila* larvae show distinct differences in morphology and physiology. J Neurobiol 43, 186-197.

- Loewen, C. A., Mackler, J. M. and Reist, N. E. (2001). *Drosophila* Synaptotagmin/null mutants survive to early adulthood. *Genesis* 31, 30-36.
- Lombardi, D., Soldati, T., Riederer, M. A., Goda, Y., Zerial, M. and Pfeffer, S. R. (1993). Rab9 functions in transport between late endosomes and the *trans*-Golgi network. *EMBO J* 12, 677-682.
- Lupashin, V. V. and Waters, M. G. (1997). t-SNARE activation through transient interaction with a rab-like guanosine triphosphatase. *Science* 276, 1255-1258.
- Mahaffey, D. T., Moore, M. S., Brodsky, F. M. and Anderson, R. G. (1989). Coat proteins isolated from clathrin-coated vesicles can assemble into coated pits. *J Cell Biol* 108, 1615-1624.
- Mahaffey, D. T., Peeler, J. S., Brodsky, F. M. and Anderson, R. G. W. (1990). Clathrin-coated pits contain an integral membrane protein that binds the AP-2 subunit with high affinity. *J Biol Chem* 265, 16514-16520.
- Marks, B. and McMahon, H. T. (1998). Calcium triggers calcineurin-dependent synaptic vesicle recycling in mammalian nerve terminals. *Curr Biol* 8, 740-749.
- Marshall, C. J. (1993). Protein prenylation: a mediator of protein-protein interactions. *Science* 259, 1865-1866.
- Martin, A. R. (1955). A further study of the statistical composition of the end-plate potential. *J Physiol* 130, 114-122.
- Martin, T. F. J. and Kowalchuk, J. A. (1997). Docked secretory vesicles undergo Ca^{2+} -activated exocytosis in a cell-free system. *J Biol Chem* 272, 14447-14453.
- Martinez, O., Schmidt, A., Salamero, J., Hoflack, B., Roa, M. and Goud, B. (1994). The small GTP-binding protein Rab6 functions in intra-Golgi transport. *J Cell Biol* 127, 1575-1588.
- Matteoli, M., Takei, K., Perin, M. S., Sudhof, T. C. and De Camilli, P. (1992). Exo-endocytotic recycling of synaptic vesicles in developing processes of cultured hippocampal neurons. *J Cell Biol* 117, 849-861.
- Maycox, P. R., Link, E., Reetz, A., Morris, S. A. and Jahn, R. (1992). Clathrin-coated vesicles in nervous tissue are involved primarily in synaptic vesicle recycling. *J Cell Biol* 118, 1379-1388.
- Mayor, S., Presley, J. F. and Maxfield, F. R. (1993). Sorting of membrane components from endosomes and subsequent recycling to the cell surface occurs by a bulk flow process. *J Cell Biol* 121, 1257-1269.
- McBride, H. M., Rybin, V., Murphy, C., Giner, A., Teasdale, R. and Zerial, M. (1999). Oligomeric complexes link Rab5 effectors with NSF and drive membrane fusion via interactions between EEA1 and Syntaxin 13. *Cell* 98, 377-386.

- McLauchlan, H., Newell, J., Morrice, N., Osborne, A., West, M. and Smythe, E. (1998). A novel role for Rab5-GDI in ligand sequestration into clathrin-coated pits. *Curr Biol* 8, 34-45.
- McNew, J. A., Parlati, F., Fukuda, R., Johnston, R. J., Paz, K., Paumet, F., Sollner, T. H. and Rothman, J. E. (2000). Compartmental specificity of cellular membrane fusion encoded in SNARE proteins. *Nature* 407, 153-159.
- McPherson, P. S., Garcia, E. P., Slepnev, V. I., *et al.* (1996). A presynaptic inositol-5-phosphatase. *Nature* 379, 353-357.
- Mellman, I. (1996). Endocytosis and molecular sorting. *Annu Rev Cell Dev Biol* 12, 575-625.
- Méresse, S., Gorvel, J. P. and Chavrier, P. (1995). The Rab7 GTPase resides on a vesicular compartment connected to lysosomes. *J Cell Biol* 108, 3349-3358.
- Mintz, I. M., Sabatini, B. L. and Regehr, W. G. (1995). Calcium control of transmitter release at a cerebellar synapse. *Neuron* 15, 675-688.
- Mitchison, T. J. (1992). Compare and contrast actin filaments and microtubules. *Mol Biol Cell* 3, 1309-1315.
- Monastirioti, M., Gorczyca, M., Rapus, J., Eckert, M., White, K. and Budnik, V. (1995). Octopamine immunoreactivity in the fruit fly *Drosophila melanogaster*. *J Comp Neurol* 356, 275-287.
- Montecucco, C. and Schiavo, G. (1995). Structure and function of tetanus and botulinum neurotoxins. *Q Rev Biophys* 28, 423-472.
- Moore, M. S., Mahaffey, D. T., Brodsky, F. M. and Anderson, R. G. (1987). Assembly of clathrin-coated pits onto purified plasma membranes. *Science* 236, 558-563.
- Morris, S. A., Schroder, S., Plessmann, U., Weber, K. and Ungewickell, E. (1993). Clathrin assembly protein AP-180: primary structure, domain organization and identification of a Clathrin binding site. *EMBO J* 12, 667-675.
- Moya, M., Roberts, D. and Novick, P. (1993). DSS4-1 is a dominant suppressor of *sec4-8* that encodes a nucleotide exchange protein that aids Sec4p function. *Nature* 361, 460-463.
- Mu, F. T., Callaghan, J. M., Steele-Mortimer, O., *et al.* (1995). EEA1, an early endosome-associated protein. EEA1 is a conserved alpha-helical peripheral membrane protein flanked by cysteine "fingers" and contains a calmodulin-binding IQ motif. *J Biol Chem* 270, 13503-13511.
- Mukherjee, S., Ghosh, R. N. and Maxfield, F. R. (1997). Endocytosis. *Physiol Rev* 77, 759-803.
- Murthy, V. N. and Stevens, C. F. (1998). Synaptic vesicles retain their identity through the endocytic cycle. *Nature* 392, 497-501.
- Neher, E. and Zucker, R. S. (1993). Multiple calcium-dependent processes related to secretion in bovine chromaffin cells. *Neuron* 10, 21-30.

- Neves, G. and Lagnado, L. (1999). The kinetics of exocytosis and endocytosis in the synaptic terminal of goldfish retinal bipolar cells. *J Physiol* 515, 181-202.
- Nielsen, E., Christoforidis, S., Uttenweiler-Joseph, S., Miaczynska, M., Dewitte, F., Wilm, M., Hoflack, B. and Zerial, M. (2000). Rabenosyn-5, a novel Rab5 effector, is complexed with hVPS45 and recruited to endosomes through a FYVE finger domain. *J Cell Biol* 151, 601-612.
- Nielsen, E., Severin, F., Backer, J. M., Hyman, A. A. and Zerial, M. (1999). Rab5 regulates motility of early endosomes on microtubules. *Nat Cell Biol* 1, 376-382.
- Nishikawa, K. and Kidokoro, Y. (1995). Junctional and extrajunctional glutamate receptor channels in *Drosophila* embryos and larvae. *J Neurosci* 15, 7905-7915.
- Nonet, M. L., Holgado, A. M., Brewer, F., *et al.* (1999). UNC-11, a *Caenorhabditis elegans* AP-180 homologue, regulates the size and protein composition of synaptic vesicles. *Mol Biol Cell* 10, 2343-2360.
- Novick, P. and Zerial, M. (1997). The diversity of Rab proteins in vesicle transport. *Curr Opin Cell Biol* 9, 496-504.
- Nuoffer, C. and Balch, W. E. (1994). GTPases: multifunctional molecular switches regulating vesicular traffic. *Annu Rev Biochem* 63, 949-990.
- Nuoffer, C., Davidson, H. W., Matteson, J., Meinkoth, J. and Balch, W. E. (1994). A GDP-bound form of Rab1 inhibits protein export from the endoplasmic reticulum and transport between Golgi compartments. *J Cell Biol* 125, 225-237.
- Nüsslein-Volhard, C. and Wieschaus, E. (1980). Mutations affecting segment number and polarity in *Drosophila*. *Nature* 287, 795-801.
- O'Kane, C. J. and Gehring, W. J. (1987). Detection *in situ* of genomic regulatory elements in *Drosophila*. *PNAS* 84, 9123-9127.
- Oheim, M., Loerke, D., Stuhmer, W. and Chow, R. H. (1998). The last few milliseconds in the life of a secretory granule in live chromaffin cells. *Eur Biophys J* 27, 83-98.
- Ohno, H., Fournier, M. C., Poy, G. and Bonifacino, J. S. (1996). Structural determinants of interaction of tyrosine-based sorting signals with the adaptor medium chains. *J Biol Chem* 271, 29009-29015.
- Ohno, H., Stewart, J., Fournier, M. C., *et al.* (1995). Interaction of tyrosine-based sorting signals with clathrin-associated proteins. *Science* 269, 1872-1875.
- Olkonen, V. M., Dupree, P., Killisch, I., Lutcke, A., Zerial, M. and Simons, K. (1993). Molecular cloning and subcellular localization of three GTP-binding proteins of the Rab subfamily. *J Cell Sci* 106, 1249-1261.
- Olkonen, V. M. and Stenmark, H. (1997). Role of Rab GTPases in membrane traffic. *Int Rev Cytol* 176, 1-85.

- Osborne, S. L., Herreros, J., Bastiaens, P. I. and Schiavo, G. (1999). Calcium-dependent oligomerization of Synaptotagmins I and II. Synaptotagmins I and II are localized on the same synaptic vesicle and heterodimerize in the presence of calcium. *J Biol Chem* 274, 59-66.
- Otto, H., Hanson, P. I. and Jahn, R. (1997). Assembly and disassembly of a ternary complex of Synaptobrevin, Syntaxin, and SNAP-25 in the membrane of synaptic vesicles. *PNAS* 94, 6197-6201.
- Oyler, G. A., Higgins, G. A., Hart, R. A., Battenberg, E., Billingsley, M., Bloom, F. E. and Wilson, M. C. (1989). The identification of a novel synaptosomal-associated protein, SNAP-25, differentially expressed by neuronal subpopulations. *J Cell Biol* 109, 3039-3052.
- Palfrey, H. C. and Artalejo, C. R. (1998). Vesicle recycling revisited: rapid endocytosis may be the first step. *Neurosci* 83, 969-989.
- Pallanck, L. and Ganetsky, B. (1999). Mechanisms of neurotransmitter release. In *Neuromuscular junctions in Drosophila*. V. Budnik, and L. S. Gramates, eds. (San Diego: Academic.), pp. 139-161.
- Parlati, F., McNew, J. A., Fukuda, R., Miller, R., Sollner, T. H. and Rothman, J. E. (2000). Topological restriction of SNARE-dependent membrane fusion. *Nature* 407, 194-198.
- Parsons, T. D., Lenzi, D., Almers, W. and Roberts, W. M. (1994). Calcium-triggered exocytosis and endocytosis in an isolated presynaptic cell: capacitance measurements in saccular hair cells. *Neuron* 13, 875-883.
- Parton, R. G., Simons, K. and Dotti, C. G. (1992). Axonal and dendritic endocytic pathways in cultured neurons. *J Cell Biol* 119, 123-137.
- Patki, V., Lawe, D. C., Corvera, S., Virbasius, J. V. and Chawla, A. (1998). A functional PtdIns(3)P-binding motif. *Nature* 394, 433-434.
- Pearse, B. M. (1975). Coated vesicles from pig brain: purification and biochemical characterization. *J Mol Biol* 97, 93-98.
- Pearse, B. M. (1976). Clathrin: a unique protein associated with intracellular transfer of membrane by coated vesicles. *PNAS* 73, 1255-1259.
- Perin, M. S., Fried, V. A., Mignery, G. A., Jahn, R. and Sudhof, T. C. (1990). Phospholipid binding by a synaptic vesicle protein homologous to the regulatory region of protein kinase C. *Nature* 345, 260-263.
- Petersen, S. A., Fetter, R. D., Noordermeer, J. N., Goodman, C. S. and DiAntonio, A. (1997). Genetic analysis of glutamate receptors in *Drosophila* reveals a retrograde signal regulating presynaptic transmitter release. *Neuron* 19, 1237-1248.
- Peterson, M. R., Burd, C. G. and Emr, S. D. (1999). Vac1p coordinates Rab and phosphatidylinositol-3-kinase signaling in Vps45p-dependent vesicle docking/fusion at the endosome. *Curr Biol* 9, 159-162.
- Pfeffer, S. R. (1994). Rab GTPases: master regulators of membrane trafficking. *Curr Opin Cell Biol* 6, 522-526.

- Pfeffer, S. R. (1996). Transport vesicle docking: SNAREs and associates. *Annu Rev Cell Dev Biol* 12, 441-461.
- Pfeffer, S. R. (1999). Transport vesicle targeting: tethers before SNAREs. *Nat Cell Biol* 1, E17-E22.
- Pfeffer, S. R., Dirac-Svejstrup, A. B. and Soldati, T. (1995). Rab GDP dissociation inhibitor: putting Rab GTPases in the right place. *J Biol Chem* 270, 17057-17959.
- Plattner, H., Artalejo, A. R. and Neher, E. (1997). Ultrastructural organization of bovine chromaffin cell cortex-analysis by cryofixation and morphometry of aspects pertinent to exocytosis. *J Cell Biol* 139, 1709-1717.
- Poirier, M. A., Hao, J. C., Malkus, P. N., Chan, C., Moore, M. F., King, D. S. and Bennett, M. K. (1998). Protease resistance of Syntaxin, SNAP-25, VAMP complexes. Implications for assembly and structure. *J Biol Chem* 273, 11370-11377.
- Poodry, C. A. and Edgar, L. (1979). Reversible alterations in the neuromuscular junctions of *Drosophila melanogaster* bearing a temperature-sensitive mutation, *shibire*. *J Cell Biol* 81, 520-527.
- Prekeris, R., Klumperman, J. and Scheller, R. H. (2000). A Rab11/Rip11 protein complex regulates apical membrane trafficking via recycling endosomes. *Mol Cell* 6, 1437-1448.
- Price, A., Seals, D., Wickner, W. and Ungermann, C. (2000). The docking stage of yeast vacuole fusion requires the transfer of proteins from a cis-SNARE complex to a Rab/Ypt protein. *J Cell Biol* 148, 1231-1238.
- Prokop, A., Landgraf, M., Rushton, E., Broadie, K. and Bate, M. (1996). Presynaptic development at the *Drosophila* neuromuscular junction: assembly and localization of presynaptic active zones. *Neuron* 17, 617-626.
- Provoda, C. J., Waring, M. T. and Buckley, K. M. (2000). Evidence for a primary endocytic vesicle involved in synaptic vesicle biogenesis. *J Biol Chem* 275, 7004-7012.
- Pumplin, D. W., Reese, T. S. and Llinas, R. (1981). Are the presynaptic membrane particles the calcium channels? *PNAS* 78, 7210-7213.
- Pyle, J. L., Kavalali, E. T., Piedras-Renteria, E. S. and Tsien, R. W. (2000). Rapid reuse of readily releasable pool vesicles at hippocampal synapses. *Neuron* 28, 221-231.
- Raiborg, C., Bache, K. G., Mehlum, A., Stang, E. and Stenmark, H. (2001a). Hrs recruits Clathrin to early endosomes. *EMBO J* 20, 5008-5021.
- Raiborg, C., Bremnes, B., Mehlum, A., Gillooly, D. J., D'Arrigo, A., Stang, E. and Stenmark, H. (2001b). FYVE and coiled-coil domains determine the specific localisation of Hrs to early endosomes. *J Cell Sci* 114, 2255-2263.
- Regazzi, R., Kikuchi, A., Takai, Y. and Wollheim, C. B. (1992). The small GTP-binding proteins in the cytosol of insulin-secreting cells are complexed to GDP dissociation inhibitor proteins. *J Biol Chem* 267, 17512-17519.

- Richards, D. A., Guatimosim, C. and Betz, W. J. (2000). Two endocytic recycling routes selectively fill two vesicle pools in frog motor nerve terminals. *Neuron* 27, 551-559.
- Riederer, M. A., Soldati, T., Shapiro, A. D., Lin, J. and Pfeffer, S. R. (1994). Lysosome biogenesis requires Rab9 function and receptor recycling from endosomes to the *trans*-Golgi network. *J Cell Biol* 125, 573-582.
- Ringstad, N., Gad, H., Low, P., Di Paolo, G., Brodin, L., Shupliakov, O. and De Camilli, P. (1999). Endophilin/SH3p4 is required for the transition from early to late stages in clathrin-mediated synaptic vesicle endocytosis. *Neuron* 24, 143-154.
- Roberts, R. L., Barbieri, M. A., Pryse, K. M., Chua, M., Morisaki, J. H. and Stahl, P. D. (1999). Endosome fusion in living cells overexpressing GFP-Rab5. *J Cell Sci* 112, 3667-3675.
- Robinson, M. S. and Bonifacino, J. S. (2001). Adaptor-related proteins. *Curr Opin Cell Biol* 13, 444-453.
- Robitaille, R., Adler, E. M. and Charlton, M. P. (1990). Strategic location of calcium channels at transmitter release sites of frog neuromuscular synapses. *Neuron* 5, 773-779.
- Rodman, J. S., Mercer, R. W. and Stahl, P. D. (1990). Endocytosis and transcytosis. *Curr Opin Cell Biol* 2, 664-672.
- Rohn, W. M., Rouille, Y., Waguri, S. and Hoflack, B. (2000). Bi-directional trafficking between the *trans*-Golgi network and the endosomal/lysosomal system. *J Cell Sci* 113, 2093-2101.
- Roos, J. and Kelly, R. B. (1998). Dap160, a neural-specific Eps15 homology and multiple SH3 domain-containing protein that interacts with *Drosophila* Dynamin. *J Biol Chem* 273, 19108-19119.
- Roos, J. and Kelly, R. B. (1999). The endocytic machinery in nerve terminals surrounds sites of exocytosis. *Curr Biol* 9, 1411-1414.
- Rosenmund, C. and Stevens, C. F. (1996). Definition of the readily releasable pool of vesicles at hippocampal synapses. *Neuron* 16, 1197-1207.
- Roth, T. F. and Porter, K. R. (1964). Yolk protein uptake in oocyte of mosquito *Aedes aegypti*. *J Cell Biol* 20, 313-324.
- Rothman, J. E. (1994). Mechanisms of intracellular protein transport. *Nature* 372, 55-63.
- Rothman, J. E. and Orci, L. (1992). Molecular dissection of the secretory pathway. *Nature* 355, 409-415.
- Rubin, G. M. and Spradling, A. C. (1982). Genetic transformation of *Drosophila* with transposable element vectors. *Science* 218, 348-353.
- Rubino, M., Miaczynska, M., Lippe, R. and Zerial, M. (2000). Selective membrane recruitment of EEA1 suggests a role in directional transport of clathrin-coated vesicles to early endosomes. *J Biol Chem* 275, 3745-3748.

- Ryan, T. A. and Smith, S. J. (1995). Vesicle pool mobilization during action potential firing at hippocampal synapses. *Neuron* 14, 983-989.
- Rybin, V., Ullrich, O., Rubino, M., Alexandrov, K., Simon, I., Seabra, M. C., Goody, R. and Zerial, M. (1996). GTPase activity of Rab5 acts as a timer for endocytic membrane fusion. *Nature* 383, 266-269.
- Saitoe, M., Tanaka, S., Takata, K. and Kidokoro, Y. (1997). Neural activity affects distribution of glutamate receptors during neuromuscular junction formation in *Drosophila* embryos. *Dev Biol* 184, 48-60.
- Salminen, A. and Novik, P. J. (1987). A Ras-like protein is required for a post-Golgi event in yeast secretion. *Cell* 49, 527-538.
- Sasaki, T., Kaibuchi, K., Kabcenell, A. K., Novick, P. J. and Takai, Y. (1991). A mammalian inhibitory GDP/GTP exchange protein (GDP dissociation inhibitor) for smg p25A is active on the yeast SEC4 protein. *Mol Cell Biol* 11, 2909-2912.
- Sasaki, T., Kikuchi, A., Araki, S., Hata, Y., Isomura, M., Kuroda, S. and Takai, Y. (1990). Purification and characterization from bovine brain cytosol of a protein that inhibits the dissociation of GDP from and the subsequent binding of GTP to smg p25A, a ras p21-like GTP-binding protein. *J Biol Chem* 265, 2333-2337.
- Sato, T. K., Rehling, P., Peterson, M. R. and Emr, S. D. (2000). Class C Vps protein complex regulates vacuolar SNARE pairing and is required for vesicle docking/fusion. *Mol Cell* 6, 661-671.
- Schiavo, G., Benfenati, F., Poulain, B., Rossetto, O., Poverino de Laureto, P., DasGupta, B. R. and Montecucco, C. (1992). Tetanus and botulinum-B neurotoxins block neurotransmitter release by proteolytic cleavage of Synaptobrevin. *Nature* 359, 832-835.
- Schikorski, T. and Stevens, C. F. (1997). Quantitative ultrastructural analysis of hippocampal excitatory synapses. *J Neurosci* 17, 5858-5867.
- Schikorski, T. and Stevens, C. F. (2001). Morphological correlates of functionally defined synaptic vesicle populations. *Nat Neurosci* 4, 391-395.
- Schlierf, B., Fey, G. H., Hauber, J., Hocke, G. M. and Rosorius, O. (2000). Rab11b is essential for recycling of Transferrin to the plasma membrane. *Exp Cell Res* 259, 257-265.
- Schlossman, D. M., Schmid, S. L., Braell, W. A. and Rothman, J. E. (1984). An enzyme that removes Clathrin coats: purification of an uncoating ATPase. *J Cell Biol* 99, 723-733.
- Schmid, A., Chiba, A. and Doe, C. Q. (1999). Clonal analysis of *Drosophila* embryonic neuroblasts: neural cell types, axon projections and muscle targets. *Development* 126, 4653-4689.
- Schmid, A., Schindelholz, B. and Zinn, K. (2002). Combinatorial RNAi: a method for evaluating the functions of gene families in *Drosophila*. *Trends Neurosci* 25, 71-74.

- Schmid, S. L. (1997). Clathrin-coated vesicle formation and protein sorting: an integrated process. *Annu Rev Biochem* 66, 511-548.
- Schmid, S. L., Fuchs, R., Male, P. and Mellman, I. (1988). Two distinct subpopulations of endosomes involved in membrane recycling and transport to lysosomes. *Cell* 52, 73-83.
- Schmidt, A., Wolde, M., Thiele, C., Fest, W., Kratzin, H., Podtelejnikov, A. V., Witke, W., Huttner, W. B. and Soeling, H.-D. (1999). Endophilin I mediates synaptic vesicle formation by transfer of arachidonate to lysophosphatidic acid. *Nature* 401, 133-149.
- Schneggenburger, R. and Neher, E. (2000). Intracellular calcium dependence of transmitter release rates at a fast central synapse. *Nature* 406, 889-893.
- Schroder, S., Morris, S. A., Knorr, R., Plessmann, U., Weber, K., Nguyen, G. V. and Ungewickell, E. (1995). Primary structure of the neuronal clathrin-associated protein Auxilin and its expression in bacteria. *Eur J Biochem* 228, 297-304.
- Schuster, C. M., Davis, G. W., Fetter, R. D. and Goodman, C. S. (1996). Genetic dissection of structural and functional components of synaptic plasticity. I. Fasciclin II controls synaptic stabilization and growth. *Neuron* 17, 641-654.
- Seabra, M. C., Brown, M. S., Slaughter, C. A., Sudhof, T. C. and Goldstein, J. L. (1992a). Purification of component A of Rab geranylgeranyl transferase: possible identity with the choroideremia gene product. *Cell* 70, 1049-1057.
- Seabra, M. C., Goldstein, J. L., Sudhof, T. C. and Brown, M. S. (1992b). Rab geranylgeranyl transferase. A multisubunit enzyme that prenylates GTP-binding proteins terminating in Cys-X-Cys or Cys-Cys. *J Biol Chem* 267, 14497-14503.
- Segev, N. (1991). Mediation of the attachment or fusion step in vesicular transport by the GTP-binding Ypt1 protein. *Science* 252, 1553-1556.
- Sever, S., Muhlberg, A. B. and Schmid, S. L. (1999). Impairment of Dynamin's GAP domain stimulates receptor-mediated endocytosis. *Nature* 398, 481-486.
- Sheff, D. R., Daro, E. A., Hull, M. and Mellman, I. (1999). The receptor recycling pathway contains two distinct populations of early endosomes with different sorting functions. *J Cell Biol* 145, 123-139.
- Shih, W., Gallusser, A. and Kirchhausen, T. (1995). A clathrin-binding site in the hinge of the beta 2 chain of mammalian AP-2 complexes. *J Biol Chem* 270, 31083-31090.
- Shraiman, B. I. (1997). On the role of assembly kinetics in determining the structure of Clathrin cages. *Biophys J* 72, 953-957.
- Shupliakov, O., Low, P., Grabs, D., Gad, H., Chen, H., David, C., Takei, K., De Camilli, P. and Brodin, L. (1997). Synaptic vesicle endocytosis impaired by disruption of dynamin-SH3 domain interactions. *Science* 276, 259-263.

- Simonsen, A., Lippe, R., Christoforidis, S., *et al.* (1998). EEA1 links PI(3)kinase function to Rab5 regulation of endosome fusion. *Nature* 394, 494-498.
- Sink, H. and Whitington, P. M. (1991a). Early ablation of target muscles modulates the arborisation pattern of an identified embryonic *Drosophila* motor axon. *Development* 113, 701-707.
- Sink, H. and Whitington, P. M. (1991b). Location and connectivity of abdominal motoneurons in the embryo and larva of *Drosophila melanogaster*. *J Neurobiol* 22, 298-311.
- Sink, H. and Whitington, P. M. (1991c). Pathfinding in the central nervous system and periphery by identified embryonic *Drosophila* motor axons. *Development* 112, 307-316.
- Sogaard, M., Tani, K., Ye, R. R., Geromanos, S., Tempst, P., Kirchhausen, T., Rothman, J. E. and Sollner, T. (1994). A Rab protein is required for the assembly of SNARE complexes in the docking of transport vesicles. *Cell* 78, 937-948.
- Soldati, T., Riederer, M. A. and Pfeffer, S. R. (1993). Rab GDI: a solubilizing and recycling factor for Rab9 protein. *Mol Biol Cell* 4, 425-434.
- Soldati, T., Shapiro, A. D., Svejstrup, A. B. and Pfeffer, S. R. (1994). Membrane targeting of the small GTPase Rab9 is accompanied by nucleotide exchange. *Nature* 369, 76-78.
- Sollner, T., Bennett, M. K., Whiteheart, S. W., Scheller, R. H. and Rothman, J. E. (1993a). A protein assembly-disassembly pathway *in vitro* that may correspond to sequential steps of synaptic vesicle docking, activation and fusion. *Cell* 75, 409-418.
- Sollner, T., Whiteheart, S. W., Brunner, M., Erdjument-Bromage, H., Geromanos, S., Tempst, P. and Rothman, J. E. (1993b). SNAP receptors implicated in vesicle targeting and fusion. *Nature* 362, 318-324.
- Sonnichsen, B., De Renzis, S., Nielsen, E., Rietdorf, J. and Zerial, M. (2000). Distinct membrane domains on endosomes in the recycling pathway visualized by multicolor imaging of Rab4, Rab5, and Rab11. *J Cell Biol* 149, 901-914.
- Sorkin, A., McKinsey, T., Shih, W., Kirchhausen, T. and Carpenter, G. (1995). Stoichiometric interaction of the epidermal growth factor receptor with the clathrin-associated protein complex AP-2. *J Biol Chem* 270, 619-625.
- Spiro, D. J., Boll, W., Kirchhausen, T. and Wessling-Resnick, M. (1996). Wortmannin alters the transferrin receptor endocytic pathway *in vivo* and *in vitro*. *Mol Biol Cell* 7, 355-367.
- Spradling, A. C. and Rubin, G. M. (1982). Transposition of cloned P-elements into *Drosophila* germ line chromosomes. *Science* 218, 341-347.
- Spruce, A. E., Breckenridge, L. J., Lee, A. K. and Almers, W. (1990). Properties of the fusion pore that forms during exocytosis of a mast cell secretory vesicle. *Neuron* 4, 643-654.

- Stenmark, H. and Aasland, R. (1999). FYVE-finger proteins - effectors of an inositol lipid. *J Cell Sci* 112, 4175-4183.
- Stenmark, H., Aasland, R., Toh, B. H. and D'Arrigo, A. (1996). Endosomal localization of the autoantigen EEA1 is mediated by a zinc-binding FYVE finger. *J Biol Chem* 271, 24048-24054.
- Stenmark, H., Parton, R. G., Steele-Mortimer, O., Luetcke, A., Gruenberg, J. and Zerial, M. (1994). Inhibition of Rab5 GTPase activity stimulates membrane fusion in endocytosis. *EMBO J* 13, 1287-1296.
- Stenmark, H., Vitale, G., Ullrich, O. and Zerial, M. (1995). Rabaptin-5 is a direct effector of the small GTPase Rab5 in endocytic membrane fusion. *Cell* 83, 423-432.
- Stevens, C. F. and Tsujimoto, T. (1995). Estimates for the pool size of releasable quanta at a single central synapse and for the time required to refill the pool. *PNAS* 92, 846-849.
- Stevens, C. F. and Williams, J. H. (2000). "Kiss-and-run" exocytosis at hippocampal synapses. *PNAS* 97, 12828-12833.
- Stewart, B. A., Atwood, H. L., Renger, J. J., Wang, J. and Wu, C. F. (1994). Improved stability of *Drosophila* larval neuromuscular preparations in haemolymph-like physiological solutions. *J Comp Neurol* 175, 179-191.
- Strom, M., Vollmer, P., Tan, T. J. and Gallwitz, D. (1993). A yeast GTPase-activating protein that interacts specifically with a member of the Ypt/Rab family. *Nature* 361, 736-739.
- Sulzer, D. and Holtzman, S. M. (1989). Acidification and endosome-like compartments in the presynaptic terminal of frog retinal photoreceptors. *J Neurocytol* 18, 529-540.
- Sun, B. and Salvaterra, P. M. (1995). Two *Drosophila* nervous system antigens, Nervana 1 and 2, are homologous to the beta subunit of Na⁺,K⁺-ATPase. *PNAS* 92, 5396-5400.
- Sutton, R. B., Fasshauer, D., Jahn, R. and Brunger, A. T. (1998). Crystal structure of a SNARE complex involved in synaptic exocytosis at 2.4 Å resolution. *Nature* 395, 347-353.
- Suzuki, K., Grinnell, A. D. and Kidokoro, Y. (2002). Hypertonicity-induced transmitter release at *Drosophila* neuromuscular junctions is partly mediated by integrins and cAMP/protein kinase A. *J Physiol* 538, 103-119.
- Swanson, M. M. and Poodry, C. A. (1981). The *shibire^{ts}* mutant of *Drosophila*: a probe for the study of embryonic development. *Dev Biol* 84, 465-470.
- Swanton, E., Sheehan, J., Bishop, N., High, S. and Woodman, P. (1998). Formation and turnover of NSF- and SNAP-containing "fusion" complexes occur on undocked, clathrin-coated vesicle-derived membranes. *Mol Biol Cell* 9, 1633-1647.
- Sweitzer, S. M. and Hinshaw, J. E. (1998). Dynamin undergoes a GTP-dependent conformational change causing vesiculation. *Cell* 93, 1021-1029.

- Takai, Y., Kaibuchi, K., Kikuchi, A. and Kawata, M. (1992). Small GTP-binding proteins. *Int Rev Cytol* 133, 187-230.
- Takei, K. and Haucke, V. (2001). Clathrin-mediated endocytosis: membrane factors pull the trigger. *Trends Cell Biol* 11, 385-391.
- Takei, K., Mundigl, O., Daniellè, L. and De Camilli, P. (1996). The synaptic vesicle cycle: A single vesicle budding step involving Clathrin and Dynamin. *J Cell Biol* 133, 1237-1250.
- Tall, G. G., Hama, H., DeWald, D. B. and Horazdovsky, B. F. (1999). The phosphatidylinositol 3-phosphate binding protein Vac1p interacts with a Rab GTPase and a Sec1p homologue to facilitate vesicle-mediated vacuolar protein sorting. *Mol Biol Cell* 10, 1873-1889.
- Tanigawa, G., Orci, L., Amherdt, M., Ravazzola, M., Helms, J. B. and Rothman, J. E. (1993). Hydrolysis of bound GTP by ARF protein triggers uncoating of Golgi-derived COP-coated vesicles. *J Cell Biol* 123, 1365-1371.
- Teichberg, S. E. and Holtzman, S. M. (1975). Circulation and turnover of synaptic vesicle membrane in cultured fetal mammalian spinal cord neurons. *J Cell Biol* 67, 215-230.
- Teng, H. and Wilkinson, R. S. (2000). Clathrin-mediated endocytosis near active zones in snake motor boutons. *J Neurosci* 20, 7986-7993.
- Thomas, D. M., Ferguson, G. D., Herschman, H. R. and Elferink, L. A. (1999). Functional and biochemical analysis of the C2 domains of Synaptotagmin IV. *Mol Biol Cell* 10, 2285-2295.
- Tisdale, E. J., Bourne, J. R., Khosravi-Far, R., Der, C. J. and Balch, W. E. (1992). GTP-binding mutants of Rab1 and Rab2 are potent inhibitors of vesicular transport from the endoplasmic reticulum to the Golgi complex. *J Cell Biol* 119, 749-761.
- Torri-Tarelli, F., Haimann, C. and Ceccarelli, B. (1987). Coated vesicles and pits during enhanced quantal release of acetylcholine at the neuromuscular junction. *J Neurocytol* 16, 205-214.
- Touchot, N., Chardin, P. and Tavittian, A. (1987). Four additional members of the Ras gene superfamily isolated by an oligonucleotide strategy: Molecular cloning of YPT-related cDNAs from a rat brain library. *PNAS* 84, 8210-8214.
- Towbin, H., Staehelin, T. and Gordon, J. (1979). Electrophoretic transfer of proteins from polyacrylamide gels to nitrocellulose sheets: procedure and some applications. *PNAS* 76, 4350-4354.
- Ullrich, O., Horiuchi, H., Bucci, C. and Zerial, M. (1994). Membrane association of Rab5 mediated by GDP-dissociation inhibitor and accompanied by GDP/GTP exchange. *Nature* 368, 157-160.
- Ullrich, O., Reinsch, S., Urbe, S., Zerial, M. and Parton, R. G. (1996). Rab11 regulates recycling through the pericentriolar recycling endosome. *J Cell Biol* 135, 913-924.

- Ullrich, O., Stenmark, H., Alexandrov, K., Huber, L. A., Kaibuchi, K., Sasaki, T., Takai, Y. and Zerial, M. (1993). Rab GDP dissociation inhibitor as a general regulator for the membrane association of Rab proteins. *J Biol Chem* 268, 18143-18150.
- Ungewickell, E. and Branton, D. (1981). Assembly units of Clathrin coats. *Nature* 289, 420-422.
- Ungewickell, E., Ungewickell, H., Holstein, S. E., Lindner, R., Prasad, K., Barouch, W., Martin, B., Greene, L. E. and Eisenberg, E. (1995). Role of Auxilin in uncoating clathrin-coated vesicles. *Nature* 378, 632-635.
- Vale, R. D., Banker, G. and Hall, Z. W. (1992). The neuronal cytoskeleton. In *An introduction to molecular neurobiology*. Z. W. Hall, ed. (Sunderland, Massachusetts, Sinauer Associates, inc.), pp. 247-280.
- Valtorta, F., Jahn, R., Fesce, R., Greengard, P. and Ceccarelli, B. (1988). Synaptophysin (p38) at the frog neuromuscular junction: its incorporation into the axolemma and recycling after intense quantal secretion. *J Cell Biol* 107, 2717-2727.
- Valtorta, F., Meldolesi, J. and Fesce, R. (2001). Synaptic vesicles: Is kissing a matter of competence? *Trends Cell Biol* 11, 324-328.
- van der Blik, A. M. and Meyerowitz, E. M. (1991). Dynamin-like protein encoded by the *Drosophila shibire* gene associated with vesicular traffic. *Nature* 351, 411-414.
- van der Sluijs, P., Hull, M., Webster, P., Male, P., Goud, B. and Mellman, I. (1992). The small GTP-binding protein Rab4 controls an early sorting event on the endocytic pathway. *Cell* 70, 729-740.
- van der Sluijs, P., Hull, M., Zahraoui, A., Tavitian, A., Goud, B. and Mellman, I. (1991). The small GTP-binding protein Rab4 is associated with early endosomes. *PNAS* 88, 6313-6317.
- Vanhaesebroeck, B., Leever, S. J., Panayotou, G. and Waterfield, M. D. (1997). Phosphoinositide-3-kinases: a conserved family of signal transducers. *Trends Biochem Sci* 22, 267-272.
- Vitale, G., Rybin, V., Christoforidis, S., Thornqvist, P., McCaffrey, M., Stenmark, H. and Zerial, M. (1998). Distinct Rab-binding domains mediate the interaction of Rabaptin-5 with GTP-bound Rab4 and Rab5. *EMBO J* 17, 1941-1951.
- Vitelli, R., Santillo, M., Lattero, D., Chiariello, M., Bifulco, M., Bruni, C. B. and Bucci, C. (1997). Role of the small GTPase Rab7 in the late endocytic pathway. *J Biol Chem* 272, 4391-4397.
- Volinia, S., Dhand, R., Vanhaesebroeck, B., MacDougall, L. K., Stein, R., Zvelebil, M. J., Domin, J., Panaretou, C. and Waterfield, M. D. (1995). A human phosphatidylinositol-3-kinase complex related to the yeast Vps34p-Vps15p protein sorting system. *EMBO J* 14, 3339-3348.
- von Ruden, L. and Neher, E. (1993). A Ca²⁺-dependent early step in the release of catecholamines from adrenal chromaffin cells. *Science* 262, 1061-1065.

- Waddell, S. and Quinn, W. G. (2001). Flies, genes, and learning. *Annu Rev Neurosci* 24, 1283-1309.
- Walworth, N. C., Brennwald, P., Kabacencell, A. K., Garrett, M. and Novick, P. (1992). Hydrolysis of GTP by Sec4 protein plays an important role in vesicular transport and is stimulated by a GTPase-activating protein in *Saccharomyces cerevisiae*. *Mol Cell Biol* 12, 2017-2028.
- Weber, T., Zemelmann, B. V., McNew, J. A., Westermann, B., Gmachl, M., Parlati, F., Sollner, T. H. and Rothman, J. E. (1998). SNAREpins: minimal machinery for membrane fusion. *Cell* 92, 759-772.
- Welinder, K. G. (1979). Amino-acid sequence studies of horseradish-peroxidase.4. Amino- and carboxyl-termini, cyanogen-bromide and tryptic fragments, the complete sequence, and some structural characteristics of horseradish peroxidase-C. *Eur J Biochem* 96, 483-502.
- Wichmann, H., Hengst, L. and Gallwitz, D. (1992). Endocytosis in yeast: Evidence for the involvement of a small GTP- binding protein (Ypt7p). *Cell* 71, 1131-1142.
- Wilcke, M., Johannes, L., Galli, T., Mayau, V., Goud, B. and Salamero, J. (2000). Rab11 regulates the compartmentalization of early endosomes required for efficient transport from early endosomes to the *trans*-Golgi network. *J Cell Biol* 151, 1207-1220.
- Wilson, J. M., de Hoop, M., Zorzi, N., Toh, B. H., Dotti, C. G. and Parton, R. G. (2000). EEA1, a tethering protein of the early sorting endosome, shows a polarized distribution in hippocampal neurons, epithelial cells, and fibroblasts. *Mol Biol Cell* 11, 2657-2671.
- Wu, M. N., Littleton, J. T., Bhat, M. A., Prokop, A. and Bellen, H. J. (1998). ROP, the *Drosophila* Sec1 homolog, interacts with Syntaxin and regulates neurotransmitter release in a dosage-dependent manner. *EMBO J* 17, 127-139.
- Yamashiro, D. J., Tycko, B., Fluss, S. R. and Maxfield, F. R. (1984). Segregation of transferrin to a mildly acidic (pH 6.5) para-Golgi compartment in the recycling pathway. *Cell* 37, 789-800.
- Yang, W. and Cerione, R. A. (1999). Endocytosis: Is Dynamin a 'blue collar' or 'white collar' worker? *Curr Biol* 9, R511-R514.
- Yoo, J. S., Grabowski, Xing, L., Trepte, H. H., Schmitt, H. D. and Gallwitz, D. (1999). Functional implications of genetic interactions between genes encoding small GTPases involved in vesicular transport in yeast. *Mol Gen Gen* 261, 80-91.
- Zenisek, D., Steyer, J. A. and Almers, W. (2000). Transport, capture and exocytosis of single synaptic vesicles at active zones. *Nature* 406, 849-854.
- Zerial, M. and McBride, H. (2001). Rab proteins as membrane organizers. *Nat Rev Mol Cell Biol* 2, 107-216.
- Zerial, M. and Stenmark, H. (1993). Rab GTPases in vesicular transport. *Curr Opin Cell Biol* 5, 613-620.

- Zhang, B., Ganetzky, B., Bellen, H. J. and Murthy, V. N. (1999). Tailoring uniform coats for synaptic vesicles during endocytosis. *Neuron* 23, 419-422.
- Zhang, B., Koh, Y. H., Beckstead, R. B., Budnik, V., Ganetzky, B. and Bellen, H. J. (1998). Synaptic vesicle size and number are regulated by a Clathrin adaptor protein required for endocytosis. *Neuron* 21, 1465-1475.
- Zhang, J. Z., Davletov, B. A., Südhof, T. C. and Anderson, R. G. W. (1994). Synaptotagmin I is a high affinity receptor for Clathrin AP-2: implications for membrane recycling. *Cell* 78, 751-760.
- Zimmerberg, J. (2000). Are the curves in all the right places? *Traffic* 1, 366-368.
- Zinsmaier, K. E., Eberle, K. K., Buchner, E., Walter, N. and Benzer, S. (1994). Paralysis and early death in cysteine string protein mutants of *Drosophila*. *Science* 263, 977-980.
- Zucker, R. S. (1989). Short-term synaptic plasticity. *Annu Rev Neurosci* 12, 13-31.
- Zucker, R. S. (1999). Calcium- and activity-dependent synaptic plasticity. *Curr Opin Neurobiol* 9, 305-313.

Lebenslauf

Tanja Wucherpfennig

- 24.09.1971** geboren in Remagen am Rhein
- Eltern: Dr. Wilhelm Wucherpfennig und Marianne Wucherpfennig, geborene Lenz
- Nationalität: deutsch
- 1978-1982** Besuch der Christian-Bitter Grundschule in Melsungen
- 1982-1988** Besuch des Gymnasiums an der Gesamtschule in Melsungen
- 1988-1991** Besuch des Geschwister-Scholl Oberstufengymnasiums in Melsungen
- 1991** Abitur
- 1991-1993** Grundstudium der Biologie an der Ruprecht-Karls-Universität in Heidelberg
- 12.10.1993** Diplom-Vorprüfung in Biologie
- 1993-1996** Hauptstudium der Biologie an der Ruprecht-Karls-Universität in Heidelberg
- 1994-1995** Studium der Biologie an der University of Glasgow, Glasgow UK
- 1996-1997** Anfertigung der Diplomarbeit am Tropeninstitut der Universität in Heidelberg, in der Abteilung von Prof. Dr. E. Hinz. "Isolierung von Antigenen aus *Onchocerca volvulus* und Bestimmung der gegen sie gerichteten humoralen Immunantwort im Menschen"
- 15.04.1997** Diplom in Biologie
- 1997-1998** Wissenschaftliche Mitarbeiterin in der Abteilung Neuropathologie, Prof. Dr. H. A. Kretschmar, am Universitätsklinikum in Göttingen
- 1998-** Anfertigung der Dissertation im Labor von Dr. Marcos González-Gaitán, am Max-Planck-Institut für biophysikalische Chemie, in der Abteilung von Prof. Dr. Herbert Jäckle, in Göttingen und
- seit 2000** am Max-Planck-Institut für molekulare Zellbiologie und Genetik in Dresden

Hiermit versichere ich, dass ich die vorliegende Dissertation selbständig und ohne unerlaubte Hilfe angefertigt und andere als die in der Dissertation angegebenen Hilfsmittel benutzt habe. Alle Stellen, die wörtlich oder sinngemäß aus veröffentlichten oder unveröffentlichten Schriften entnommen sind, habe ich als solche kenntlich gemacht. Kein Teil dieser Arbeit ist in einem anderen Promotions- oder Habilitationsverfahren verwendet worden.

(Tanja Wucherpfennig)